COMPLICATED DYNAMICS OF A THREE SPECIES CHEMOSTAT FOOD CHAIN

By

SPIRO DAOUSSIS, B.Sc., M.Sc.

A Thesis

Submitted to the School of Graduate Studies

in Partial Fulfilment of the Requirements

for the Degree

Doctor of Philosophy

McMaster University

COMPLICATED DYNAMICS OF A THREE SPECIES CHEMOSTAT FOOD CHAIN

DOCTOR OF PHILOSOPHY (1997)
(Mathematics)

McMaster University
Hamilton, Ontario

TITLE: COMPLICATED DYNAMICS OF A THREE SPECIES CHEMOSTAT FOOD CHAIN

AUTHOR: Spiro Daoussis
B.Sc. (McMaster University)
M.Sc. (McMaster University)

SUPERVISOR: Professor G.S.K. Wolkowicz

NUMBER OF PAGES: vii, 144

.... to my loving wife Victoria

Acknowledgements

I am deeply indebted to my supervisor Dr. G.S.K. Wolkowicz. Her patience, guidance, insight and friendship are deeply appreciated and will be forever remembered.

I would like to thank the Natural Sciences and Engineering Research Council of Canada and the Department of Mathematics for their financial support. I would also like to thank my supervisory committee members, Dr. J. Chadam, Dr. A. Peirce and Dr. T. Hurd for their financial assistance and their helpful comments and suggestions in preparing this thesis.

To all my friends, thank you and of course, cheers! Your friendships have had an immeasurable impact on my life. A special thank you to Dr. B. Müller, Dr. M. Clase, Mike (Narl) Pfau, Rob (Bob-o) Stamicar, Franco (Guinny) Guerriero, Paul (Captain Kirk) Stephenson, Eric (Rabbit) Derbez, Sean (Milo) Hill and Tarit (Foreign Minister) Saha for often turning a routine day into an interesting, unpredictable event.

Finally, I would like to extend my gratitude and a profound thank you to my father, Jerry, and my wife, Victoria. Their unconditional love and support never fails to amaze and inspire me.

Abstract

We consider a model of the chemostat that involves a three species food chain with no imposed periodicities. The bottom trophic level species depends on a single, essential, growth-limiting nutrient. For a particular choice of prototype response functions, numerical simulations exhibit complicated dynamical behavior for reasonable parameter values. Using bifurcation theory methods we show the possibility of chaotic dynamics in a neighborhood of a particular equilibrium point. Moreover, we examine the role of each of the response functions with respect to the dynamics (i.e. chaos) of the model by systematically changing one response function at a time from linear to a more biologically reasonable Michaelis-Menten response function.

Contents

Chapter 1

Introduction

1.1 The Chemostat

The chemostat is a laboratory apparatus used for the continuous culture of microbial organisms. It provides a controlled environment for the study of microorganism growth under nutrient limitation. The first description of the chemostat is due to both Monod [33] and Novick and Szilard [34], however, the term 'chemostat' is attributed to Novick and Szilard. The apparatus itself is relatively simple. It consists of three chambers : a feed vessel, a culture (or growth) vessel and a collection vessel. Nutrients are pumped at a constant rate from the feed vessel into the culture vessel and simultaneously, medium is pumped out of the culture vessel, at the same rate, into the collection vessel. Thus, constant volume is maintained in the culture vessel. With the exception of the nutrients under consideration, the feed vessel contains sufficient levels of all other required nutrients. The culture vessel is well stirred, thus nutrients, organisms and byproducts are removed in proportion to their concentrations in the culture vessel. All other parameters that may affect growth (i.e. temperature, light, pH conditions etc...) are kept constant.

One of the attractive attributes of the chemostat, from a experimental point of view, is that it allows the experimenter to make measurements based on the contents of the collection vessel without disturbing the behavior in the culture vessel, hence reducing the risk of tainting the experiment.

Over the years, the chemostat has played an important role in industry. It has been used in industrial processes such as water purification and waste decomposition ([10], [28], [54]), and commercially for the production of 'useful' microorganisms ([19], [42]). The chemostat also plays a key role in theoretical ecology (see, for example, [4], [9], [47]). It provides a model of microorganism interactions in a very simple lake. Surface waters of lakes are host to planktonic communities comprised of a variety of microbial organisms such as bacteria and unicellular algae. These planktonic communities are entirely dependent on the availability of nutrients in the surface waters (Hutchinson [24]).

However, natural occurring planktonic communities often deviate from the ideal laboratory conditions of the chemostat. For example, in nature it is rare to have a uniform distribution of planktonic communities across the surface waters of a lake. Distribution of these communities can depend on such things as shoreline stuctures (i.e. bays, coves etc...). Shoreline structures can provide protection against the general circulation of the open water and wind action, and hence allow the plankton to flourish in numbers in these areas (Welch [48]). Thus when we refer to the chemostat as a model of a lake, we are refering to an extremely simple, and perhaps artificial lake, characterized by near uniform distributions of shoreline profiles, temperature, light etc.

Also, the well stirred hypothesis of the chemostat can be violated when one considers seasonal weather changes. As pointed out in Waltman, Hubbell and Hsu [47],

> '...in deeper lakes and oceans, gradients of water density established in

summer prevent complete mixing of the water column, thereby cutting off the supply of nutrients to the surface waters from bottom sediments or nutrient-rich older and denser waters below. In the spring and fall, however, heating and cooling of the surface waters, respectively, equalize the water densities throughout the water colunm, and more nearly complete mixing occurs.'

Despite this deviation, predictions based on chemostat studies are still successful. This is due to the fact that the same nutrients remain limiting to the planktonic communities during the fluctuation or rapidly become limiting again after the fluctuation has subsided ([47]).

As a result, the chemostat is an extremely good theoretical and experimental tool that can uncover and probe complex mechanisms that govern microbial interactions in nature. All chemostat parameters, species' specific or otherwise, are measurable. The experimental work can confirm the theoretical work (see for example [23] and the subsequent experiments of Hansen and Hubbell [17]), and the ecology guides both the theoretical and experimental work of the chemostat.

We refer the reader to Smith and Waltman [41], and the references therein, for a survey of the various chemostat models.

1.2 Background Material

Models of biological systems are often parameter dependent and varying one or more of these parameters can change the dynamical behavior of the model. For example, consider pure competition in the chemostat with a single growth-limiting nutrient and equal dilution rates. Let S^0 denote the concentration of nutrient in the feed vessel. For S^0 sufficiently small, we have wash out of the

competitors (see, for example, [1], [8], [22], [23], [33], [43], [46], [51] and [52]). That is, all populations are driven to extinction. However, for sufficiently large S^0, one competitor population can survive. This change in dynamical behavior as S^0 passes through a critical value is called a 'bifurcation'. S^0 is called the 'bifurcation parameter' and the critical value of S^0 that produces this change is called the 'bifurcation value'.

Consider the following example of a one dimensional, one parameter dependent vector field, demonstrating an elementary bifurcation and the relevance of nonhyperbolicity of the fixed point.

Example A: Consider the following vector field

$$x' = f(x,\mu) = \mu x - x^2,\ x \in \mathbf{R},\ \mu \in \mathbf{R}. \tag{1.1}$$

It is easy to check that $f(0,0) = 0$ and $(\partial f/\partial x)(0,0) = 0$. The fixed points of (1.1) are $x = 0$ and $x = \mu$ and for $\mu = 0$, $x = 0$ is a nonhyperbolic fixed point. For $\mu < 0$, the fixed point $x = 0$ is stable while $x = \mu$ is unstable. At $\mu = 0$ the two fixed points coalesce and there is an exchange of stability, that is for $\mu > 0$, $x = 0$ is unstable and $x = \mu$ is stable. Thus there is a bifurcation at the critical value $\mu = 0$.

A bifurcation occurs for a dynamical system if the phase portrait undergoes a topological qualitative change. More precisely, there is no smooth deformation of the curves of one phase portrait to the curves of the other phase portrait as in Example A.

Many bifurcations occur when the vector field becomes nonhyperbolic. Studying bifurcation points of vector fields aids in the understanding of the

dynamical behavior of the vector field. That is, consideration of small perturbations of a vector field at a bifurcation point reveals all possible dynamical behavior of the system in a neighborhood of the bifurcation point.

There are two classifications of bifurcations: global and local. Global bifurcations can often be very difficult to deal with analytically. However, local bifurcations can readily be dealt with analytically. What is a local bifurcation? First we need the notion of a 'perturbation' of a vector field.

Let $f(\mathbf{x};p)$ and $g(\mathbf{x};p,\mu)$ be C^r vector fields in $\mathbf{R}^n$, with $p \in \mathbf{R}^p$ and $\mu \in \mathbf{R}^q$. Assume both f and g are continuous functions of the parameters. If $f(\mathbf{x};p) \neq g(\mathbf{x};p,\mu)$ but $f(\mathbf{x};p) = g(\mathbf{x};p,0)$, then we say that $g(\mathbf{x};p,\mu)$ is a 'perturbation' or 'unfolding' of $f(\mathbf{x};p)$.

An ordinary point of a vector field is any point other than a fixed point. The Flow Box Theorem ([2]) tells us that there is no topological qualitative change in the vector field for small perturbations in a neighborhood of an ordinary point. Hence, in order to produce qualitative change in a vector field we need to consider perturbations of the vector field in a neighborhood of a fixed point. The Hartman-Grobman Theorem ([2]) tells us that there is no qualitative change in a vector field due to small perturbations in a neighborhood of a hyperbolic fixed point. Thus we need to consider nonhyperbolic fixed points. Nonhyperbolic fixed points have at least one associated eigenvalue with zero real part. Small perturbations in a neighborhood of a nonhyperbolic fixed point can change the sign of the real part of the eigenvalue. Hence, it can change the local stability of the fixed point. If such a change occurs, we then say a 'local' bifurcation has occurred about the fixed point.

Example B: Consider the vector field

$$x' = f(x,\mu) = \mu - x^3, \ x \in \mathbf{R}, \ \mu \in \mathbf{R}. \tag{1.2}$$

Once again $f(0,0) = 0$ and $(\partial f/\partial x)(0,0) = 0$, and $x = 0$, at $\mu = 0$, is again a nonhyperbolic fixed point. However, unlike in the previous example, here the dynamics are qualitatively the same for $\mu < 0$ and $\mu > 0$. Namely, there is a unique stable fixed point and no bifurcation occurs.

An unfolding (perturbation) of a vector field that yields all possible topologically distinct dynamical behavior is called a 'versal' unfolding. A versal unfolding that uses the minimum number of parameters is called a 'universal' unfolding. The number of parameters required for a universal unfolding is called the 'codimension' of the bifurcation. Hence, every bifurcation is at least codimension one. The bifurcation of example A is a codimension one bifurcation, also known as a 'transcritical' bifurcation. For a more detailed consideration of codimension one bifurcation (i.e. pitchfork, saddle-node, etc...) and bifurcations in general, we refer the reader to Wiggins [49], [50].

Local bifurcation of fixed points can be determined by studying their associated eigenvalues and Taylor series expansions. There are however bifurcations that cannot be determined in this manner. We refer to these bifurcations as global bifurcations. For smooth vector fields in $\mathbf{R}^n$, global bifurcations can be a result of saddle connections between invariant sets of the flow (i.e. fixed points, limit cycles, etc...) breaking under small perturbations. There are two types of saddle connections: homoclinic and heteroclinic orbits. A homoclinic orbit, or loop, is created by a trajectory forming a loop which is closed by a saddle type point. The stable and unstable manifolds of the saddle type point cross away from the point, and since we are considering smooth vector fields, this implies that these two manifolds must coincide.

A heteroclinic loop is formed by a series of at least two trajectories connecting saddle points. The stable manifold of one saddle point crosses the

unstable manifold of the other saddle point. Once again, this implies that they must coincide.

Consider a smooth parameter dependent vector field in $\mathbf{R}^n$. Let μ be the bifurcation parameter that moves the vector field through a global bifurcation. As μ passes through the bifurcation value, the local stability of the saddle points does not change. However the global dynamics can be drastically affected. As μ moves through the bifurcation value there is usually the creation of a limit cycle. Moreover, global bifurcations can produce chaotic dynamics. For example, a two dimensional, parameter dependent, discrete dynamical system possessing a homoclinic or heteroclinic loop can be chaotic (Wiggins [50]) for certain parameter ranges. The chaotic behavior here is associated with local stretching, contracting and folding of regions near bifurcation.

For smooth autonomous vector fields, chaotic dynamics are only possible in $\mathbf{R}^n$ for $n > 2$ (Peixoto's Thm.). However, one can determine chaos in many vector fields by identifying global bifurcations for an associated $(n-1)$ dimensional Poincare map. One is usually restricted to computer simulations in order to locate and identify global bifurcations of vector fields.

Unlike the case for global bifurcations, there are analytical reduction methods that simplify the study of local bifurcations. One such method is the theory of **normal forms**, which will we use in our work and thus briefly outline below.

Consider the n dimensional vector field

$$\dot{\mathbf{v}} = G(\mathbf{v}) \text{ for } \mathbf{v} \in \mathbf{R}^n, \tag{1.3}$$

where G is C^r, and r is to be determined later. Assume that (1.3) has a fixed point at $\mathbf{v} = \mathbf{v}_0$. We outline the method of computation of the 'normal form' of (1.3), about $\mathbf{v}_0$, as given in Wiggins [49]. First, translate the fixed point to

the origin and then separate the linear part of the vector field to obtain

$$\dot{\mathbf{u}} = Dg(\mathbf{0})\mathbf{u} + \overline{g}(\mathbf{u}), \tag{1.4}$$

where $\mathbf{u} = \mathbf{v} - \mathbf{v}_0$, $G(\mathbf{u} + \mathbf{v}_0) \equiv g(\mathbf{u})$ and $\overline{g}(\mathbf{u}) = g(\mathbf{u}) - Dg(\mathbf{0})\mathbf{u}$. Let T denote the similarity transformation that takes the matrix $Dg(\mathbf{0})$ in (1.4) into J, a matrix in real Jordan canonical form. That is, under the transformation $\mathbf{u} = T\mathbf{x}$, (1.4) becomes

$$\begin{aligned} \dot{\mathbf{x}} &= T^{-1}Dg(\mathbf{0})T\mathbf{x} + T^{-1}\overline{g}(T\mathbf{x}) \,, \\ &\equiv J\mathbf{x} + F(\mathbf{x}). \end{aligned}$$

Next, find the Taylor expansion of $F(\mathbf{x})$ about the origin. That is,

$$\dot{\mathbf{x}} = J\mathbf{x} + F_2(\mathbf{x}) + F_3(\mathbf{x}) + ... + F_{r-1}(\mathbf{x}) + \mathcal{O}(\mathbf{x}^r), \tag{1.5}$$

where $F_i(\mathbf{x})$ for $i = 2, ..r-1$, are the order i terms in the Taylor expansion. Notice that up to this point we have simplified the linear terms as much as possible. We now seek to simplify the higher order terms in (1.5). We want to simplify the second order terms without changing the linear terms. After accomplishing this, we want to simplify third order terms without changing the second order and linear terms. We can continue in this manner to any desired order $r^* \leq r - 1$.

We begin with order 2 and introduce the near linear transformation

$$\mathbf{x} = \mathbf{y} + h_2(\mathbf{y}), \tag{1.6}$$

where $h_2(\mathbf{y})$ is order 2 and will be determined later. Substituting (1.6) into (1.5) we obtain

$$(I_n + Dh_2(\mathbf{y}))\,\dot{\mathbf{y}} = J\mathbf{y} + Jh_2(\mathbf{y}) + F_2(\mathbf{y} + h_2(\mathbf{y})) + F_3(\mathbf{y} + h_2(\mathbf{y})) + \mathcal{O}(4), \tag{1.7}$$

where I_n denotes the $n \times n$ identity matrix. Note that

$$\begin{aligned} F_2(\mathbf{y}+h_2(\mathbf{y})) &= F_2(\mathbf{y}) + DF_2(\mathbf{y})h_2(\mathbf{y}) + F_2(h_2(\mathbf{y})), \\ F_3(\mathbf{y}+h_2(\mathbf{y})) &= F_3(\mathbf{y}) + DF_3(\mathbf{y})h_2(\mathbf{y}) + \mathcal{O}(5). \end{aligned}$$

Regrouping terms in (1.7) by order we have

$$(I_n + Dh_2(\mathbf{y}))\,\dot{\mathbf{y}} = J\mathbf{y} + Jh_2(\mathbf{y}) + F_2(\mathbf{y}) + \overline{F}_3(\mathbf{y}) + \mathcal{O}(4), \tag{1.8}$$

where

$$\overline{F}_3(\mathbf{y}) = DF_2(\mathbf{y})h_2(\mathbf{y}) + F_3(\mathbf{y}).$$

For a $n \times n$ matrix $A = (a_{ij})$, we define the norm of A as

$$||A||_{mat} = \max_{i,j} |a_{ij}|.$$

Then for $||Dh_2(\mathbf{y})||_{mat} < 1$ we have

$$(I_n + Dh_2(\mathbf{y}))^{-1} = \sum_{n=0}^{\infty} (-1)^n (Dh_2(\mathbf{y}))^n = I_n - Dh_2(\mathbf{y}) + (Dh_2(\mathbf{y}))^2 + \mathcal{O}(3). \tag{1.9}$$

For $||y||$ sufficiently small, $||Dh_2(\mathbf{y})||_{mat}$ can be made arbitrarily small and thus $(I_n + Dh_2(\mathbf{y}))^{-1}$ exists. Apply (1.9) to equation (1.8) to obtain

$$\dot{\mathbf{y}} = J\mathbf{y} + Jh_2(\mathbf{y}) - Dh_2(\mathbf{y})J\mathbf{y} + F_2(\mathbf{y}) + \tilde{F}_3(\mathbf{y}) + \mathcal{O}(4), \tag{1.10}$$

where

$$\tilde{F}_3(\mathbf{y}) = (Dh_2(\mathbf{y}))^2 J\mathbf{y} - Dh_2(\mathbf{y})Jh_2(\mathbf{y}) - Dh_2(\mathbf{y})F_2(\mathbf{y}) + \overline{F}_3(\mathbf{y}).$$

So far we have not specified $h_2(\mathbf{y})$. We would like to choose $h_2(\mathbf{y})$ such that

$$Jh_2(\mathbf{y}) - Dh_2(\mathbf{y})J\mathbf{y} = -F_2(\mathbf{y}), \tag{1.11}$$

and thus remove all second order terms in (1.10). However, in general this is not possible. Below we outline a method describing how to choose $h_2(\mathbf{y})$ such

that we are only left with the 'essential' second order terms, denoted $F_2^r(\mathbf{y})$. For now assume $h_2(\mathbf{y})$ has been determined. Equation (1.10) then takes the form

$$\dot{\mathbf{y}} = J\mathbf{y} + F_2^r(\mathbf{y}) + \tilde{F}_3(\mathbf{y}) + \mathcal{O}(4). \tag{1.12}$$

We now seek to simplify the third order terms in (1.12). Introduce the near identity transformation

$$\mathbf{y} = \mathbf{y} + h_3(\mathbf{y}),$$

where $h_3(\mathbf{y})$ is third order in $\mathbf{y}$. Applying the above transformation to (1.12) and proceeding as we did for the second order terms, we have

$$\begin{aligned}(I_n + Dh_3(\mathbf{y}))\,\dot{\mathbf{y}} &= J\mathbf{y} + Jh_3(\mathbf{y}) + F_2^r(\mathbf{y} + h_3(\mathbf{y})) + \tilde{F}_3(\mathbf{y} + h_3(\mathbf{y})) + \mathcal{O}(4) \\ &= J\mathbf{y} + Jh_3(\mathbf{y}) + F_2^r(\mathbf{y}) + \tilde{F}_3(\mathbf{y}) + \mathcal{O}(4).\end{aligned}$$

For $||\mathbf{y}||$ sufficiently small, $(I_n + Dh_3(\mathbf{y}))^{-1}$ exists and we have

$$\begin{aligned}\dot{\mathbf{y}} &= \{I_n - Dh_3(\mathbf{y}) + \mathcal{O}(4)\}\left\{J\mathbf{y} + Jh_3(\mathbf{y}) + F_2^r(\mathbf{y}) + \tilde{F}_3(\mathbf{y}) + \mathcal{O}(4)\right\} \\ &= J\mathbf{y} + F_2^r(\mathbf{y}) + Jh_3(\mathbf{y}) - Dh_3(\mathbf{y})J\mathbf{y} + \tilde{F}_3(\mathbf{y}) + \mathcal{O}(4).\end{aligned} \tag{1.13}$$

We would like to choose $h_3(\mathbf{y})$ such that

$$Jh_3(\mathbf{y}) - Dh_3(\mathbf{y})J\mathbf{y} = -\tilde{F}_3(\mathbf{y}), \tag{1.14}$$

and thus eliminate all third order terms (1.13). In general this is not possible. Thus we choose $h_3(\mathbf{y})$ in such a manner as to leave only the 'essential' third order terms, $F_3^r(\mathbf{y})$.

The procedure can continue to the desired order $r^* \leq r - 1$. Notice that at each application of a transformation of the form $\mathbf{y} = \mathbf{y} + h_k(\mathbf{y})$, the $k+1$ order terms are changed but not the lower order terms.

We now quickly outline how to determine $h_k(\mathbf{y})$. First let H_k^n denote the space of vector-valued monomials of degree k, in $\mathbf{R}^n$. For example, take

the standard ordered basis of $\mathbf{R}^2$, and let the coordinates with respect to this basis be denoted by x and y. Then H_2^2 is given by

$$H_2^2 = span\left\{\begin{pmatrix} x^2 \\ 0 \end{pmatrix}, \begin{pmatrix} xy \\ 0 \end{pmatrix}, \begin{pmatrix} y^2 \\ 0 \end{pmatrix}, \begin{pmatrix} 0 \\ x^2 \end{pmatrix}, \begin{pmatrix} 0 \\ xy \end{pmatrix}, \begin{pmatrix} 0 \\ y^2 \end{pmatrix}\right\},$$

and the set of vectors above are referred to as the standard ordered basis of H_2^2.

Next, reconsider equation (1.11). Clearly, $h_2(\mathbf{y}) \in H_2^n$ and the map

$$h_2(\mathbf{y}) \mapsto Dh_2(\mathbf{y})J\mathbf{y} - Jh_2(\mathbf{y})$$

is a linear map of H_2^n into H_2^n. Moreover, for $h_k(\mathbf{y}) \in H_k^n$ we have the linear map of H_k^n into H_k^n given by

$$h_k(\mathbf{y}) \mapsto Dh_k(\mathbf{y})J\mathbf{y} - Jh_k(\mathbf{y}).$$

This map is often denoted as

$$L_J(h_k(\mathbf{y})) \equiv -(Dh_k(\mathbf{y})J\mathbf{y} - Jh_k(\mathbf{y})) \equiv [h_k(\mathbf{y}), J\mathbf{y}],$$

for the Lie bracket operation on the vector fields $h_k(\mathbf{y})$ and $J\mathbf{y}$ ([21]).

The task of solving equation (1.11) and determining $h_2(\mathbf{y})$ is now much easier if we work in the linear space setting of L_J. Solving equation (1.11) is like solving a linear system $Ax = b$. To see this let B_2 denote the standard ordered basis of H_2^n. By determining the action of L_J on each basis vector of B_2, we can construct a matrix representation of L_J with respect to B_2, say M_2. Then, since $F_2(\mathbf{y}) \in H_2^n$, equation (1.11) is equivalent to

$$M_2 \cdot h_2(\mathbf{y}) = -F_2(\mathbf{y}). \tag{1.15}$$

If the above equation has a solution, then all second order terms can be omitted. That is if F_2 is in the range of L_J, then $L_J(H_2^n) = H_2^n$ and all second

order terms can be eliminated. However, in general, equation (1.15) may have no solution.

If equation (1.15) has no solution then proceed as follows. First, H_2^n can be represented (non uniquely) as

$$H_2^n = L_J(H_2^n) \oplus G_2,$$

where G_2 is a space complementary to $L_J(H_2^n)$. If $F_2 \notin L_J(H_2^n)$, then choose $h_2(\mathbf{y})$ such that only second order terms in G_2 are left. That is,

$$F_2^r(\mathbf{y}) \in G_2.$$

Determine G_2 in the following manner. First, note that $L_J(H_2^n)$ is the column space of M_2. Choose G_2 to be the orthogonal complement of M_2, that is, G_2 can be chosen to be the nullspace of the transpose of M_2. Next, choose bases for $L_J(H_2^n)$ and G_2. Concatenate the two bases to form a new basis of H_2^n. Now rewrite F_2 with respect to this new basis and decompose F_2 into

$$F_2 = F_2^L + F_2^r, \text{ where } F_2^L \in L_J(H_2^n) \text{ and } F_2^r \in G_2.$$

Finally, determine $h_2(\mathbf{y})$ by solving the linear system

$$M_2 \cdot h_2 = -F_2^L.$$

By iteration determine each h_k. The above is summarized in the following theorem.

Normal Form Theorem : (Wiggins [49])

By a sequence of analytic coordinate changes (1.5) *can be transformed into*

$$\dot{\mathbf{y}} = J\mathbf{y} + F_2^r(\mathbf{y}) + F_3^r(\mathbf{y}) + \ldots + F_{r-1}^r(\mathbf{y}) + \mathcal{O}(|\mathbf{y}|^r), \tag{1.16}$$

where $F_k^r(\mathbf{y}) \in G_k$, $2 \leq k \leq r-1$, *and* G_k *is a space complementary to* $L_J(H_k^n)$. *Equation* (1.16) *is said to be in normal form.*

We conclude this section with a few general remarks on normal forms. First, notice that a normal form computation is solely dependent on the linear part of the vector field. Thus a particular normal form can represent a large class of vector fields with similar linear part. Secondly, since the choice of G_k is not unique, normal forms (unlike Taylor series) are not unique. Thus determining a universal unfolding for a normal form is crucial if one wants to compare the dynamical behavior of the normal form to the behavior of the original vector field.

1.3 Thesis Outline

In this thesis, motivated by the results of Hastings and Powell ([18]), we consider a model of a three species food chain in the chemostat (super-predator, predator, prey) without any imposed periodicities. Numerical work on this model seems to indicate chaotic dynamical behavior for certain parameter regions when all response functions are of Michaelis-Menten form ([41]). The work in this thesis centers around two questions. First, what are the bifurcations that lead to chaos? Secondly, how are these bifurcations related to the structure (i.e. nonlinearity) of the response functions? In an attempt to answer these questions, we begin by considering the mathematically simplest example of the model which is described by linear response functions. We then change one uptake function one at a time, from linear to Michaelis-Menten, and determine what new bifurcations have been introduced to the model. That is, we systematically build towards the known chaotic model of three Michaelis-Menten response functions.

This thesis is organized in the following manner. In Chapter 2 we give the mathematical description of the model for general monotone uptake

functions along with the necessary biological constraints. In addition, we give a non-dimensional version of the model and introduce notation for the fixed points. Finally, we present some preliminary results and give conditions for the global asymptotic stability of the wash-out state and the single species survival state.

In Chapter 3 we restrict our attention to prototype response functions and consider three examples of the model. The first example (Case 1) incorporates linear response functions. In this case we are able to give a complete global analysis of the model. Example 2 (Case 2) consists of changing the super-predator's response function from linear type to Michaelis-Menten type. We present some global stability results for this case and also give a necessary and sufficient condition for uniform persistence. The final example of the model (Case 3), that we consider in this chapter, is given by Michaelis-Menten response functions for both super-predator and predator. We show the existence of a codimension 2 bifurcation on one of the faces of $\mathbf{R}^4$. We conclude the chapter with some numerical simulations of this example.

Chapter 4 contains the normal form calculation of the codimension 2 bifurcation of Case 3. We introduce an unfolding for the normal form and then describe the bifurcations of this unfolding. We end Chapter 4 with a comparison of the bifurcation behavior of the unfolded normal form to the dynamics of the original vector field. In Chapter 5 we consider one last example of the model (Intermediate case). This case consists of a Michaelis-Menten response function for the predator and linear response functions for both prey and super-predator. Once again, this case has the same codimension 2 bifurcation, but appears not to be chaotic. We conclude this chapter with a comparison of bifurcation behavior of Case 2, Case 3, and the Intermediate

case. Finally, Chapter 6 contains a summary and discussion of our results. Appendices A and B contain Maple programs for the calculation of the normal form of Chapter 4 and the calculation of the associated 3-jet, respectively.

Chapter 2

Three Species Food Chain in the Chemostat

2.1 The Model

We consider a model of a food chain in the chemostat described by the following system of ordinary differential equations :

$$\begin{aligned} S'(t) &= (S^0 - S(t))D - \tfrac{x_1(t)h(S(t))}{\zeta} , \\ x_1'(t) &= x_1(t)(-D + h(S(t))) - \tfrac{x_2(t)p_1(x_1(t))}{\eta_1} , \\ x_2'(t) &= x_2(t)(-D + p_1(x_1(t))) - \tfrac{x_3(t)p_2(x_2(t))}{\eta_2} , \\ x_3'(t) &= x_3(t)(-D + p_2(x_2(t))) , \end{aligned} \tag{2.1}$$

$$S(0) = S_0 \geq 0 \text{ and } x_i(0) = x_{i0} \geq 0 \text{ for } i = 1, 2, 3.$$

The culture vessel is assumed to be well-stirred so that spatial variation can be neglected and for convenience the volume of the culture vessel is assumed to be one cubic unit. $S(t)$ denotes the nutrient concentration and $x_i(t)$, $i = 1, 2, 3$, denote the concentrations of microorganisms in the culture vessel

at time t. Population x_3 is the top predator in the food chain. Population x_3 consumes population x_2. Population x_2 in turn consumes population x_1, and population x_1 consumes the nutrient S. The functional response of population x_1 on nutrient S is given by $h(S)$, with corresponding growth yield constant ζ. Thus, $h(S)/\zeta$ is the rate of consumption of nutrient S for population x_1 and so we assume that consumption of nutrient by the microorganism is proportional to conversion to biomass. Similarly, $p_i(x_i)$, $i = 1, 2$, denotes the functional response of predator x_{i+1} on prey x_i and $p_i(x_i)/\eta_i$ is assumed to denote the prey uptake function for the respective predator. Thus, the constants η_i, $i = 1, 2$, are the growth yield constants for the respective predator populations. S^0 denotes the concentration of nutrient in the feed vessel and D denotes the dilution rate. The species' death rates are assumed to be insignificant compared to the dilution rate and are neglected.

We make the following assumptions concerning the functions $p_i(x_i)$ and $h(S)$ in system (2.1) :

$$\begin{gathered} p_i, h : \mathbf{R}_+ \to \mathbf{R}_+ \ ; \\ p_i, h \text{ are continuously differentiable} \ ; \\ h'(S) \geq 0 \ \text{ for all } S \in \mathbf{R}_+ \ ; \\ p_i'(x_i) \geq 0 \ \text{ for all } x_i \in \mathbf{R}_+ \ ; \\ p_i(0) = 0 \text{ and } h(0) = 0. \end{gathered} \tag{2.2}$$

The following substitutions help simplify the analysis of system (2.1) :

$$\begin{gathered} \overline{t} = tD \ ; \ \overline{S} = S \ ; \ \overline{x}_1 = \tfrac{x_1}{\zeta} \ ; \ \overline{x}_2 = \tfrac{x_2}{\zeta\eta_1} \ ; \ \overline{x}_3 = \tfrac{x_3}{\zeta\eta_1\eta_2} \ ; \\ \overline{h}(\overline{S}) = \tfrac{h(S)}{D} \ ; \ \overline{p}_i(\overline{x}_i) = \tfrac{p_i(x_i)}{D} \text{ for } i = 1, 2. \end{gathered}$$

Omitting the bars, to simplify the notation, the scaled version of system

(2.1) can be written as follows :

$$\begin{aligned} S'(t) &= S^0 - S(t) - x_1(t)h(S(t)) \,, \\ x_1'(t) &= x_1(t)(-1 + h(S(t))) - x_2(t)p_1(x_1(t)) \,, \\ x_2'(t) &= x_2(t)(-1 + p_1(x_1(t))) - x_3(t)p_2(x_2(t)) \,, \\ x_3'(t) &= x_3(t)(-1 + p_2(x_2(t))) \,, \end{aligned} \tag{2.3}$$

$$S_0 \geq 0, \; x_{i0} \geq 0, \; \text{for } i = 1,2,3.$$

There is no loss of generality if we analyze system (2.3) instead of system (2.1). We identify $(S, x_1, x_2, x_3) - space$ with $\mathbf{R}^4_+$.

From the assumptions in (2.2) it follows that there exist uniquely defined positive extended real numbers λ and δ_i, $i = 1,2$, such that

$$\begin{aligned} h(S) < 1 \quad &\text{if} \quad S < \lambda \,, \\ h(S) > 1 \quad &\text{if} \quad S > \lambda \,, \\ p_i(x_i) < 1 \quad &\text{if} \quad x_i < \delta_i \,, \\ p_i(x_i) > 1 \quad &\text{if} \quad x_i > \delta_i. \end{aligned}$$

Hence λ and δ_i $(i = 1,2)$ denote the break-even concentrations of nutrient and prey respectively. Prototypes of monotone response functions commonly used in the literature ([25], [33], [46]) are :

$$\begin{array}{lll} (i) & p(x) = x/\delta & \text{Lotka} - \text{Volterra} \\ (ii) & p(x) = mx/(\delta(m-1) + x), \; m > 1 & \text{Michaelis} - \text{Menten} \\ (iii) & p(x) = mx^2/(a+x)(b+x), \; m > 1 & \text{Sigmodial} \,. \end{array} \tag{2.4}$$

We will focus the majority of our attention on response functions of types (i) and (ii).

The critical points of system (2.3) will be denoted by

$$\begin{aligned} E_0 &= (S^0, 0, 0, 0) , \\ E_\lambda &= (\lambda, S^0 - \lambda, 0, 0) , \\ E_{\delta_2} &= (S^0, 0, \delta_2, -\delta_2) , \\ E_{S^*} &= (S^*, \delta_1, x_2^*, 0) , \\ E^\Delta &= (S^\Delta, x_1^\Delta, \delta_2, x_3^\Delta) , \end{aligned}$$

where S^* must satisfy $S^0 - S^* = \delta_1 h(S^*)$, $x_2^* = \delta_1(-1 + h(S^*))$ and S^Δ, x_1^Δ must satisfy $S^0 - S^\Delta = x_1^\Delta h(S^\Delta)$ and $x_1^\Delta(-1 + h(S^\Delta)) = \delta_2 p_1(x_1^\Delta)$ with $x_3^\Delta = \delta_2(-1 + p_1(x_1^\Delta))$. Note that there may be more than one fixed point of the form E^Δ.

We say that a critical point exists if and only if all of its components are nonnegative. Hence E_λ exists provided $\lambda \leq S^0$. E_{S^*} exists provided $S^* \geq \lambda$. E^Δ exists provided $x_1^\Delta \geq \delta_1$. Note that E_{δ_2} cannot occur in the nonnegative cone due to the biological constraint $\delta_2 > 0$.

2.2 Preliminary Results

As is the case with any reasonable model of the chemostat, the solutions of system (2.3) are well behaved which is the content of our first proposition.

Proposition 2.1 *All solutions $S(t)$, $x_i(t)$ for $i = 1, 2, 3$ of system (2.3) for which $x_{i0} > 0$ $(i = 1, 2, 3)$ are (i) positive and (ii) bounded for $t > 0$.*

Proof : (i) If $S(0) = 0$ then $S'(0) = S^0 > 0$. Suppose there exists a first $t_0 > 0$ such that $S(t_0) = 0$ and $S(t) > 0$ for $0 < t < t_0$. Then $S'(t_0) \leq 0$, but from (2.3) $S'(t_0) = S^0 > 0$, which is a contradiction.

Next, since the boundary faces $x_i \equiv 0$ $(i = 1, 2, 3)$ are invariant, by the uniqueness of solutions of initial value problems, they cannot be reached in

finite time by any trajectory originating in the interior of $\mathbf{R}^4_+$. Therefore, for all $t > 0$, $x_i(t) > 0$ for $i = 1, 2, 3$.

(ii) Let

$$z(t) = S(t) + \sum_{i=1}^{3} x_i(t) \ .$$

Then adding the equations in (2.3) we obtain $z'(t) = S^0 - z(t)$. Solving this first order differential equation leads to $z(t) = S^0 + (z_0 - S^0)e^{-t}$, and thus $z(t) = S^0$ as $t \to \infty$. In particular, $S(t) + \sum_{i=1}^{3} x_i(t) = S^0 > 0$ as $t \to \infty$, and since by part (i) solutions are positive, it follows that all solutions are bounded. □

Proposition 2.2 *The simplex,*

$$\Im = \{(S, x_1, x_2, x_3) \in \mathbf{R}^4_+ : S, x_i \geq 0, \ S + \sum_{i=1}^{3} x_i = S^0\} \tag{2.5}$$

is a global attractor for system (2.3).

Proof : See the proof of Proposition 2.1 part (ii).

Remark : Let $\gamma(t) = (S(t), x_1(t), x_2(t), x_3(t))$ be a solution of system (2.1) and let Ω denote the omega limit set of $\gamma(t)$. By Propositions 2.1 and 2.2, Ω is a nonempty, invariant, compact and connected subset of $\mathbf{R}^4_+$ (see [16], Thm. 8.1).

The following theorem is concerned with the extinction of the populations $x_i(t)$ due to insufficient nutrient amount. The extinction is independent of predation. We will first require the following proposition and a lemma due to Miller ([32]) which we state below for the sake of completeness.

Proposition 2.3 *For all solutions of system (2.3),*

(i) Given any $\varepsilon > 0$, $S(t) < S^0 + \varepsilon$ *for all sufficiently large* t.

(ii) If there exists $t_0 > 0$ *such that* $S(t) < S^0$, *then* $S(t) < S^0$ *for all* $t \geq t_0$.

Proof : (i) By Proposition 2.1 all solutions of (2.3) are positive and bounded and thus

$$\begin{aligned} S'(t) &= S^0 - S(t) - x_1(t)h(S(t)) \\ &\leq S^0 - S(t)\ , \end{aligned}$$

which implies that given any $\varepsilon > 0$

$$\begin{aligned} S(t) &\leq S^0 + (S_0 - S^0)e^{-t} \\ &< S^0 + \varepsilon, \text{ for all sufficiently large } t. \end{aligned}$$

(ii) Assume there exists a first $t_1 > t_0$ such that $S(t_1) = S^0$. Then $S(t) < S^0$ for all $t_0 \leq t < t_1$, and so $S'(t_1) \geq 0$. However,

$$S'(t_1) = -x_1(t_1)h(S(t_1)) < 0$$

which is a contradiction. □

In addition to the above propositions we will need the following lemma due to Miller ([32]).

Lemma 2.4 *Let* $w(t) \in C^2(t_0, \infty)$, $w(t) \geq 0$ *and* $K > 0$.

(i) If $w'(t) \geq 0$, $w(t)$ *bounded and* $w''(t) \leq K$ *for all* $t \geq t_0$, *then* $w'(t) \to 0$ *as* $t \to \infty$.

(ii) If $w'(t) \leq 0$, $w''(t) \geq -K > -\infty$ *for all* $t \geq t_0$, *then* $w'(t) \to 0$ *as* $t \to \infty$.

Theorem 2.5 *For all solutions of system (2.3), if* $S^0 < \lambda$ *then* $x_i(t) \to 0$ $(i = 1, 2, 3)$ *as* $t \to \infty$.

Proof : If $S^0 < \lambda$ then $h(S^0) < 1$ and by the continuity of $h(S(t))$, there exists $\varepsilon > 0$ such that $h(S^0 + \varepsilon) < 1$. By Proposition 2.3 part (i), $S(t) < S^0 + \varepsilon$ for all sufficiently large t. Since all solutions are positive and bounded, $x_1'(t) < 0$ for all sufficiently large t. By Lemma 2.4, $x_1'(t) \to 0$ as $t \to \infty$. However

$$\limsup_{t\to\infty} h(S(t)) < h(S^0 + \varepsilon) < 1 \ .$$

This and (2.3) imply that $x_1(t) \to 0$ as $t \to \infty$.

Next, since $\lim_{t\to\infty} x_1(t) = 0$, then for an arbitrary $\varepsilon > 0$, there exists t_0 sufficiently large such that for all $t \geq t_0$, we have $-1 + p_1(x_1(t)) < 0$ which implies that $x_2'(t) < 0$. As before, we have by Lemma 2.4 $x_2'(t) \to 0$ as $t \to \infty$. By (2.3), we obtain $x_2(t) \to 0$ as $t \to \infty$. Similarly, we have $x_3(t) \to 0$ as $t \to \infty$. □

2.3 Stability of E_0 and E_λ

In this section we concern ourselves with the global stability of the fixed points E_0 and E_λ of system (2.3). Whenever possible, the results of this section are obtained for response functions satisfying only the basic assumptions in (2.2). In certain cases, the results are restricted to the prototype response functions given in (2.4).

For $S^0 < \lambda$, E_0 is the only fixed point in the nonnegative cone $\mathbf{R}^4_+$. The Jacobian of (2.3) evaluated at $E_0 = (S^0, 0, 0, 0)$ is

$$\begin{pmatrix} -1 & -h(S^0) & 0 & 0 \\ 0 & -1 + h(S^0) & 0 & 0 \\ 0 & 0 & -1 & 0 \\ 0 & 0 & 0 & -1 \end{pmatrix}$$

and the associated eigenvalues for E_0 are $-1,-1,-1,-1+h(S^0)$. Hence, E_0 is locally asymptotically stable provided $-1+h(S^0)<0$ (i.e. $S^0<\lambda$). Under the condition $S^0<\lambda$, E^0 is not only locally asymptotically stable but also globally asymptotically stable.

Theorem 2.6 *If $S^0<\lambda$ then $E_0=(S^0,0,0,0)$ is globally asymptotically stable for system (2.3).*

Proof : Let $P\in\{(S,x_1,x_2,x_3)\in\mathbf{R}^4_+ : x_i>0,\ i=1,2,3\}$ and let $\Omega(P)$ denote the omega limit set of P. If $Q=(\overline{S},\overline{x}_1,\overline{x}_2,\overline{x}_3)\in\Omega(P)$, then by Theorem 2.5, $\overline{x}_i=0$ for $i=1,2,3$. On the subspace $\{(\overline{S},0,0,0)\in\mathbf{R}^4_+\}$ system (2.3) reduces to

$$S'(t)=S^0-S(t).$$

Hence, by Proposition 2.2, $S(t)\to S^0$ as $t\to\infty$. If $Q\in\Omega(P)$, then the entire trajectory through Q is in $\Omega(P)$, and since $\Omega(P)$ is closed then $E_0\in\Omega(P)$. Since $S^0<\lambda$, E_0 is locally asymptotically stable. Therefore $\{E_0\}=\Omega(P)$, and thus E_0 is globally asymptotically stable for system (2.3). □

For system (2.3), when $S^0=\lambda$, E_0 and E_λ coalesce. As S^0 increases past λ, E_0 becomes unstable with a three dimensional stable manifold and a one dimensional unstable manifold. Simultaneously, E_λ enters the nonnegative cone $\mathbf{R}^4_+$. The Jacobian of (2.3) evaluated at $E_\lambda=(\lambda,S^0-\lambda,0,0)$ is

$$\begin{pmatrix} -1-(S^0-\lambda)h'(\lambda) & -1 & 0 & 0 \\ (S^0-\lambda)h'(\lambda) & 0 & -p_1(S^0-\lambda) & 0 \\ 0 & 0 & -1+p_1(S^0-\lambda) & 0 \\ 0 & 0 & 0 & -1 \end{pmatrix}$$

and the associated eigenvalues for E_λ are $-1,-1,-(S^0-\lambda)h'(\lambda)$, and $-1+p_1(S^0-\lambda)$. Thus $E_\lambda\in\mathbf{R}^4_+$ and is locally asymptotically stable provided

$\lambda < S^0 < \lambda + \delta_1$, and the exchange of stability between E_0 and E_λ is via a transcritical bifurcation. In order to show global stability for E_λ we will require the following preparatory results.

Proposition 2.7 *If $\lambda < S^0$, then $S(t) < S^0$ for all sufficiently large t.*

Proof : Let $\lambda < S^0$ and assume $S(t) > S^0$ for all sufficiently large t. Then $S'(t) < 0$ for all sufficiently large t, and $S(t) \downarrow S^* \geq S^0$. If $S^* > S^0$ then $S'(t) \leq (S^0 - S^*) < 0$, which implies that $S(t) \downarrow -\infty$, a contradiction.

Next, if $S^* = S^0$, since by Proposition 2.2

$$S(t) + \sum_{i=1}^{3} x_i(t) \to S^0 \text{ as } t \to \infty,$$

and since solutions are positive and bounded, it follows that $x_i(t) \to 0$ as $t \to \infty$. However, since by assumption $\lambda < S^0 < S(t)$ for all sufficiently large t, then

$$\begin{aligned} x_1'(t) &= x_1(t)(-1 + h(S(t))) - x_2(t)p_1(x_1(t)) \\ &> 0 \text{ for all sufficiently large } t \ . \end{aligned}$$

This contradicts $x_1(t) \to 0$ as $t \to \infty$. Thus for sufficiently large t, by Proposition 2.3 (ii), $S(t) < S^0$ if $\lambda < S^0$. □

Next, consider the system of differential equations

$$\mathbf{x}'(t) = \mathbf{f}(\mathbf{x}(t)) \tag{2.6}$$

where $\mathbf{f} : \mathcal{G}^* \subseteq \mathbf{R}^n \to \mathbf{R}^n$ is a continuous vector-valued function.

Definition 2.8 *A function V on $\mathcal{G} \subseteq \mathcal{G}^*$ is called a Liapunov function for (2.6) if :*

(i) V is continuously differentiable on $\mathcal{G}$,

(ii) V not continuous at $\mathbf{x} \in \overline{\mathcal{G}}$ implies that

$$\lim_{\mathbf{x} \to \overline{\mathbf{x}}} V(\mathbf{x}) = \infty \ , \text{ for } \mathbf{x} \in \mathcal{G},$$

(iii) $\dot{V} = \nabla V \cdot \mathbf{f} \leq 0$ *on* $\mathcal{G}$.

The following modification of the LaSalle Extension Theorem, given in LaSalle [29], is due to Wolkowicz and Zhiqi [53] and as they point out the proof only requires a minor modification to the proof given in Hale [16].

Theorem 2.9 *(Modified LaSalle Extension Theorem)*
Assume that V is a Liapunov function for (2.6) on $\mathcal{G} \subseteq \mathcal{G}^*$. Define $\mathcal{E} = \{\mathbf{x} \in \overline{\mathcal{G}} \cap \mathcal{G}^* : \dot{V}(\mathbf{x}) = 0\}$. Let $\mathcal{M}$ denote the largest invariant subset of $\mathcal{E}$. Then every bounded (for $t \geq 0$) trajectory of (2.6) that remains in $\mathcal{G}$ (for $t \geq 0$) approaches the set $\mathcal{M}$ as $t \to \infty$.

To obtain global stability for E_λ, under the condition $\lambda < S^0 < \lambda + \delta_1$, we restrict $p_1(x_1)$ to be one of the **prototype** response functions given in (2.4). The response functions $h(S)$ and $p_2(x_2)$ are still general monotone uptake functions satisfying only the assumptions in (2.2).

Lemma 2.10 *Let the response function $p_1(x_1)$ be any one of the prototype functions given in (2.4). Then, for $\lambda < S^0 < \lambda + \delta_1$ there exists a scalar $\alpha > 0$ such that*

$$\max_{0 < x_1 < \delta_1} g(x_1) \leq \alpha \leq \min_{\delta_1 < x_1 < \infty} g(x_1)$$

where

$$g(x_1) = \frac{(x_1 - (S^0 - \lambda))p_1(x_1)}{x_1(-1 + p_1(x_1))}.$$

Proof : See Wolkowicz and Zhiqi [53].

Theorem 2.11 *Let $p_1(x_1)$ be one of the prototype response functions given in (2.4) and let $\lambda < S^0 < \lambda + \delta_1$. Then $E_\lambda = (\lambda, S^0 - \lambda, 0, 0)$ is globally asymptotically stable for system (2.3) with respect to $int\mathbf{R}^4_+$.*

Proof : By Proposition 2.7, it is enough to show global stability on the set $\mathcal{G} = \{(S, x_1, x_2, x_3) \in \mathbf{R}^4_+ : S \in (0, S^0)$ and $x_i \in (0, \infty)$ $i = 1, 2, 3.\}$. Define a Liapunov function $V(S, x_1, x_2, x_3)$ on the set $\mathcal{G}$ by

$$V(S, x_1, x_2, x_3) = \int_\lambda^S \frac{(-1 + h(\xi))(S^0 - \lambda)}{(S^0 - \xi)} d\xi + \{x_1 - \overline{x}_1 - \overline{x}_1 \ln(\frac{x_1}{\overline{x}_1})\} + \sum_{i=2}^{3} \alpha_i x_i$$

where $\overline{x}_1 = S^0 - \lambda$ and $\alpha_2, \alpha_3 > 0$ real scalars. Then the time derivative of $V(S, x_1, x_2, x_3)$ calculated along solutions of (2.3) is :

$$\begin{aligned} \dot{V}(S, x_1, x_2, x_3) &= \tfrac{(-1+h(S))(S^0-\lambda)}{(S^0-S)} S' + (1 - \tfrac{S^0-\lambda}{x_1}) x_1' + \textstyle\sum_{i=2}^{3} \alpha_i x_i' \\ &= x_1(-1 + h(S)) - x_1 h(S) \tfrac{(-1+h(S))(S^0-\lambda)}{S^0-S} \\ &+ \alpha_2 x_2(-1 + p_1(x_1)) - x_2 p_1(x_1) \tfrac{(x_1-(S^0-\lambda))}{x_1} - \alpha_3 x_3 \, . \end{aligned}$$

Choosing $\alpha_2 = \alpha_3$ we have

$$\begin{aligned} \dot{V}(S, x_1, x_2, x_3) &= x_1(-1 + h(S)) \left\{1 - \tfrac{h(S)(S^0-\lambda)}{S^0-S}\right\} \\ &+ x_2 \left\{\alpha_2(-1 + p_1(x_1)) - \tfrac{(x_1-(S^0-\lambda))}{x_1} p_1(x_1)\right\} \qquad (2.7) \\ &- \alpha_2 x_3 \, . \end{aligned}$$

The first term in (2.7) is always non-positive for $0 < S < S^0$ and is zero for $S \in [0, S^0]$ if and only if $S = \lambda$ or $x_1 = 0$. By Lemma 2.10, we can choose $\alpha_2 > 0$ such that the second term in (2.7) is always non-positive and equal to zero if and only if $x_2 = 0$. Similarly, since solutions are positive and bounded and $\alpha_2 > 0$, the third term in (2.7) is non-positive and equal to zero if and only if $x_3 = 0$. By the Modified LaSalle Extension Theorem 2.9 every bounded solution of (2.3) is contained in $\mathcal{G}$, and thus by Lemma 2.7 every solution of (2.3), approaches the set $\mathcal{M}$, the largest invariant subset of

$\mathcal{E} = \{(S, x_1, x_2, x_3) \in \overline{\mathcal{G}} : \dot{V}\ (S, x_1, x_2, x_3) = 0\}$. The set $\mathcal{M}$ consists of points of the form $(S, 0, 0, 0)$ for $S \in [0, S^0]$, and $(\lambda, x_1, 0, 0)$ for $x_1 \in [0, \infty)$.

First, consider points of the form $(S, 0, 0, 0)$ for $S \in [0, S^0)$. If any such point is in the omega limit set of any solution initiating in $int\mathbf{R}^4_+$, then since the entire trajectory through any point in Ω must lie in Ω, this would imply that Ω is not compact, a contradiction. If $S = S^0$, then $E^0 = (S^0, 0, 0, 0)$ is a saddle fixed point whose stable manifold does not intersect $int\mathbf{R}^4_+$. This implies that $\Omega \neq \{E^0\}$ and hence some other point of $\mathcal{E}$ must lie in Ω. Next, consider points of the form $(\lambda, x_1, 0, 0)$ for $x_1 > 0$ since if $x_1 = 0$ we are back in the previous case. If any such point with $x_1 > 0$ is in the omega limit set, Ω, of any solution initiating in $int\mathbf{R}^4_+$, then $E_\lambda \in \Omega$ since E_λ is globally asymptotically stable on the subspace $\{(S, x_1, 0, 0) : S \geq 0\ , x_1 > 0\}$. However, E_λ is locally asymptotically stable with respect to $\mathbf{R}^4_+$ and hence if $E_\lambda \in \Omega$ then $\Omega = \{E_\lambda\}$. Since E_λ is the only possible point in Ω, and Ω is nonempty, then $\Omega = \{E_\lambda\}$ and E_λ is globally asymptotically stable with respect to $int\mathbf{R}^4_+$. □

Theorems 2.6 and 2.11 illustrate that there is an orderly transfer of global stability from one fixed point, E_0, to another fixed point, E_λ, as the parameter S^0 increases through the value λ. When $S^0 = \lambda + \delta_1$, E_λ and $E_{S^\bullet}$ coalesce. Simultaneously, as S^0 increases past $\lambda + \delta_1$, we have $E_{S^\bullet}$ entering the nonnegative cone and E_λ becoming unstable. For general monotone response functions, the global stability description of $E_{S^\bullet}$ is at best difficult. As a result, in the following chapter we consider three specific cases of the model given by (2.3). In the first case we will consider, all three response functions will be assumed to be of Lotka-Volterra form. In case two, $h(S)$ and $p_1(x_1)$ will be Lotka-Volterra and $p_2(x_2)$ is Michaelis-Menten. In case three, $h(S)$ is Lotka-Volterra and $p_i(x_i)$, $i = 1, 2$, are Michaelis-Menten.

Chapter 3

Dynamical Effects of Different Prototype Response Functions

In this chapter we consider three different scenarios of model (2.3), each described by a different combination of prototype response functions. In the first scenario all response functions are of Lotka-Volterra type. That is, $h(S) = S/\lambda$ and $p_i(x_i) = x_i/\delta_i$ for $i = 1, 2$. We will refer to this case as the linear response functions case. In the second case, $h(S)$ and $p_1(x_1)$ are linear uptake functions and $p_2(x_2) = m_2 x_2/(\delta_2(m_2 - 1) + x_2)$ is a Michaelis-Menten uptake function. We will refer to this case as the one Michaelis-Menten response function case. Lastly we consider the scenario when $h(S)$ is linear and $p_i(x_i)$ $(i = 1, 2)$ are both Michaelis-Menten response functions. This case will be referred to as the two Michaelis-Menten response functions case. By considering these three cases we hope to extend the stability description of the chemostat model in (2.3). Specifically, we want to consider the dynamics of the model when $S^0 > \lambda + \delta_1$.

3.1 Case 1: Linear Response Functions

For this particular choice of functional responses, system (2.3) becomes

$$\begin{aligned} S' &= S^0 - S - x_1\tfrac{S}{\lambda}\,, \\ x_1' &= x_1(-1+\tfrac{S}{\lambda}) - x_2\tfrac{x_1}{\delta_1}\,, \\ x_2' &= x_2(-1+\tfrac{x_1}{\delta_1}) - x_3\tfrac{x_2}{\delta_2}\,, \\ x_3' &= x_3(-1+\tfrac{x_2}{\delta_2})\,. \end{aligned} \tag{3.1}$$

We begin by examining the local stability of the fixed point $E_{S^*} = (S^*, \delta_1, x_2^*, 0)$, where $S^* = \lambda S^0/(\lambda+\delta_1)$ and $x_2^* = \delta_1(S^0-\lambda-\delta_1)/(\lambda+\delta_1)$. When $S^0 = \lambda+\delta_1$, E_λ and E_{S^*} coalesce. E_λ loses stability via a transcritical bifurcation as S^0 increases past $\lambda+\delta_1$. At the same time E_{S^*} enters the nonnegative cone $\mathbf{R}^4_+$. The Jacobian of (3.1) evaluated at $E_{S^*} = (S^*, \delta_1, x_2^*, 0)$ is

$$\begin{pmatrix} -1-\frac{\delta_1}{\lambda} & -\frac{S^*}{\lambda} & 0 & 0 \\ \frac{\delta_1}{\lambda} & -1+\frac{S^*}{\lambda}-\frac{x_2^*}{\delta_1} & -1 & 0 \\ 0 & \frac{x_2^*}{\delta_1} & 0 & -\frac{x_2^*}{\delta_2} \\ 0 & 0 & 0 & -1+\frac{x_2^*}{\delta_2} \end{pmatrix}$$

and the associated eigenvalues of E_{S^*} are

$$-1+\frac{x_2^*}{\delta_2},\ -1,\ \text{and}\ \frac{1}{2}\left\{-\frac{\delta_1}{\lambda} \pm \sqrt{\frac{\delta_1^2}{\lambda^2}-\frac{4}{\lambda}(S^0-\lambda-\delta_1)}\right\}.$$

Thus $E_{S^*} \in \mathbf{R}^4_+$ and is locally asymptotically stable provided

$$\lambda+\delta_1 < S^0 < (\lambda+\delta_1)(1+\frac{\delta_2}{\delta_1}).$$

In this instance, the local stability criterion is sufficient for global stability of E_{S^*} which is the content of the following theorem.

Theorem 3.1 *If* $\lambda+\delta_1 < S^0 < (\lambda+\delta_1)(1+\delta_2/\delta_1)$ *then* $E_{S^*} = (S^*, \delta_1, x_2^*, 0)$ *is globally asymptotically stable for system (3.1) with respect to* $int\mathbf{R}^4_+$.

Proof : Define a Liapunov function $V : int\mathbf{R}^4_+ \to \mathbf{R}$ by

$$\begin{aligned} V(S,x_1,x_2,x_3) &= S - S^* - S^*\ln(\tfrac{S}{S^*}) + x_1 - \delta_1 - \delta_1\ln(\tfrac{x_1}{\delta_1}) \\ &+ x_2 - x_2^* - x_2^*\ln(\tfrac{x_2}{x_2^*}) + x_3. \end{aligned}$$

The time derivative of $V(S,x_1,x_2,x_3)$ calculated along solutions of (3.1) is given by

$$\dot{V}\,(S,x_1,x_2,x_3) = (1-\frac{S^*}{S})S' + (1-\frac{\delta_1}{x_1})x_1' + (1-\frac{x_2^*}{x_2})x_2' + x_3'.$$

Substituting the equations for S', x_i' $(i = 1,2,3)$ into the above expression yields

$$\begin{aligned} \dot{V}\,(S,x_1,x_2,x_3) &= \tfrac{(S-S^*)}{S}(S^0 - S) + x_1(-1 + \tfrac{S^*}{\lambda}) - \delta_1(-1 + \tfrac{S}{\lambda} - \tfrac{x_2}{\delta_1}) \\ &- x_2^*(-1 + \tfrac{x_1}{\delta_1} - \tfrac{x_3}{\delta_2}) - x_2 - x_3 \\ &= \tfrac{(S-S^*)}{S}(S^0 - S) + x_1(-1 + \tfrac{S^*}{\lambda} - \tfrac{x_2^*}{\delta_1}) \\ &+ x_2^* - \delta_1(-1 + \tfrac{S}{\lambda}) + \tfrac{x_3}{\delta_2}(x_2^* - \delta_2). \end{aligned}$$

Replacing x_2^* with $\delta_1(S^0 - \lambda - \delta_1)/(\lambda + \delta_1)$ gives

$$\begin{aligned} \dot{V}\,(S,x_1,x_2,x_3) &= \tfrac{(S-S^*)}{S}(S^0 - S) + \tfrac{\delta_1}{\lambda}(S^* - S) + \tfrac{x_3}{\delta_2}(x_2^* - \delta_2) \\ &= -\tfrac{(\lambda+\delta_1)}{\lambda S}(S - S^*)^2 + \tfrac{x_3}{\delta_2}(x_2^* - \delta_2). \end{aligned} \tag{3.2}$$

The first term above is clearly non-positive. By the assumption that $S^0 < (\lambda + \delta_1)(1 + \delta_2/\delta_1)$, $x_2^* < \delta_2$ and thus the second term is also non-positive. Moreover,

$$\dot{V}\,(S,x_1,x_2,x_3) = 0 \Leftrightarrow S = S^* \text{ and } x_3 = 0.$$

Hence V is a Liapunov function for (3.1) with respect to $int\mathbf{R}^4_+$. Since all solutions of (3.1) are positive and bounded, then by the LaSalle Extension Theorem, every solution of (3.1) approaches $\mathcal{M}$, where $\mathcal{M}$ is the largest invariant subset of

$$\mathcal{E} = \{(S,x_1,x_2,x_3) \in int\mathbf{R}^4_+ : \dot{V}\,(S,x_1,x_2,x_3) = 0\}.$$

Since $S = S^* = S^0\lambda/(\lambda+\delta_1)$ then $S' = 0 = S^0 - S^* - x_1S^*/\lambda$ and hence $x_1 = \delta_1$. Similarly, since $x_1 = \delta_1$ then $x_1' = 0 = \delta_1(-1 + S^*/\lambda) - x_2$ and thus $x_2 = \delta_1(S^0-\lambda-\delta_1)/(\lambda+\delta_1) \equiv x_2^*$. Therefore, if $\lambda+\delta_1 < S^0 < (\lambda+\delta_1)(1+\delta_2/\delta_1)$ then $\mathcal{E} = \mathcal{M} = \{E_{S^*}\}$, and E_{S^*} is globally asymptotically stable with respect to $int\mathbf{R}^4_+$. □

For the linear functional response case there is a unique interior fixed point $E^\Delta = (S^\Delta, x_1^\Delta, \delta_2, x_3^\Delta)$ given by

$$\begin{aligned} S^\Delta &= \lambda(1+\tfrac{\delta_2}{\delta_1}) , \\ x_1^\Delta &= \tfrac{\delta_1 S^0}{\delta_1+\delta_2} - \lambda , \\ x_3^\Delta &= \tfrac{\delta_2 S^0}{\delta_1+\delta_2} - \delta_2(1+\tfrac{\lambda}{\delta_1}) . \end{aligned} \tag{3.3}$$

For $E^\Delta \in \mathbf{R}^4_+$ we require $x_1^\Delta, x_3^\Delta \geq 0$, in particular

$$\begin{aligned} x_1^\Delta \geq 0 &\Leftrightarrow S^0 \geq \lambda(1+\tfrac{\delta_2}{\delta_1}) , \\ x_3^\Delta \geq 0 &\Leftrightarrow S^0 \geq (\lambda+\delta_1)(1+\tfrac{\delta_2}{\delta_1}) . \end{aligned} \tag{3.4}$$

Therefore, $E^\Delta \in \mathbf{R}^4_+$ if and only if $S^0 \geq (\lambda+\delta_1)(1+\delta_2/\delta_1)$. The Jacobian of (3.1) evaluated at E^Δ is

$$\begin{pmatrix} -1-\frac{x_1^\Delta}{\lambda} & -\frac{S^\Delta}{\lambda} & 0 & 0 \\ \frac{x_1^\Delta}{\lambda} & 0 & -\frac{x_1^\Delta}{\delta_1} & 0 \\ 0 & \frac{\delta_2}{\delta_1} & 0 & -1 \\ 0 & 0 & \frac{x_3^\Delta}{\delta_2} & 0 \end{pmatrix}$$

and the associated characteristic equation is

$$r^4+r^3\{1+\frac{x_1^\Delta}{\lambda}\}+r^2\{\frac{x_1^\Delta\delta_2}{\delta_1^2}+\frac{x_3^\Delta}{\delta_2}+\frac{x_1^\Delta S^\Delta}{\lambda^2}\}+r\{(1+\frac{x_1^\Delta}{\lambda})(\frac{x_3^\Delta}{\delta_2}+\frac{x_1^\Delta\delta_2}{\delta_1^2})\}+\frac{x_1^\Delta x_3^\Delta S^\Delta}{\lambda^2\delta_2} = 0,$$

or equivalently,

$$(r+1)(r^3 + a_1r^2 + a_2r + a_3) = 0 \tag{3.5}$$

where

$$\begin{aligned} a_1 &= \tfrac{x_1^\Delta}{\lambda}\ , \\ a_2 &= \tfrac{x_1^\Delta}{\lambda\delta_1}(\lambda+\delta_1)(1+\tfrac{\delta_2}{\delta_1}) - (\tfrac{x_1^\Delta}{\lambda}+1)\ , \\ a_3 &= \tfrac{x_1^\Delta x_3^\Delta}{\lambda\delta_2}(1+\tfrac{\delta_2}{\delta_1})\ . \end{aligned}$$

By the Routh-Hurwitz criterion ([15]), for all the roots of (3.5) to have negative real parts we require $a_1, a_3 > 0$ and $a_1a_2 - a_3 > 0$. Clearly $a_1, a_3 > 0$ and

$$\begin{aligned} a_1a_2 - a_3 &= \tfrac{x_1^\Delta}{\lambda}\left\{\tfrac{x_1^\Delta}{\lambda\delta_1}(1+\tfrac{\delta_2}{\delta_1})(\lambda+\delta_1) - (\tfrac{x_1^\Delta}{\lambda}+1) - \tfrac{x_3^\Delta}{\delta_2}(1+\tfrac{\delta_2}{\delta_1})\right\} \\ &= \tfrac{x_1^\Delta\delta_2}{\lambda\delta_1}(\tfrac{x_1^\Delta}{\lambda}+1) > 0\ . \end{aligned}$$

Hence when $E^\Delta \in \mathbf{R}^4_+$, it is locally asymptotically stable.

When $S^0 = (\lambda+\delta_1)(1+\delta_2/\delta_1)$, $E_{S^\bullet}$ and E^Δ coalesce. As S^0 increases past $(\lambda+\delta_1)(1+\delta_2/\delta_1)$, $E_{S^\bullet}$ becomes unstable and simultaneously E^Δ enters $int\mathbf{R}^4_+$ and is locally asymptotically stable. The exchange of stability occurs via a transcritical bifurcation. As was the case for $E_{S^\bullet}$, in this case the local asymptotic stablity of E^Δ is enough to ensure that it is globally asymptotically stable.

Theorem 3.2 *If* $S^0 > (\lambda+\delta_1)(1+\delta_2/\delta_1)$ *then* $E^\Delta = (S^\Delta, x_1^\Delta, \delta_2, x_3^\Delta)$ *is globally asymptotically stable for system (3.1) with respect to* $int\mathbf{R}^4_+$.

Proof : Define a Liapunov function $V : int\mathbf{R}^4_+ \to \mathbf{R}$ by

$$\begin{aligned} V(S,x_1,x_2,x_3) &= S - S^\Delta - S^\Delta\ln(\tfrac{S}{S^\Delta}) + x_1 - x_1^\Delta - x_1^\Delta\ln(\tfrac{x_1}{x_1^\Delta}) \\ &+ x_2 - \delta_2 - \delta_2\ln(\tfrac{x_2}{\delta_2}) + x_3 - x_3^\Delta - x_3^\Delta\ln(\tfrac{x_3}{x_3^\Delta}). \end{aligned}$$

The time derivative of $V(S,x_1,x_2,x_3)$ calculated along solutions of (3.1) is given by

$$\dot{V}\ (S,x_1,x_2,x_3) = (1-\frac{S^\Delta}{S})S' + (1-\frac{x_1^\Delta}{x_1})x_1' + (1-\frac{\delta_2}{x_2})x_2' + (1-\frac{x_3^\Delta}{x_3})x_3'.$$

Substituting the equations for S', x_i' $(i = 1,2,3)$ into the above expression yields

$$\begin{aligned}
\dot{V}(S,x_1,x_2,x_3) &= (S^0 - S)\tfrac{(S-S^\Delta)}{S} + x_1\left\{\tfrac{S^\Delta}{\lambda} - \tfrac{\delta_2}{\delta_1} - 1\right\} \\
&+ x_2\left\{\tfrac{x_1^\Delta}{\delta_1} - \tfrac{x_3^\Delta}{\delta_2} - 1\right\} - x_1^\Delta(-1 + \tfrac{S}{\lambda}) + \delta_2 + x_3^\Delta \\
&= (S^0 - S)\tfrac{(S-S^\Delta)}{S} + x_1^\Delta\left\{\tfrac{\delta_2}{\delta_1} + 1 - \tfrac{S}{\lambda}\right\} \\
&= (S - S^\Delta)\left\{\tfrac{S^0-S}{S} - \tfrac{x_1^\Delta}{\lambda}\right\}.
\end{aligned}$$

Replacing x_1^Δ with $-\lambda + (\delta_1 S^0)/(\delta_1 + \delta_2)$ gives

$$\begin{aligned}
\dot{V}(S,x_1,x_2,x_3) &= (S - S^\Delta)\left\{\tfrac{S^0}{S} - \tfrac{\delta_1 S^0}{\lambda(\delta_1+\delta_2)}\right\} \\
&= -\tfrac{S^0}{SS^\Delta}(S - S^\Delta)^2.
\end{aligned} \tag{3.6}$$

Clearly (3.6) is non-positive and equal to zero if and only if $S = S^\Delta$. Hence V is a Liapunov function for (3.1) with respect to $int\mathbf{R}^4_+$. Since all solutions of (3.1) are positive and bounded, then by the LaSalle Extension Theorem, every solution of (3.1) approaches $\mathcal{M}$, where $\mathcal{M}$ is the largest invariant subset of

$$\mathcal{E} = \{(S,x_1,x_2,x_3) \in int\mathbf{R}^4_+ : \dot{V}(S,x_1,x_2,x_3) = 0\}.$$

Since $S = S^\Delta = \lambda(1 + \delta_2/\delta_1)$ then $S' = 0 = S^0 - S^\Delta - x_1 S^\Delta/\lambda$ and hence $x_1 \equiv x_1^\Delta = -\lambda + (\delta_1 S^0)/(\delta_1 + \delta_2)$. Similarly, since $x_1 = x_1^\Delta$ then $x_1' = 0 = x_1^\Delta(-1 + S^\Delta/\lambda) - x_2 x_1^\Delta/\delta_1$ and thus $x_2 = \delta_2$. Finally, since $x_2 = \delta_2$ then $x_2' = 0 = \delta_2(-1 + x_1^\Delta/\delta_1) - x_3$ and hence $x_3 \equiv x_3^\Delta = -\delta_2(1+\lambda/\delta_1) + (\delta_2 S^0)/(\delta_1+\delta_2)$. Therefore, if $S^0 > (\lambda+\delta_1)(1+\delta_2/\delta_1)$ then $\mathcal{E} = \mathcal{M} = \{E^\Delta\}$, and E^Δ is globally asymptotically stable with respect to $int\mathbf{R}^4_+$. □

In light of Theorems 3.1 and 3.2, the food chain in (3.1) cannot exhibit any complex behavior such as limit cycle stability. The food chain in (3.1) is characterized by an orderly transfer of global stability from one fixed point to another via transcritical bifurcations. At each stage of this transfer, conditions become sufficient such that a new population survives.

3.2 Case 2: One Michaelis-Menten Response Function

For this particular choice of functional responses, system (2.3) becomes

$$\begin{aligned} S' &= S^0 - S - x_1\tfrac{S}{\lambda}\ , \\ x_1' &= x_1(-1+\tfrac{S}{\lambda}) - x_2\tfrac{x_1}{\delta_1}\ , \\ x_2' &= x_2(-1+\tfrac{x_1}{\delta_1}) - x_3\tfrac{m_2x_2}{\delta_2(m_2-1)+x_2}\ , \\ x_3' &= x_3(-1+\tfrac{m_2x_2}{\delta_2(m_2-1)+x_2})\ , \end{aligned} \tag{3.7}$$

where $m_2 > 1$. The local stability description of $E_{S^*} = (S^*, \delta_1, x_2^*, 0)$, where $S^* = \lambda S^0/(\lambda+\delta_1)$ and $x_2^* = \delta_1(S^0-\lambda-\delta_1)/(\lambda+\delta_1)$, is similar to case 1. E_λ and E_{S^*} coalesce when $S^0 = \lambda+\delta_1$ and E_λ loses stability via a transcritical bifurcation as S^0 increases past $\lambda+\delta_1$. At the same time E_{S^*} enters the nonnegative cone $\mathbf{R}^4_+$. For this case the associated eigenvalues of E_{S^*} are

$$-1+\frac{m_2x_2^*}{\delta_2(m_2-1)+x_2^*},\ -1,\ \text{and}\ \frac{1}{2}\left\{-\frac{\delta_1}{\lambda} \pm \sqrt{\frac{\delta_1^2}{\lambda^2}-\frac{4}{\lambda}(S^0-\lambda-\delta_1)}\right\}$$

and hence $E_{S^*} \in \mathbf{R}^4_+$ (i.e. $S^0 > \lambda+\delta_1$) and is locally asymptotically stable (i.e. $x_2^* < \delta_2$) provided

$$\lambda+\delta_1 < S^0 < (\lambda+\delta_1)(1+\frac{\delta_2}{\delta_1})\ .$$

Theorem 3.3 *If $\lambda+\delta_1 < S^0 < (\lambda+\delta_1)(1+\delta_2/\delta_1)$, then $E_{S^*} = (S^*, \delta_1, x_2^*, 0)$ is globally asymptotically stable for system (3.7) with respect to $int\mathbf{R}^4_+$.*

Proof : Define a Liapunov function $V : int\mathbf{R}^4_+ \to \mathbf{R}$ by

$$\begin{aligned} V(S,x_1,x_2,x_3) &= S - S^* - S^*\ln(\tfrac{S}{S^*}) + x_1 - \delta_1 - \delta_1\ln(\tfrac{x_1}{\delta_1}) \\ &+ x_2 - x_2^* - x_2^*\ln(\tfrac{x_2}{x_2^*}) + \alpha x_3 \end{aligned}$$

where $\alpha > 0$ is a scalar. The time derivative of $V(S, x_1, x_2, x_3)$ calculated along solutions of (3.7) is given by

$$\dot{V}(S, x_1, x_2, x_3) = (1 - \frac{S^*}{S})S' + (1 - \frac{\delta_1}{x_1})x_1' + (1 - \frac{x_2^*}{x_2})x_2' + \alpha x_3'.$$

Substituting the equations for S', x_i' $(i = 1, 2, 3)$ into the above expression yields

$$\begin{aligned} \dot{V}(S, x_1, x_2, x_3) &= \tfrac{(S-S^*)}{S}(S^0 - S) + x_1\left\{-1 + \tfrac{S^*}{\lambda} - \tfrac{x_2^*}{\delta_1}\right\} + x_2^* - \delta_1(-1 + \tfrac{S}{\lambda}) \\ &+ x_3\left\{\alpha(-1 + p_2(x_2)) - \tfrac{(x_2 - x_2^*)}{x_2}p_2(x_2)\right\} \end{aligned}$$

where $p_2(x_2) = m_2 x_2/(\delta_2(m_2 - 1) + x_2)$. Replacing x_2^* with $\delta_1(S^0 - \lambda - \delta_1)/(\lambda + \delta_1)$ gives

$$\begin{aligned} \dot{V}(S, x_1, x_2, x_3) &= \tfrac{(S-S^*)}{S}(S^0 - S) + \tfrac{\delta_1}{\lambda}(S^* - S) \\ &+ x_3\left\{\alpha(-1 + p_2(x_2)) - \tfrac{(x_2 - x_2^*)}{x_2}p_2(x_2)\right\} \\ &= -\tfrac{(\lambda+\delta_1)}{\lambda S}(S - S^*)^2 \\ &+ x_3\left\{\alpha(-1 + p_2(x_2)) - \tfrac{(x_2 - x_2^*)}{x_2}p_2(x_2)\right\}. \end{aligned} \tag{3.8}$$

For $x_2 \in [0, \delta_2) \cup (\delta_2, \infty)$ define

$$g(x_2) = \frac{(x_2 - x_2^*)p_2(x_2)}{x_2(-1 + p_2(x_2))} = \frac{m_2(x_2 - x_2^*)}{(m_2 - 1)(x_2 - \delta_2)}.$$

Differentiating with respect to x_2 we obtain

$$g'(x_2) = \frac{m_2(x_2^* - \delta_2)}{(m_2 - 1)(x_2 - \delta_2)^2} < 0 \text{ for } x_2 \in (0, \delta_2) \cup (\delta_2, \infty),$$

and thus

$$\max_{0 < x_2 < \delta_2} g(x_2) = g(0) = \frac{m_2 x_2^*}{(m_2 - 1)\delta_2} > 0$$

and

$$\min_{\delta_2 < x_2 < \infty} g(x_2) = \lim_{x_2 \to \infty} g(x_2) = \frac{m_2}{m_2 - 1} > 0.$$

Since by assumption $x_2^* < \delta_2$, there exists a scalar $\alpha > 0$ such that

$$\max_{0<x_2<\delta_2} g(x_2) < \alpha < \min_{\delta_2<x_2<\infty} g(x_2) \, . \tag{3.9}$$

The first term in (3.8) is clearly non-positive and by (3.9) above, the second term in (3.8) is also non-positive. Moreover,

$$\dot{V}\,(S, x_1, x_2, x_3) = 0 \Leftrightarrow S = S^* \text{ and } x_3 = 0.$$

Hence V is a Liapunov function for (3.7) with respect to $int\mathbf{R}_+^4$. Since all solutions of (3.7) are positive and bounded, then by the LaSalle Extension Theorem, every solution of (3.7) approaches $\mathcal{M}$, where $\mathcal{M}$ is the largest invariant subset of

$$\mathcal{E} = \{(S, x_1, x_2, x_3) \in int\mathbf{R}_+^4 : \dot{V}\,(S, x_1, x_2, x_3) = 0\}.$$

Since $S = S^* = S^0\lambda/(\lambda + \delta_1)$, then $S' = 0 = S^0 - S^* - x_1 S^*/\lambda$ and hence $x_1 = \delta_1$. Similarly, since $x_1 = \delta_1$, then $x_1' = 0 = \delta_1(-1 + S^*/\lambda) - x_2$ and thus $x_2 = \delta_1(S^0 - \lambda - \delta_1)/(\lambda + \delta_1) \equiv x_2^*$. Therefore, if $\lambda + \delta_1 < S^0 < (\lambda + \delta_1)(1 + \delta_2/\delta_1)$, then $\mathcal{E} = \mathcal{M} = \{E_{S^*}\}$, and E_{S^*} is globally asymptotically stable with respect to $int\mathbf{R}_+^4$. □

As was the case for the linear functional response model (3.1), system (3.7) has a unique interior fixed point $E^\Delta = (S^\Delta, x_1^\Delta, \delta_2, x_3^\Delta)$ where S^Δ, x_1^Δ and x_3^Δ are given by (3.3). Similarly, $E^\Delta \in \mathbf{R}_+^4$ if and only if $x_3^\Delta \geq 0$ (i.e. $S^0 \geq (\lambda + \delta_1)(1 + \delta_2/\delta_1)$). The Jacobian of (3.7) evaluated at E^Δ is

$$\begin{pmatrix} -1 - \frac{x_1^\Delta}{\lambda} & \frac{S^\Delta}{\lambda} & 0 & 0 \\ \frac{x_1^\Delta}{\lambda} & 0 & -\frac{x_1^\Delta}{\delta_1} & 0 \\ 0 & \frac{\delta_2}{\delta_1} & \frac{x_3^\Delta}{\delta_2 m_2} & -1 \\ 0 & 0 & \frac{x_3^\Delta(m_2-1)}{\delta_2 m_2} & 0 \end{pmatrix}$$

and the associated characteristic equation is

$$r^4 + r^3\left\{1 + \frac{x_1^\Delta}{\lambda} - \frac{x_3^\Delta}{\delta_2 m_2}\right\} + r^2\left\{\frac{x_3^\Delta(m_2-1)}{\delta_2 m_2} + \frac{x_1^\Delta \delta_2}{\delta_1^2} + \frac{x_1^\Delta S^\Delta}{\lambda^2} - \frac{x_3^\Delta}{\delta_2 m_2}(1 + \frac{x_1^\Delta}{\lambda})\right\}$$
$$+r\left\{(1 + \frac{x_1^\Delta}{\lambda})\left(\frac{x_3^\Delta(m_2-1)}{\delta_2 m_2} + \frac{x_1^\Delta \delta_2}{\delta_1^2}\right) - \frac{x_1^\Delta x_3^\Delta S^\Delta}{\lambda^2 \delta_2 m_2}\right\} + \frac{x_1^\Delta x_3^\Delta S^\Delta(m_2-1)}{\lambda^2 m_2} = 0$$

or equivalently,

$$(r+1)(r^3 + b_1 r^2 + b_2 r + b_3) = 0 \tag{3.10}$$

where

$$\begin{aligned} b_1 &= \frac{x_1^\Delta}{\lambda} - \frac{x_3^\Delta}{\delta_2 m_2}\,, \\ b_2 &= \frac{x_3^\Delta}{\delta_2 m_2}\left\{(m_2 - 1) - \frac{x_1^\Delta}{\lambda}\right\} + \frac{x_1^\Delta \delta_2}{\delta_1}(\frac{1}{\lambda} + \frac{1}{\delta_1})\,, \\ b_3 &= \frac{x_1^\Delta x_3^\Delta S^\Delta(m_2-1)}{\lambda^2 m_2}(1 + \frac{\delta_2}{\delta_1})\,. \end{aligned}$$

By the Routh-Hurwitz criterion, for all the roots of (3.10) to have negative real parts we require $b_1, b_3 > 0$ and $b_1 b_2 - b_3 > 0$ (note that this implies $b_2 > 0$). When $S^0 = (\lambda + \delta_1)(1 + \delta_2/\delta_1)$, E_{S^*} and E^Δ coalesce. As S^0 increases past $(\lambda + \delta_1)(1 + \delta_2/\delta_1)$, E_{S^*} becomes unstable and simultaneously E^Δ enters $int\mathbf{R}_+^4$ and is at least initially locally asymptotically stable. Clearly $b_3 > 0$, since $m_2 > 1$. Also $b_1 > 0$ since

$$0 < (-1 + \frac{\delta_1}{\lambda})\frac{S^0}{\delta_1 + \delta_2} + \frac{\lambda}{\delta_1} = \frac{x_1^\Delta}{\lambda} - \frac{x_3^\Delta}{\delta_2} < b_1 < \frac{x_1^\Delta}{\lambda}\,.$$

However, the sign of $b_1 b_2 - b_3$ is unknown. In fact, it appears that $b_1 b_2 - b_3$ can change sign, which implies that E^Δ can undergo a Hopf bifurcation.

Example 1 : Let $S^0 = 3.45$, $\lambda = \delta_1 = 0.9$ and $\delta_2 = 0.3$. The interior fixed point is $E^\Delta = (1.2, 1.6875, 0.3, 0.2625)$ and the associated characteristic equation (3.10) becomes

$$(r+1)\left\{r^3 + r^2\left(1.875 - \frac{0.875}{m_2}\right) + r\left(2.125 - \frac{2.5156}{m_2}\right) + 2.1875\left(\frac{m_2 - 1}{m_2}\right)\right\} = 0\,.$$

Let $m_2 \in [1.2, 2]$. From Figure 3.1 we see that on the interval $[1.2, 2]$, b_2 as a function of m_2 is a positive increasing function. In addition, there is a unique

value $m_2 = m_2^* \approx 1.74$ such that $b_1b_2 - b_3 = 0$ on $[1.2, 2]$. Thus for $m_2 \in [1.2, 2]$, we have $b_i > 0$ and

$$\begin{aligned} b_1b_2 - b_3 &< 0 \text{ on } [1.2, m_2^*) \ , \\ b_1b_2 - b_3 &> 0 \text{ on } (m_2^*, 2] \ . \end{aligned}$$

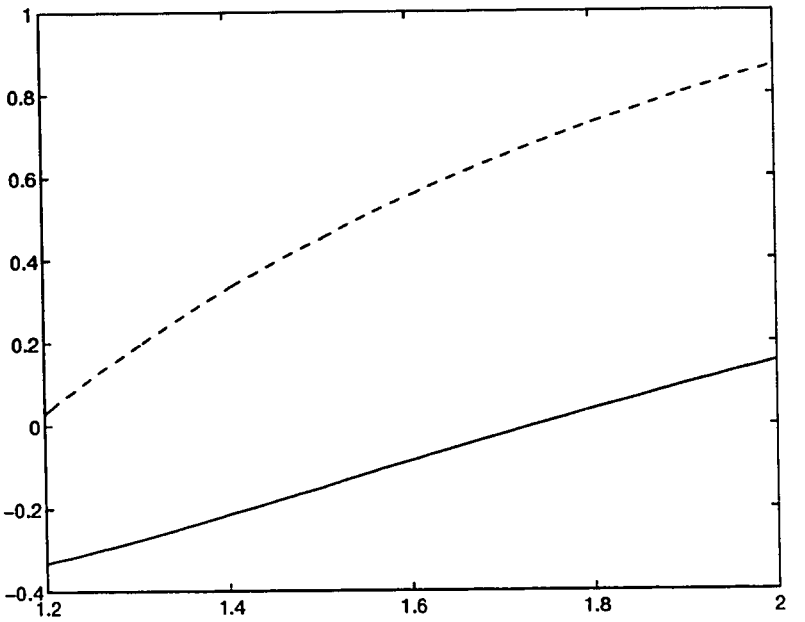

Figure 3.1 : Plot of $b_1b_2 - b_3$ and b_2 vs. m_2. b_2 is the dashed curve and $b_1b_2 - b_3$ is the solid curve.

In general, for $b_i > 0$ $(i = 1, 2, 3)$ and $b_1b_2 - b_3 = 0$ we have a pair of pure imaginary roots. This can easily be verified by substituting $r = \pm iw$ $(w > 0)$ into $r^3 + b_1r^2 + b_2r + b_3 = 0$ with $b_i > 0$. In particular, for $m_2 = m_2^*$ we have the pair of pure imaginary roots $r = \pm 0.235i$. For m_2 slightly greater than m_2^*, E^Δ is locally asymptotically stable. As m_2 becomes less than m_2^*, E^Δ seems to lose stability via a supercritical Hopf bifurcation. Figure 3.2 depicts sustained oscillations in $int\mathbf{R}_+^4$ for $m_2 = 1.475$.

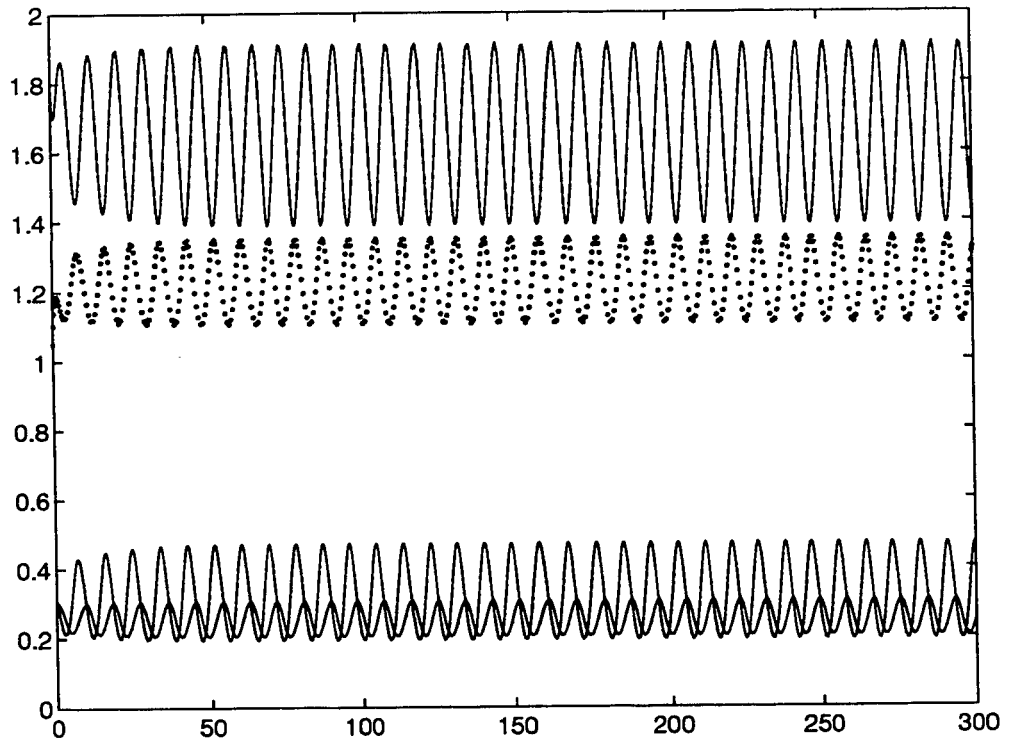

Figure 3.2 : Sustained oscillations for the chemostat model in (3.7) with $m_2 = 1.475$. The plots in order (top to bottom) are $x_1(t)$, $S(t)$, $x_2(t)$ and $x_3(t)$ vs. t.

The presence of an interior Hopf bifurcation makes it difficult to determine conditions that ensure the global stability of E^{Δ}. Unlike the linear response functions case, here the condition $S^0 > (\lambda + \delta_1)(1 + \delta_2/\delta_1)$ is not sufficient for global stability of E^{Δ}. However, under the condition $S^0 > (\lambda + \delta_1)(1 + \delta_2/\delta_1)$ we still can describe the global behavior of solutions in terms of coexistence of the species x_i. This is the subject of the following subsection.

3.2.1 Persistence of System (3.7)

We begin with the definition of persistence as given in [5] and [6], and the statement of the Butler-McGehee Lemma (whose proof may be found in Freedman and Waltman [12]). This Lemma will be used extensively to prove our results.

Definition 3.4 *Let* $\mathbf{x}' = \mathbf{f}(\mathbf{x}(t))$ *be a system of differential equations, where* $\mathbf{f}$ *is a continuous vector valued function in* $\mathbf{x} = (x_1, ..., x_n) \in \mathbf{R}^n$.
(i) The system of differential equations is weakly persistent if all solutions with $x_i(0) > 0$ *for* $i = 1, ..., n$ *satisfy*

$$\limsup_{t\to\infty} x_i(t) > 0 \text{ for } i = 1, ..., n.$$

(ii) The system of differential equations is persistent if all solutions with $x_i(0) > 0$ *for* $i = 1, ..., n$ *satisfy*

$$\liminf_{t\to\infty} x_i(t) > 0 \text{ for } i = 1, ..., n.$$

(iii) The system of differential equations is uniformly persistent if there exists $\varepsilon > 0$ *such that all solutions with* $x_i(0) > 0$ *for* $i = 1, ..., n$ *satisfy*

$$\liminf_{t\to\infty} x_i(t) \geq \varepsilon \text{ for } i = 1, ..., n.$$

Lemma 3.5 *Let* P *be an isolated hyperbolic critical point in the omega limit set* $\Omega(X)$ *of an orbit through* X *of a dynamical system. Then, either* $\Omega(X) = \{P\}$, *or there exist points* P^s *and* P^u, *satisfying* $P^s \in W^s(P)\backslash\{P\}$ *and* $P^u \in W^u(P)\backslash\{P\}$, *where* $W^s(P)$ *and* $W^u(P)$ *denote the stable and unstable manifolds of* P *respectively.*

Recall that in the linear response function case, the condition $S^0 > (\lambda + \delta_1)(1 + \delta_2/\delta_1)$ was necessary and sufficient to show that E^Δ was globally asymptotically stable with respect to solutions with positive initial conditions.

This is an example of persistence. Although the condition $S^0 > (\lambda + \delta_1)(1 + \delta_2/\delta_1)$ is not sufficient to prove an analog of Theorem 3.2 for system (3.7), it is however sufficient to show persistence of system (3.7).

Proposition 3.6 *Let $\gamma(t) = (S(t), x_1(t), x_2(t), x_3(t))$ be a solution of system (3.7). Then*

(i) $\liminf_{t\to\infty} S(t) > 0$,

(ii) if $\lambda < S^0$ *and* $x_{10} > 0$ *then* $\liminf_{t\to\infty} x_1(t) > 0$,

(iii) if $\lambda + \delta_1 < S^0$ *and* $x_{i0} > 0$ *for* $i = 1, 2$, *then* $\liminf_{t\to\infty} x_2(t) > 0$,

(iv) if $(\lambda + \delta_1)(1 + \delta_2/\delta_1) < S^0$ *and* $x_{i0} > 0$ *for* $i = 1, 2, 3$, *then* $\liminf_{t\to\infty} x_3(t) > 0$, *and hence system (3.7) is persistent.*

Proof : Let Ω denote the omega limit set of $\gamma(t)$. All solutions are positive and bounded, thus $\Omega \subset \mathbf{R}^4_+$ is a nonempty, compact, invariant set with respect to system (3.7).

(i) Since $x_1(t)$ is positive and bounded, then by (2.2) and (3.7), $S'(t) > 0$ if $S(t)$ is sufficiently close to zero. Hence, it follows that any point in Ω must satisfy $\liminf_{t\to\infty} S(t) > 0$.

(ii) Assume $\lambda < S^0$ and $x_{10} > 0$. Suppose $E_0 \in \Omega$. For $\lambda < S^0$, E_0 is an unstable hyperbolic fixed point with a three dimensional stable manifold

$$W^s(E_0) = \{(S, x_1, x_2, x_3) \in \mathbf{R}^4_+ : S, x_2, x_3 \geq 0 \text{ and } x_1 = 0\}.$$

From (3.7) and the proof of Theorem 2.5 it is clear that E_0 is globally asymptotically stable with respect to solutions initiating in its stable manifold. Since $\gamma(0) \notin W^s(E_0)$ then $\Omega \neq \{E_0\}$. Therefore, by Lemma 3.5, there exists $R^s \in (W^s(E_0)\backslash\{E_0\}) \cap \Omega$ and hence $cl\mathcal{O}(R^s) \subset \Omega$. But then, as $t \to -\infty$, either $\mathcal{O}(R^s)$ becomes unbounded or one of the components of the trajectory becomes negative. In either case we have a contradiction since the entire trajectory through any point in Ω must lie in Ω. Therefore $E_0 \notin \Omega$.

Next, suppose $\liminf_{t\to\infty} x_1(t) = 0$. Then there exists a point $R = (\overline{S}, 0, \overline{x}_2, \overline{x}_3) \in \Omega$, which implies that $cl\mathcal{O}(R) \subset \Omega$. By Proposition 2.2 and from the proof of Theorem 2.5 it follows that $\overline{x}_2(t), \overline{x}_3(t) \to 0$ and $\overline{S}(t) \to S^0$ as $t \to \infty$ and thus $E_0 \in \Omega$, which is a contradiction. Hence $\liminf_{t\to\infty} x_1(t) > 0$.

(iii) Assume $\lambda + \delta_1 < S^0$ and $x_{10}, x_{20} > 0$. By part *(ii)* we have $E_0 \notin \Omega$. Suppose $E_\lambda \in \Omega$. For $\lambda + \delta_1 < S^0$, E_λ is an unstable hyperbolic fixed point with a three dimensional stable manifold

$$W^s(E_\lambda) = \{(S, x_1, x_2, x_3) \in \mathbf{R}^4_+ : x_1 > 0 \text{ and } x_2 = 0\}.$$

From (3.7) and the proof of Theorem 2.5 it is clear that E_λ is globally asymptotically stable with respect to solutions initiating in its stable manifold. Since $x_{20} > 0$, $\gamma(0) \notin W^s(E_\lambda)$ and so $\Omega \neq \{E_\lambda\}$. Therefore, by Lemma 3.5, there exists $Q^s \in (W^s(E_\lambda) \backslash \{E_\lambda\}) \cap \Omega$ and hence $cl\mathcal{O}(Q^s) \subset \Omega$. But then, as $t \to -\infty$, either $cl\mathcal{O}(Q^s)$ becomes unbounded or leaves the positive cone or $E_0 \in cl\mathcal{O}(Q^s) \subset \Omega$. In any case, we have a contradiction, and thus $E_\lambda \notin \Omega$.

Next, suppose $\liminf_{t\to\infty} x_2(t) = 0$. From the proof of Theorem 2.5 it follows that $x_3(t) \to 0$ as $t \to \infty$. Thus, there exists a point $Q = (\overline{S}, \overline{x}_1, 0, 0) \in \Omega$, and hence $cl\mathcal{O}(Q) \subset \Omega$. On the subspace $\mathcal{T}_1 = \{(S, x_1, 0, 0) \in \mathbf{R}^4_+ : x_1 > 0\}$ system (3.7) reduces to

$$\begin{aligned} S'(t) &= S^0 - S(t) - x_1(t)h(S(t)) \\ x_1'(t) &= x_1(t)(-1 + h(S(t))) \end{aligned}$$

and thus E_λ is globally attracting with respect to all solutions initiating in $\mathcal{T}_1$. Therefore $E_\lambda \in cl\mathcal{O}(Q) \subset \Omega$, a contradiction. Thus $\liminf_{t\to\infty} x_2(t) > 0$.

(iv) Assume $(\lambda + \delta_1)(1 + \delta_2/\delta_1) < S^0$ and $x_{i0} > 0$ for $i = 1, 2, 3$. By parts *(ii)* and *(iii)* we have E_0, $E_\lambda \notin \Omega$. Suppose $E_{S^*} \in \Omega$. For $(\lambda + \delta_1)(1 + \delta_2/\delta_1) < S^0$, E_{S^*} is an unstable hyperbolic fixed point with a three dimensional stable

manifold

$$W^s(E_{S^\bullet}) = \{(S, x_1, x_2, x_3) \in \mathbf{R}^4_+ : x_1, x_2 > 0 \text{ and } x_3 = 0\}.$$

From (3.7), it is clear that $E_{S^\bullet}$ is globally asymptotically stable with respect to solutions initiating in its stable manifold. As before, since $x_{30} > 0$ then $\gamma(0) \notin W^s(E_{S^\bullet})$ and so $\Omega \neq \{E_{S^\bullet}\}$. Thus, by Lemma 3.5, there exists $P^s \in (W^s(E_{S^\bullet}) \backslash \{E_{S^\bullet}\}) \cap \Omega$ and hence $cl\mathcal{O}(P^s) \subset \Omega$. But then, as $t \to -\infty$, either $cl\mathcal{O}(P^s)$ becomes unbounded or leaves the positive cone or E_0 and/or $E_\lambda \in cl\mathcal{O}(P^s) \subset \Omega$. In any case, we have a contradiction and thus $E_{S^\bullet} \notin \Omega$.

Next, suppose $\liminf_{t\to\infty} x_3(t) = 0$. Then there exists a point $P = (\overline{S}, \overline{x}_1, \overline{x}_2, 0) \in \Omega$, which implies that $cl\mathcal{O}(P) \subset \Omega$. On the subspace $\mathcal{T}_2 = \{(S, x_1, x_2, 0) \in \mathbf{R}^4_+ : x_1, x_2 > 0\}$ system (3.7) reduces to

$$\begin{aligned} S'(t) &= S^0 - S(t) - x_1(t)h(S(t)) \\ x_1'(t) &= x_1(t)(-1 + h(S(t))) - x_2(t)p_1(x_1(t)) \\ x_2'(t) &= x_2(t)(-1 + p_1(x_1(t))) \end{aligned}$$

and thus $E_{S^\bullet}$ is globally attracting with respect to all solutions initiating in $\mathcal{T}_2$. Therefore $E_{S^\bullet} \in cl\mathcal{O}(P) \subset \Omega$, a contradiction. Thus $\liminf_{t\to\infty} x_3(t) > 0$. □

If a dynamical system is uniformly persistent, then there exists a compact attractor in the interior. For system (3.7), this would imply that all solutions eventually approach a compact invariant set in $int\mathbf{R}^4_+$. To show uniform persistence for system (3.7) we will utilize a theorem of Butler, Freedman and Waltman ([5]). Before we give a statement of this theorem we state a few preparatory definitions.

Definition 3.7 *Let $\mathcal{F}$ be a dynamical system on $\mathbf{R}^n_+$. Denote the boundary of $\mathbf{R}^n_+$ by $\partial\mathbf{R}^n_+$ and let $\partial\mathcal{F}$ denote the dynamical system $\mathcal{F}$ restricted to $\partial\mathbf{R}^n_+$.*

(i) The dynamical system $\mathcal{F}$ is said to be **dissipative** *if for each $\mathbf{x} \in \mathbf{R}^n_+$, the omega limit set of $\mathbf{x}$ is nonempty ($\Omega(\mathbf{x}) \neq \emptyset$) and $\Omega(\mathcal{F}) = \cup_{\mathbf{x} \in \mathbf{R}^n_+} \Omega(\mathbf{x})$ has compact closure.*

(ii) A nonempty subset $M \subset \mathbf{R}^n_+$, invariant with respect to $\mathcal{F}$, is said to be an **isolated invariant set** *if it is the maximal invariant set in some neighborhood of itself.*

(iii) $\partial\mathcal{F}$ is said to be **isolated** *if there exists a covering $\mathcal{M}$ of $\Omega(\partial\mathcal{F})$ of pairwise disjoint, compact, isolated invariant sets $M_1, ..., M_k$ for $\partial\mathcal{F}$ such that each M_i is also isolated for $\mathcal{F}$. $\mathcal{M}$ is then called an* **isolated covering**.

(iv) The **stable set** *$W^+(M)$ of an isolated invariant set M is defined to be $\{\mathbf{x} \in \mathbf{R}^n_+ : \Omega(\mathbf{x}) \neq \emptyset, \Omega(\mathbf{x}) \subset M\}$ and the* **unstable set** *$W^-(M)$ is defined to be $\{\mathbf{x} \in \mathbf{R}^n_+ : \alpha(\mathbf{x}) \neq \emptyset, \alpha(\mathbf{x}) \subset M\}$, where α denotes the alpha limit set.*

(v) Let M, N be isolated invariant sets (not necessarily distinct). We say that M is **chained** *to N, denoted $M \rightarrow N$, if there exists $\mathbf{x} \notin M \cup N$ such that $\mathbf{x} \in W^-(M) \cap W^+(N)$.*

(vi) A **chain** *of isolated invariant sets is a finite sequence $M_1, ..., M_k$, such that $M_1 \rightarrow M_2 \rightarrow .... \rightarrow M_k$. The chain is called a* **cycle** *if $M_k = M_1$.*

(vii) $\partial\mathcal{F}$ will be called **acyclic** *if there exists some isolated covering $\mathcal{M} = \cup_{i=1}^k M_i$ of $\Omega(\partial\mathcal{F})$ such that no subset of the $\{M_i\}$ forms a cycle.*

Remarks : (1) The property of $\partial\mathcal{F}$ being isolated is a hyperbolicity condition. It prevents fixed points (or other invariant sets such as periodic orbits) from accumulating on the boundary $\partial\mathbf{R}^n_+$.

(2) The definitions of $W^+(M)$ and $W^-(M)$ coincide with the definitions of local stable and unstable manifolds if M is a fixed point, periodic orbit, or in general if M is compact ([20], [40]).

(3) $\partial\mathcal{F}$ being acyclic prevents homoclinic and heteroclinic cycles from forming on the boundary $\partial\mathbf{R}^n_+$.

Theorem 3.8 *Let $\mathcal{F}$ be a continuous flow on a locally compact metric space E with boundary ∂E. Let $\partial\mathcal{F}$ be the restriction of $\mathcal{F}$ to ∂E. Assume that*

(i) $\mathcal{F}$ is dissipative,

(ii) $\mathcal{F}$ is weakly persistent,

(iii) $\partial\mathcal{F}$ is isolated,

(iv) $\partial\mathcal{F}$ is acyclic.

Then $\mathcal{F}$ is uniformly persistent.

The dynamical system given by (3.7) is not invariant on the boundary $\partial\mathbf{R}^4_+$. The $(x_1, x_2, x_3)-$face repels into $int\mathbf{R}^4_+$. However, Theorem 3.8 can be modified to apply to this situation ([44]). Let B denote the $(x_1, x_2, x_3)-$face and let $A = \partial\mathbf{R}^4_+ \backslash B$. Then $\partial\mathbf{R}^4_+ = A \cup B$ and $\mathcal{F}$, the associated flow of (3.7), is invariant on A. If $\partial\mathcal{F}_A$, the restriction of $\mathcal{F}$ to A, satisfies conditions (iii) and (iv) of Theorem 3.8, then $\mathcal{F}$ is uniformly persistent.

Condition (i) holds for system (3.7) by Proposition 2.2 and the remark that followed it. Condition (ii) holds since we have proved the stronger assertion of persistence in Proposition 3.6. By Theorems 2.6, 2.11, and 3.3, the only invariant sets on $\partial\mathbf{R}^4_+$ are the fixed points E_0, E_λ and $E_{S^\bullet}$. They are clearly isolated and thus form a trivial isolated covering of $\Omega(\partial\mathcal{F}_A)$. Hence $\partial\mathcal{F}_A$ is isolated. Moreover, since the transfers of global stability from E_0 to E_λ, and from E_λ to $E_{S^\bullet}$ are via transcritical bifurcations, we have the following chains on $\partial\mathbf{R}^4_+$:

$$E_0 \to E_\lambda,\ E_\lambda \to E_{S^\bullet} \text{ and } E_0 \to E_\lambda \to E_{S^\bullet}.$$

Thus no subset of $\{E_0, E_\lambda, E_{S^\bullet}\}$ forms a cycle, and $\partial\mathcal{F}_A$ is acyclic. Hence for $S^0 > (\lambda + \delta_1)(1 + \delta_2/\delta_1)$, system (3.7) is **uniformly persistent**.

3.3 Case 3: Two Michaelis-Menten Response Functions

For this choice of functional responses, system (2.3) becomes

$$\begin{aligned} S' &= S^0 - S - x_1\tfrac{S}{\lambda}\,, \\ x_1' &= x_1(-1+\tfrac{S}{\lambda}) - x_2\tfrac{m_1x_1}{\delta_1(m_1-1)+x_1}\,, \\ x_2' &= x_2(-1+\tfrac{m_1x_1}{\delta_1(m_1-1)+x_1}) - x_3\tfrac{m_2x_2}{\delta_2(m_2-1)+x_2}\,, \\ x_3' &= x_3(-1+\tfrac{m_2x_2}{\delta_2(m_2-1)+x_2})\,, \end{aligned} \tag{3.11}$$

with $m_i > 1$ for $i = 1, 2$. The food chain in (3.11) has five fixed points that may exist in the nonnegative cone, $\mathbf{R}^4_+$. They are E_0, E_λ, $E_{S^\bullet}$ and two interior fixed points given by

$$E_i^\Delta = (S_i^\Delta, x_{1i}^\Delta, \delta_2, x_{3i}^\Delta) \text{ for } i = 1, 2,$$

where

$$\begin{aligned} x_{1i}^\Delta &= \tfrac{-u+(-1)^{i+1}\sqrt{u^2-4v}}{2}\,, \\ x_{3i}^\Delta &= \delta_2(-1+\tfrac{m_1x_{1i}^\Delta}{\delta_1(m_1-1)+x_{1i}^\Delta})\,, \\ S_i^\Delta &= \tfrac{S^0\lambda}{x_{1i}^\Delta+\lambda}\,, \end{aligned} \tag{3.12}$$

with

$$\begin{aligned} u &= m_1(\delta_1+\delta_2) - S^0 - \delta_1 + \lambda\,, \\ v &= m_1\lambda(\delta_1+\delta_2) + \delta_1(S^0 - S^0m_1 - \lambda). \end{aligned}$$

The local stability description of $E_{S^\bullet} = (S^*, \delta_1, x_2^*, 0)$ is similar to the previous two cases. When $S^0 = \lambda + \delta_1$, E_λ and $E_{S^\bullet}$ coalesce and E_λ loses stability via a transcritical bifurcation as S^0 increases past $\lambda+\delta_1$. Simultaneously, $E_{S^\bullet}$ enters $\mathbf{R}^4_+$. The associated eigenvalues of $E_{S^\bullet}$ are

$$-1,\ -1+\frac{m_2x_2^*}{\delta_2(m_2-1)+x_2^*} \text{ and } \frac{1}{2}\left\{-\gamma \pm \sqrt{\gamma^2 - \frac{4(S^0-\lambda-\delta_1)(m_1-1)}{\lambda m_1}}\right\}\,,$$

where

$$\gamma = \frac{\delta_1}{\lambda} - \frac{S^0 - \lambda - \delta_1}{m_1(\lambda + \delta_1)}. \tag{3.13}$$

Thus $E_{S^*} \in int\mathbf{R}^4_+$ (i.e. $S^0 > \lambda + \delta_1$) and is locally asymptotically stable provided

$$\lambda + \delta_1 < S^0 < \begin{cases} (\lambda + \delta_1)(1 + \frac{\delta_2}{\delta_1}) \text{ i.e. } x_2^* < \delta_2, \\ \\ (\lambda + \delta_1)(1 + \frac{m_1\delta_1}{\lambda}) \text{ i.e. } \gamma > 0. \end{cases} \tag{3.14}$$

At this point, unfortunately, global stability information is not easily obtained. As a result, to facilitate the further analysis of system (3.11), we utilize the existence of the globally attracting simplex $\Im$ in Proposition 2.2 to reduce the dimension of the model by one. Using $S + \sum_{i=1}^3 x_i = S^0$, the four dimensional system in (3.11) can be written as the following three dimensional system

$$\begin{aligned} x_1' &= x_1(-1 + \tfrac{S^0 - x_1 - x_2 - x_3}{\lambda}) - x_2 \tfrac{m_1 x_1}{\delta_1(m_1 - 1) + x_1}, \\ x_2' &= x_2(-1 + \tfrac{m_1 x_1}{\delta_1(m_1 - 1) + x_1}) - x_3 \tfrac{m_2 x_2}{\delta_2(m_2 - 1) + x_2}, \\ x_3' &= x_3(-1 + \tfrac{m_2 x_2}{\delta_2(m_2 - 1) + x_2}). \end{aligned} \tag{3.15}$$

Notice that the omega limit sets of system (3.15) are also omega limit sets of the four dimensional system (3.11) (see [45] and the references therein). For system (3.15) the fixed point in the x_1x_2—plane, when it exists, will be denoted by $E^3_{S^*}$, and similarly the two interior fixed points will be denoted by E^{Δ}_{3i} for $i = 1, 2$. Denote the associated eigenvalues of $E^3_{S^*}$ by

$$r_{1,2} = \frac{1}{2}\left\{-\gamma \pm \sqrt{\gamma^2 - \frac{4(S^0 - \lambda - \delta_1)(m_1 - 1)}{\lambda m_1}}\right\} \text{ and}$$

$$r_3 = -1 + \frac{m_2 x_2^*}{\delta_2(m_2 - 1) + x_2^*},$$

where γ is given by (3.13).

First consider the pair of eigenvalues $r_{1,2}$. At $S^0 = (\lambda + \delta_1)(1 + \frac{m_1\delta_1}{\lambda})$ (i.e. $\gamma = 0$) we have a pair of complex eigenvalues with $\mathbf{Re}(r_{1,2}) = 0$ and $\mathbf{Im}(r_{1,2}) = \pm 1/\lambda\sqrt{(m_1 - 1)(\lambda + \delta_1)\delta_1} > 0$. Using S^0 as the bifurcation parameter we have

$$\mathbf{Re}(r_{1,2}(S^0)) = -\frac{\gamma}{2} ,$$

which implies

$$\frac{d}{dS^0}(\mathbf{Re}(r_{1,2}(S^0))) = \frac{1}{2m_1(\lambda + \delta_1)} \neq 0.$$

Thus $E^3_{S^\bullet}$ undergoes a Hopf bifurcation with critical bifurcation value $S^0 = (\lambda + \delta_1)(1 + \frac{m_1\delta_1}{\lambda})$. Figure 3.3 depicts a periodic orbit which emerged from a Hopf bifurcation about $E^3_{S^\bullet}$. The periodic orbit appears to be stable with respect to initial conditions $x_{10}, x_{20} > 0$ and $x_{30} = 0$.

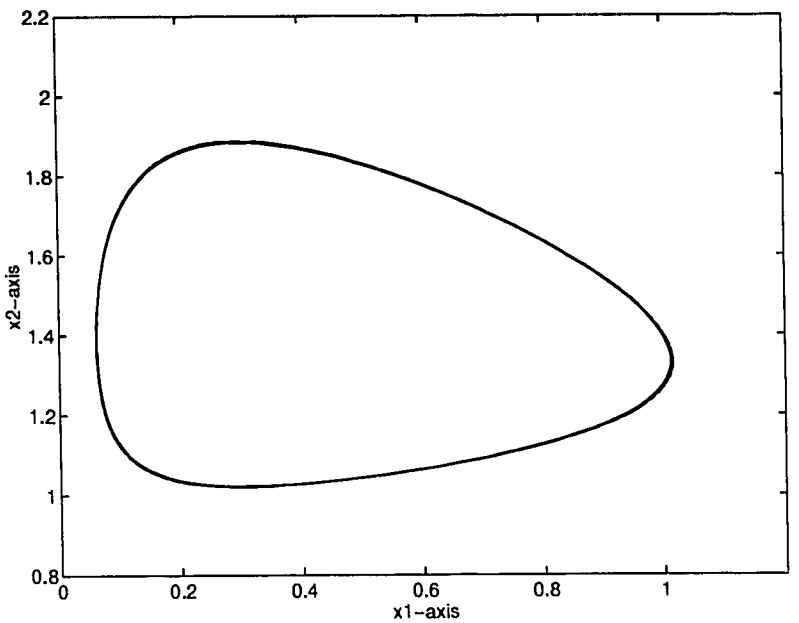

Figure 3.3 : A limit cycle in the x_1x_2−plane for $\lambda = 0.2$, $\delta_1 = 0.3$, $\delta_2 = 0.96$, $m_1 = 2.5$, $m_2 = 3.0$ and $S^0 = 3.0$. The limit cycle appears to be stable with respect to the x_1x_2-plane.

Next consider the real eigenvalue r_3. At $S^0 = (\lambda + \delta_1)(1 + \delta_2/\delta_1)$ (i.e. $x_2^* = \delta_2$) we have $r_3 = 0$ and $E^3_{S^\bullet} = (\delta_1, \delta_2, 0)$. Moreover, the interior fixed

points $E_{3i}^{\Delta} = (x_{1i}^{\Delta}, \delta_2, x_{3i}^{\Delta})$ are given by

$$x_{11}^{\Delta} = \delta_1 \qquad x_{12}^{\Delta} = \beta$$

and

$$x_{31}^{\Delta} = 0 \qquad x_{32}^{\Delta} = \delta_2(-1 + \tfrac{m_1\beta}{\delta_1(m_1-1)+\beta})$$

where $\beta = (\delta_1+\delta_2)\{\frac{\lambda}{\delta_1} - (m_1-1)\} - \lambda$. Hence at $S^0 = (\lambda+\delta_1)(1+\delta_2/\delta_1)$, $E_{S^*}^3$ and E_{31}^{Δ} coalesce. As S^0 increases past the critical value $(\lambda+\delta_1)(1+\delta_2/\delta_1)$, $E_{S^*}^3$ increases the dimension of its unstable manifold by one while simultaneously, E_{31}^{Δ} increases the dimension of its stable manifold by one. This exchange of stability occurs via a transcritical bifurcation. Whether E_{31}^{Δ} enters or exits the positive cone depends on the value of β. We examine this statement more carefully below.

From (3.12) it is clear that we may have none, one, or two fixed points E_{3i}^{Δ} in $int\mathbf{R}_+^3$, depending on the sign of u^2-4v, and u. Moreover, a saddle-node bifurcation involving the fixed points E_{3i}^{Δ} may occur.

Example 2: Let $\lambda = \delta_2 = 0.2$, $\delta_1 = 0.1$, $m_1 = 1.1$ and $m_2 = 2.0$. For $S^0 = 0.81$, the fixed points E_{3i}^{Δ} do not exist in $\mathbf{R}^3$. At approximately $S^0 = 0.818900967$ we have $E_{31}^{\Delta} = E_{32}^{\Delta} = (0.1945, 0.2, 0.0092)$ with associated eigenvalues $0.0371 \pm 0.3593i$ and 0. For $S^0 = 0.82$, we have two fixed points $E_{31}^{\Delta} = (0.21, 0.2, 0.01)$ and $E_{32}^{\Delta} = (0.18, 0.2, 0.0084)$. Hence the interior fixed points E_{3i}^{Δ} emerge through a saddle-node bifurcation.

For the parameter values given in Example 2, the Hopf bifurcation in the x_1x_2-plane occurs at $S^0 = 0.4650$ and the transcritical bifurcation in the x_1x_2-plane occurs at $S^0 = 0.9$. Notice that the saddle-node bifurcation in Example 2 occurs in $int\mathbf{R}_+^3$, and moreover it occurs after the planar Hopf bifurcation but prior to the planar transcritical bifurcation. This observation

is true in general for system (3.15). That is to say, **if** a saddle-node bifurcation occurs in $int\mathbf{R}^3_+$, then it occurs in the above order. This can be deduced from the following two observations.

First, consider what is required for both fixed points E^{Δ}_{3i} to exist simultaneously in $int\mathbf{R}^3_+$. From (3.12) we see that it is necessary that $x^{\Delta}_{11}, x^{\Delta}_{12} > \delta_1$. Thus we must have at least $u^2 - 4v > 0$ and $u < 0$, which implies $x^{\Delta}_{11} > x^{\Delta}_{12}$. If $x^{\Delta}_{12} > \delta_1$, then by simple algebraic manipulation we have $S^0 < (\lambda + \delta_1)(1 + \delta_2/\delta_1)$. As a result, if a saddle-node bifurcation of E^{Δ}_{3i} occurs in the positive cone, it must occur before the planar transcritical bifurcation. As S^0 increases past $(\lambda + \delta_1)(1 + \delta_2/\delta_1)$, one of E^{Δ}_{3i} exits the positive cone through the planar transcritical bifurcation. Conversely, if the saddle-node bifurcation of E^{Δ}_{3i} occurs outside the positive cone, then one of the fixed points E^{Δ}_{3i} enters the positive cone via the planar transcritical bifurcation.

Secondly, assume that a saddle-node bifurcation of E^{Δ}_{3i} occurs in $int\mathbf{R}^3_+$. For this to occur we require at least $u^2 - 4v = 0$ and $-u > 2\delta_1$. Note that $-u > 2\delta_1 \Leftrightarrow S^0 > (\lambda + \delta_1) + m_1(\delta_1 + \delta_2)$. If the saddle-node bifurcation in the positive cone is to occur before the planar Hopf bifurcation then we need

$$(\lambda + \delta_1) + m_1(\delta_1 + \delta_2) < S^0 < (\lambda + \delta_1)(1 + \frac{m_1\delta_1}{\lambda}) \Leftrightarrow \delta_2 < \frac{\delta_1^2}{\lambda}$$

however, this would imply

$$(\lambda + \delta_1)(1 + \frac{\delta_2}{\delta_1}) < (\lambda + \delta_1) + (\delta_1 + \delta_2) < (\lambda + \delta_1) + m_1(\delta_1 + \delta_2).$$

Hence if the saddle-node bifurcation in the positive cone occurs before the planar Hopf bifurcation, then it must also occur after the planar transcritical bifurcation. A contradiction.

In summary, system (3.15) can undergo both a Hopf and transcritical bifurcation about E_{S^*}. There is a saddle-node bifurcation of the fixed points

E_{3i}^{Δ} that may occur in the positive cone. This is not the complete local bifurcation description of system (3.15). In the following subsection we consider several numerical simulations of (3.15) that illustrate several other bifurcation phenomena of the model.

We conclude this section with a persistence result for model (3.11). Notice that the condition for persistence given in the proposition below is not a necessary and sufficient one, but simply a sufficient condition.

Proposition 3.9 *Let* $\gamma(t) = (S(t), x_1(t), x_2(t), x_3(t))$ *be a solution of system (3.11). Then*
(i) $\liminf_{t\to\infty} S(t) > 0$,
(ii) *if* $\lambda < S^0$ *and* $x_{10} > 0$ *then* $\liminf_{t\to\infty} x_1(t) > 0$,
(iii) *if* $\lambda + \delta_1 < S^0$ *and* $x_{i0} > 0$ *for* $i = 1, 2$, *then* $\liminf_{t\to\infty} x_2(t) > 0$,
(iv) *if* $(\lambda+\delta_1)(1+\delta_2/\delta_1) < S^0 < (\lambda+\delta_1)(1+m_1\delta_1/\lambda)$ *and* $x_{i0} > 0$ *for* $i = 1, 2, 3$, *then* $\liminf_{t\to\infty} x_3(t) > 0$, *and hence system (3.11) is uniformly persistent.*

Proof : (i) By an argument similar to that given in Proposition 3.6, it follows that any point in the omega limit set of $\gamma(t)$ must satisfy $\liminf_{t\to\infty} S(t) > 0$.

(ii) + (iii) Notice that in these two cases we may have $S^0 > (\lambda + \delta_1)(1 + m_1\delta_1/\lambda)$. If this is the case, then there exists a periodic orbit on the Sx_1x_2-face. However, the periodic orbit is not contained in the stable manifold of E_0 or E_λ. Hence, by an argument similar to that given in Proposition 3.6 it follows that $\liminf_{t\to\infty} x_1(t) > 0$ and $\liminf_{t\to\infty} x_2(t) > 0$.

(iv) Since $(\lambda+\delta_1)(1+\delta_2/\delta_1) < S^0 < (\lambda+\delta_1)(1+m_1\delta_1/\lambda)$, then again by an argument similar to that given in Proposition 3.6, we have $\liminf_{t\to\infty} x_3(t) > 0$. □

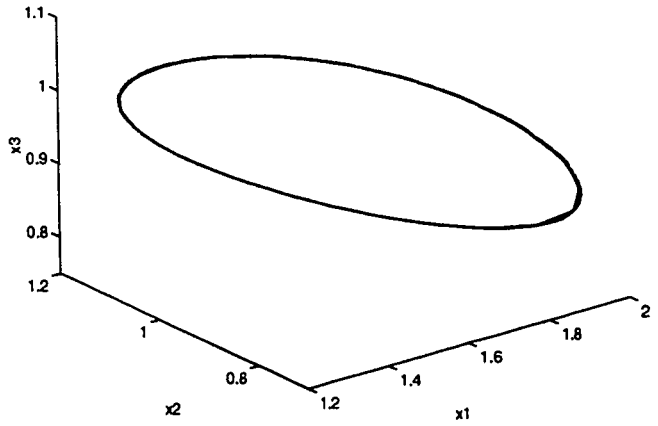

Figure 3.4 : An interior limit cycle for $\lambda = 0.2$, $\delta_1 = 0.3$, $\delta_2 = 0.96$, $m_1 = 2.5$, $m_2 = 3.0$ and $S^0 = 4.0$. The limit cycle appears to be stable with respect to initial conditions $x_{i0} > 0$.

3.3.1 Numerical Simulations of System (3.15)

In this section we present several observations based on numerical simulations, for different parameter values and initial conditions, for system (3.15). Recall from the previous section that we computed a condition for a Hopf bifurcation to occur in the x_1x_2-plane. Figure 3.3 depicts such a limit cycle in the x_1x_2-plane which emerged from $E^3_{S^*}$. For this particular choice of parameters, the limit cycle seems to be stable with respect to initial conditions $x_{10}, x_{20} > 0$ and $x_{30} = 0$.

Any one of the five parameters $S^0, \lambda, \delta_1, \delta_2$ and m_1 can be used as a bifurcation parameter. However, we use the operating parameter S^0 as the bifurcation parameter, since it is the most accessible parameter to the experimenter. In all of the simulations $\lambda = 0.2, \delta_1 = 0.3, \delta_2 = 0.96, m_1 = 2.5$ and $m_2 = 3$. As a result, $E^{\Delta}_{32} = (x^{\Delta}_{1_2}, \delta_2, x^{\Delta}_{3_2})$ remains outside the nonnegative cone.

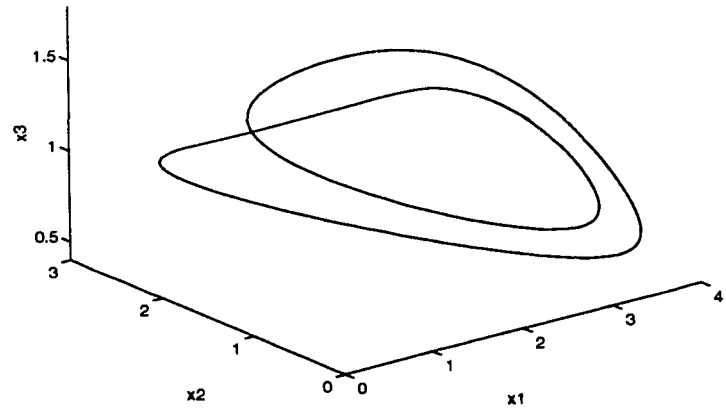

Figure 3.5 : A period 2 limit cycle for $\lambda = 0.2$, $\delta_1 = 0.3$, $\delta_2 = 0.96$, $m_1 = 2.5$, $m_2 = 3.0$ and $S^0 = 5.0$.

Near $S^0 = 2.0$, $E^3_{S\bullet}$ is a sink. As S^0 increases, $E^3_{S\bullet}$ undergoes a transcritical bifurcation at $S^0 = 2.1$ giving rise to the interior fixed point E^{Δ}_{31}. For $S^0 \in (2.1, 2.375)$, E^{Δ}_{31} is a sink and $E^3_{S\bullet}$ is a saddle with the x_1x_2-plane as its stable manifold. As a result, there is a saddle connection between $E^3_{S\bullet}$ and E^{Δ}_{31}. At $S^0 = 2.375$, $E^3_{S\bullet}$ undergoes a Hopf bifurcation giving rise to a limit cycle in the x_1x_2-plane. As S^0 increases a little further, the radius of the limit cycle grows resulting in an attracting cone in the interior on which trajectories spiral away from the x_1x_2-plane and up to E^{Δ}_{31}. Next, as S^0 increases further E^{Δ}_{31} appears to undergo a Hopf bifurcation. The resulting interior limit cycle seems to be stable with respect to initial conditions $x_{i0} > 0$, for $i = 1, 2, 3$ (Figure 3.4). At this point a further increase in S^0 results in a cascade of period doubling limit cycles. At each stage of the period doubling the resulting higher period limit cycle appears to be stable (Figures 3.5 and 3.6). The period doubling continues until eventually we reach the attractor in Figure 3.7.

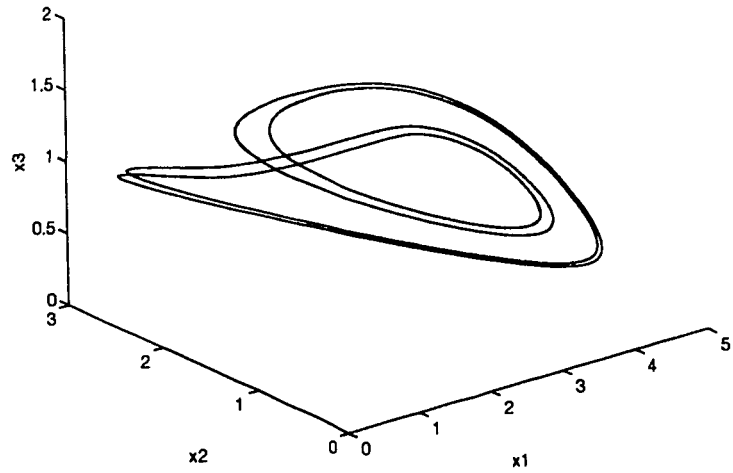

Figure 3.6 : A period 4 limit cycle for $\lambda = 0.2$, $\delta_1 = 0.3$, $\delta_2 = 0.96$, $m_1 = 2.5$, $m_2 = 3.0$ and $S^0 = 5.2$.

Figure 3.8 depicts the attractor for a set of parameter values different from the ones in Figure 3.7. The attractor in Figure 3.8 is reminiscent of the "tea-cup" attractor of Hastings and Powell ([18]). In fact, most of the above observations were also made by Hastings and Powell ([18]) for their food chain model. In related work by Klebanoff ([26]) some numerical evidence of a second route to chaos in the Hastings' model was presented, namely a Sil'nikov type bifurcation of limit cycles. In the following chapter, we shall see that the normal form analysis predicts this type of bifurcation for system (3.15) and we present some numerical evidence to support the existence of this bifurcation phenomenon for the model in (3.15).

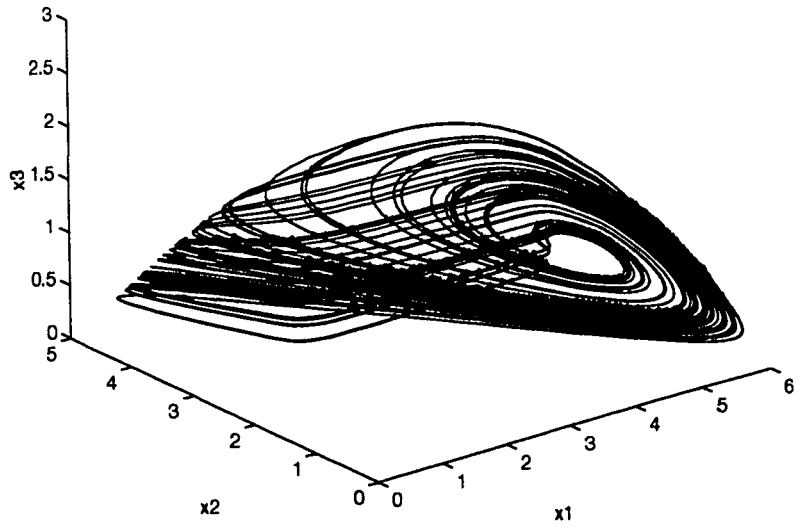

Figure 3.7 : An attractor for the chemostat in (3.15) for $\lambda = 0.2$, $\delta_1 = 0.3$, $\delta_2 = 0.96$, $m_1 = 2.5$, $m_2 = 3.0$ and $S^0 = 6.0$.

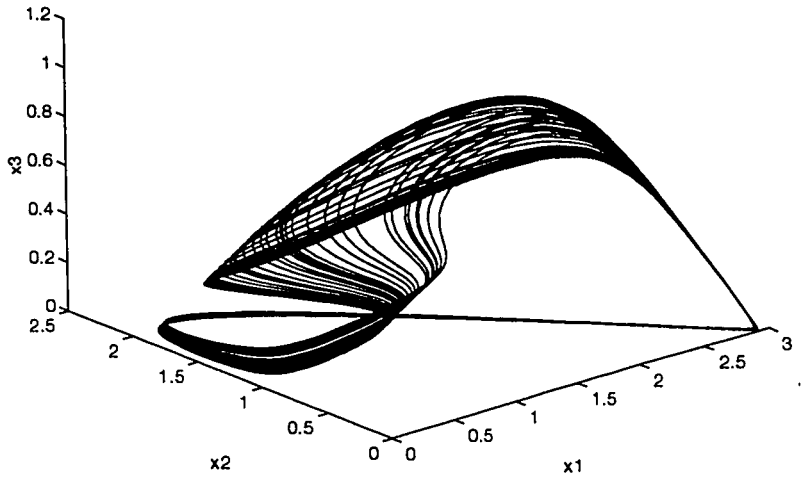

Figure 3.8 : An attractor for the chemostat model in (3.15) with $\lambda = 0.2$, $\delta_1 = 0.3$, $\delta_2 = 0.2$, $m_1 = 2.5$, $m_2 = 3.0$ and $S^0 = 3.12$.

Chapter 4

Normal Form

Our model of a food chain in the chemostat given in (3.15) is similar to a three species food chain of the form

$$\begin{aligned} x_1' &= f_1(x_1, x_2) , \\ x_2' &= f_2(x_1, x_2, x_3) , \\ x_3' &= f_3(x_2, x_3) , \end{aligned} \tag{4.1}$$

where f_i is the per-capita growth rate of species i. One of the defining properties for such a food chain (4.1) is the absence of direct interaction between species x_1 and x_3, that is $\partial f_1/\partial x_3 = \partial f_3/\partial x_1 = 0$. This is not the case for our model. However, the two models do share other characteristic traits.

Typically in food chains of the type given by (4.1) there are coupled predator-prey oscillations with higher trophic level species oscillating at lower amplitudes than the bottom trophic level species. This is also the case for our model (see Figure 3.2 for example). Furthermore, systems like the one in (4.1) exhibit persistence of species at the bottom trophic levels in the absence of higher trophic level species. This holds true for our model as well ([7]). Hence in both systems (3.15) and (4.1) one expects a fixed point of the form $(\overline{x}_1, \overline{x}_2, 0)$, with $(\overline{x}_1, \overline{x}_2, 0)$ having an unstable eigenspace transverse to the

x_1x_2-plane. Motivated by these similarities of the models, we adopt a normal form approach to our model, similar to the one used by Klebanoff ([26]).

4.1 Normal Form Computation

In this section we compute a normal form for system (3.15) expanded about the fixed point $E^3_{S^*}$. Under the conditions

$$\begin{aligned} S^0 - (\lambda + \delta_1)(1 + \tfrac{\delta_2}{\delta_1}) &= 0\ , \\ S^0 - (\lambda + \delta_1)(1 + \tfrac{m_1\delta_1}{\lambda}) &= 0\ , \end{aligned} \tag{4.2}$$

$E^3_{S^*}$ is a nonhyperbolic fixed point with associated eigenvalues

$$r_{1,2} = \pm\frac{i}{\lambda}\sqrt{\frac{(\lambda+\delta_1)(\lambda\delta_2 - \delta_1^2)}{\delta_1}} = \pm i\omega \text{ and } r_3 = 0.$$

Notice that under the conditions in (4.2) we must have $m_1 = (\lambda\delta_2)/\delta_1^2$, and this gives a condition for which system (3.15) undergoes a bifurcation of codimension two or greater. It is under the conditions in (4.2) that we wish to compute a normal form for system (3.15), since this is where the linear part of the vector field is most degenerate. That is, the linear part of the vector field in (3.15) at bifurcation is

$$\begin{pmatrix} 0 & \omega & 0 \\ -\omega & 0 & 0 \\ 0 & 0 & 0 \end{pmatrix}. \tag{4.3}$$

Next, consider a vector field with Taylor expansion (up to third order)

given by

$$\begin{pmatrix} \dot{x}_1 \\ \dot{x}_2 \\ \dot{x}_2 \end{pmatrix} = \begin{pmatrix} 0 & \omega & 0 \\ -\omega & 0 & 0 \\ 0 & 0 & 0 \end{pmatrix} \begin{pmatrix} x_1 \\ x_2 \\ x_3 \end{pmatrix} + \begin{pmatrix} a_{11} & a_{12} & a_{22} & a_{23} & a_{33} & a_{13} \\ b_{11} & b_{12} & b_{22} & b_{23} & b_{33} & b_{13} \\ c_{11} & c_{12} & c_{22} & c_{23} & c_{33} & c_{13} \end{pmatrix} \begin{pmatrix} x_1^2 \\ x_1x_2 \\ x_2^2 \\ x_2x_3 \\ x_3^2 \\ x_1x_3 \end{pmatrix}$$

$$+ \begin{pmatrix} a_{111} & a_{112} & a_{122} & a_{222} & a_{223} & a_{233} & a_{333} & a_{113} & a_{133} & a_{123} \\ b_{111} & b_{112} & b_{122} & b_{222} & b_{223} & b_{233} & b_{333} & b_{113} & b_{133} & b_{123} \\ c_{111} & c_{112} & c_{122} & c_{222} & c_{223} & c_{233} & c_{333} & c_{113} & c_{133} & c_{123} \end{pmatrix} \begin{pmatrix} x_1^3 \\ x_1^2x_2 \\ x_1x_2^2 \\ x_2^3 \\ x_2^2x_3 \\ x_2x_3^2 \\ x_3^3 \\ x_1^2x_3 \\ x_1x_3^2 \\ x_1x_2x_3 \end{pmatrix}.$$

In general, the normal form (up to third order) of any vector field with Taylor expansion as above is of the form ([26])

$$\begin{aligned} x_1' &= wx_2 + c_1x_2x_3 + c_2x_1x_3 + c_3x_1(x_1^2+x_2^2) - c_4x_2(x_1^2+x_2^2) \\ &\quad -c_5x_2x_3^2 + c_6x_1x_3^2 + O(4)\ , \\ x_2' &= -wx_1 + c_2x_2x_3 - c_1x_1x_3 + c_4x_1(x_1^2+x_2^2) + c_3x_2(x_1^2+x_2^2) \\ &\quad +c_6x_2x_3^2 + c_5x_1x_3^2 + O(4)\ , \\ x_3' &= c_7(x_1^2+x_2^2) + c_8x_3^2 + c_9x_3(x_1^2+x_2^2) + c_{10}x_3^3 + O(4)\ . \end{aligned} \tag{4.4}$$

In cylindrical coordinates ($r^2 = x_1^2 + x_2^2$ and $\theta = \tan^{-1}(x_2/x_1)$), the

normal form in (4.4) is

$$\begin{aligned}
\dot{r} &= c_2 r x_3 + c_6 r x_3^2 + c_3 r^3 + O(4) \ , \\
\dot{\theta} &= -w - c_1 x_3 + c_4 r^2 + c_5 x_3^2 + O(3) \ , \\
\dot{x}_3 &= c_7 r^2 + c_8 x_3^2 + c_9 r^2 x_3 + c_{10} x_3^3 + O(4) \ ,
\end{aligned} \tag{4.5}$$

where

$$\begin{aligned}
c_1 &= \tfrac{a_{23}-b_{13}}{2}, \\
c_2 &= \tfrac{a_{13}+b_{23}}{2},
\end{aligned}$$

$$\begin{aligned}
c_3 = {} & \tfrac{3a_{111}+a_{122}+b_{112}+3b_{222}}{8} - \tfrac{a_{11}a_{12}}{8\omega} - \tfrac{a_{12}a_{22}}{8\omega} + \tfrac{a_{11}b_{11}}{4\omega} + \tfrac{b_{11}b_{12}}{8\omega} \\
& - \tfrac{a_{22}b_{22}}{4\omega} + \tfrac{b_{12}b_{22}}{8\omega} - \tfrac{3a_{23}c_{11}}{16\omega} - \tfrac{3b_{13}c_{11}}{16\omega} + \tfrac{3a_{13}c_{12}}{16\omega} + \tfrac{b_{23}c_{12}}{16\omega} \\
& - \tfrac{a_{23}c_{22}}{16\omega} - \tfrac{b_{13}c_{22}}{16\omega},
\end{aligned}$$

$$\begin{aligned}
c_4 = {} & -\tfrac{a_{112}+3a_{222}-3b_{111}-b_{122}}{8} + \tfrac{a_{11}^2}{6\omega} + \tfrac{a_{12}^2}{24\omega} + \tfrac{5a_{11}a_{22}}{12\omega} + \tfrac{5a_{22}^2}{12\omega} \\
& - \tfrac{a_{12}b_{11}}{24\omega} + \tfrac{5b_{11}^2}{12\omega} - \tfrac{5a_{11}b_{12}}{24\omega} - \tfrac{a_{22}b_{12}}{24\omega} + \tfrac{b_{12}^2}{24\omega} - \tfrac{5a_{12}b_{22}}{24\omega} + \tfrac{5b_{11}b_{22}}{12\omega} \\
& + \tfrac{b_{22}^2}{6\omega} - \tfrac{a_{13}c_{11}}{16\omega} + \tfrac{b_{23}c_{11}}{16\omega} - \tfrac{a_{23}c_{12}}{16\omega} + \tfrac{3b_{13}c_{12}}{16\omega} - \tfrac{3a_{13}c_{22}}{16\omega} + \tfrac{3b_{23}c_{22}}{16\omega},
\end{aligned}$$

$$\begin{aligned}
c_5 = {} & -\tfrac{a_{233}-b_{133}}{2} + \tfrac{a_{13}^2}{8\omega} + \tfrac{a_{23}^2}{8\omega} + \tfrac{a_{22}a_{33}}{\omega} - \tfrac{a_{33}b_{12}}{2\omega} + \tfrac{a_{23}b_{12}}{4\omega} + \tfrac{b_{13}^2}{8\omega} \\
& - \tfrac{a_{13}b_{23}}{4\omega} + \tfrac{b_{23}^2}{8\omega} - \tfrac{a_{12}b_{33}}{2\omega} + \tfrac{b_{11}b_{33}}{\omega} + \tfrac{a_{33}c_{13}}{\omega} + \tfrac{b_{33}c_{23}}{\omega} - \tfrac{a_{13}c_{33}}{4\omega} + \tfrac{b_{23}c_{33}}{4\omega},
\end{aligned}$$

$$\begin{aligned}
c_6 = {} & \tfrac{a_{133}+b_{233}}{2} - \tfrac{a_{12}a_{33}}{2\omega} - \tfrac{a_{33}b_{22}}{\omega} + \tfrac{a_{11}b_{33}}{\omega} + \tfrac{b_{12}b_{33}}{2\omega} \\
& - \tfrac{b_{33}c_{13}}{\omega} + \tfrac{a_{33}c_{23}}{\omega} - \tfrac{a_{23}c_{33}}{4\omega} - \tfrac{b_{13}c_{33}}{4\omega},
\end{aligned}$$

$$\begin{aligned}
c_7 &= \tfrac{c_{11}+c_{22}}{2}, \\
c_8 &= c_{33},
\end{aligned}$$

$$\begin{aligned}
c_9 = {} & \tfrac{c_{113}+c_{223}}{2} + \tfrac{a_{23}c_{11}}{2\omega} + \tfrac{b_{13}c_{11}}{2\omega} - \tfrac{a_{13}c_{12}}{2\omega} + \tfrac{b_{11}c_{13}}{2\omega} \\
& + \tfrac{b_{22}c_{13}}{2\omega} - \tfrac{a_{11}c_{23}}{2\omega} - \tfrac{a_{22}c_{23}}{2\omega} + \tfrac{c_{12}c_{33}}{2\omega},
\end{aligned}$$

$$c_{10} = c_{333} + \frac{b_{33}c_{13}}{\omega} - \frac{a_{33}c_{23}}{\omega} \ .$$

Next, for the vector field in (3.15), we begin by shifting $E^3_{S^*} = (\delta_1, \delta_2, 0)$ to the origin and then calculating the Taylor expansion up to third order to obtain

$$\begin{aligned}
\dot{x}_1 &= -\left(\tfrac{\lambda+\delta_1}{\lambda}\right) x_2 - \tfrac{\delta_1}{\lambda} x_3 - \tfrac{\delta_1^2}{\lambda^2\delta_2} x_1^2 + \left(\tfrac{\delta_1^2-\lambda\delta_2-\delta_1\delta_2}{\lambda\delta_1\delta_2}\right) x_1x_2 - \tfrac{1}{\lambda} x_1x_3 \\
&\quad -\delta_1\left(\tfrac{\lambda\delta_2-\delta_1^2}{\lambda^3\delta_2^2}\right) x_1^3 + \left(\tfrac{\lambda\delta_2-\delta_1^2}{\lambda^2\delta_2^2}\right) x_1^2x_2 + O(4)\ , \\
\dot{x}_2 &= \left(\tfrac{\lambda\delta_2-\delta_1^2}{\lambda\delta_1}\right) x_1 - x_3 - \left(\tfrac{\lambda\delta_2-\delta_1^2}{\lambda^2\delta_2}\right) x_1^2 + \left(\tfrac{\lambda\delta_2-\delta_1^2}{\lambda\delta_1\delta_2}\right) x_1x_2 - \left(\tfrac{m_2-1}{\delta_2 m_2}\right) x_2x_3 \\
&\quad +\delta_1\left(\tfrac{\lambda\delta_2-\delta_1^2}{\lambda^3\delta_2^2}\right) x_1^3 - \left(\tfrac{\lambda\delta_2-\delta_1^2}{\lambda^2\delta_2^2}\right) x_1^2x_2 + \left(\tfrac{m_2-1}{\delta_2^2 m_2^2}\right) x_2^2x_3 + O(4)\ , \\
\dot{x}_3 &= \left(\tfrac{m_2-1}{\delta_2 m_2}\right) x_2x_3 - \left(\tfrac{m_2-1}{\delta_2^2 m_2^2}\right) x_2^2x_3 + O(4).
\end{aligned}$$

Applying the similarity transformation

$$\begin{pmatrix} x_1 \\ x_2 \\ x_3 \end{pmatrix} = T \begin{pmatrix} u_1 \\ u_2 \\ u_3 \end{pmatrix}$$

where

$$T = \begin{pmatrix} 0 & \sqrt{\frac{\delta_1(\lambda+\delta_1)}{\lambda\delta_2-\delta_1^2}} & 1 \\ 1 & 0 & -\frac{\lambda\delta_2-\delta_1^2}{\lambda(\lambda+\delta_1)} \\ 0 & 0 & \frac{\lambda\delta_2-\delta_1^2}{\lambda\delta_1} \end{pmatrix}\ , \tag{4.6}$$

to the vector field above we get

$$\begin{pmatrix} \dot{u}_1 \\ \dot{u}_2 \\ \dot{u}_3 \end{pmatrix} = \begin{pmatrix} 0 & \omega & 0 \\ -\omega & 0 & 0 \\ 0 & 0 & 0 \end{pmatrix} \begin{pmatrix} u_1 \\ u_2 \\ u_3 \end{pmatrix} + \begin{pmatrix} 0 & a_{12} & a_{22} & a_{23} & a_{33} & a_{13} \\ 0 & b_{12} & b_{22} & b_{23} & b_{33} & b_{13} \\ 0 & 0 & 0 & 0 & c_{33} & c_{13} \end{pmatrix} \begin{pmatrix} u_1^2 \\ u_1u_2 \\ u_2^2 \\ u_2u_3 \\ u_3^2 \\ u_1u_3 \end{pmatrix}$$

$$+\begin{pmatrix} 0 & 0 & a_{122} & a_{222} & a_{223} & a_{233} & a_{333} & a_{113} & a_{133} & a_{123} \\ 0 & 0 & b_{122} & b_{222} & b_{223} & b_{233} & b_{333} & b_{113} & b_{133} & b_{123} \\ 0 & 0 & 0 & 0 & 0 & 0 & c_{333} & c_{113} & c_{133} & 0 \end{pmatrix} \begin{pmatrix} u_1^3 \\ u_1^2 u_2 \\ u_1 u_2^2 \\ u_2^3 \\ u_2^2 u_3 \\ u_2 u_3^2 \\ u_3^3 \\ u_1^2 u_3 \\ u_1 u_3^2 \\ u_1 u_2 u_3 \end{pmatrix}$$

where

$$\omega = \frac{1}{\lambda}\sqrt{\frac{(\lambda+\delta_1)(\lambda\delta_2-\delta_1^2)}{\delta_1}},$$

$$a_{12} = \frac{1}{\lambda\delta_2}\sqrt{\frac{(\lambda+\delta_1)(\lambda\delta_2-\delta_1^2)}{\delta_1}},$$

$$a_{22} = -\frac{(\lambda+\delta_1)\delta_1}{\lambda^2\delta_2},$$

$$a_{23} = -\sqrt{\frac{\lambda\delta_2-\delta_1^2}{\delta_1(\lambda+\delta_1)}}\left(\frac{2\lambda\delta_1+\lambda\delta_2+\delta_1^2}{\lambda^2\delta_2}\right),$$

$$a_{33} = -\frac{(\lambda\delta_2-\delta_1^2)\{\lambda\delta_2-\delta_1^2+\delta_1 m_2(\lambda+\delta_2+2\delta_1)\}}{\lambda\delta_1\delta_2 m_2(\lambda+\delta_1)^2},$$

$$a_{13} = \frac{(\lambda\delta_2-\delta_1^2)(\lambda+\delta_1 m_2)}{\lambda\delta_1\delta_2 m_2(\lambda+\delta_1)},$$

$$b_{12} = -\frac{\lambda\delta_2-\delta_1^2+\delta_1\delta_2}{\lambda\delta_1\delta_2},$$

$$b_{22} = -\sqrt{\frac{\delta_1(\lambda+\delta_1)}{\lambda\delta_2-\delta_1^2}}\left(\frac{\delta_1}{\lambda^2\delta_2}\right),$$

$$b_{23} = -\frac{\delta_1(\delta_1^2+2\lambda\delta_1+\lambda\delta_2)}{\lambda^2\delta_2(\lambda+\delta_1)},$$

$$b_{33} = \sqrt{\frac{\lambda\delta_2-\delta_1^2}{\delta_1(\lambda+\delta_1)}}\frac{\{(\lambda\delta_2-\delta_1^2)(m_2-1)-\delta_1 m_2(\delta_1+\delta_2)\}}{\lambda\delta_2 m_2(\lambda+\delta_1)},$$

$$b_{13} = -\sqrt{\frac{\lambda\delta_2-\delta_1^2}{\delta_1(\lambda+\delta_1)}}\frac{\{m_2(\lambda\delta_2-\delta_1^2)+\lambda\delta_1(m_2-1)+\delta_1\delta_2 m_2\}}{\lambda\delta_1\delta_2 m_2},$$

$$c_{33} = -\frac{(m_2-1)(\lambda\delta_2-\delta_1^2)}{\lambda\delta_2 m_2(\lambda+\delta_1)},$$

$$c_{13} = \frac{m_2-1}{\delta_2 m_2},$$

$$a_{122} = -\frac{(\lambda+\delta_1)\delta_1}{\lambda^2\delta_2^2},$$

$$a_{222} = \sqrt{\frac{\delta_1(\lambda+\delta_1)}{\lambda\delta_2-\delta_1^2}}\left(\frac{\lambda+\delta_1}{\lambda^3\delta_2^2}\right),$$

$$a_{223} = \frac{\delta_1(2\delta_1^2+\lambda\delta_2+3\lambda\delta_1)}{\lambda^3\delta_2^2},$$

$$a_{233} = \sqrt{\frac{\lambda\delta_2-\delta_1^2}{\delta_1(\lambda+\delta_1)}}\left\{\frac{\delta_1(\delta_1^2+2\lambda\delta_2+3\lambda\delta_1)}{\lambda^3\delta_2^2}\right\},$$

$$a_{333} = \frac{(\lambda\delta_2-\delta_1^2)}{\lambda^2\delta_1\delta_2^2 m_2^2(\lambda+\delta_1)^3}\Big\{(m_2-1)(\lambda^2\delta_2^2+\delta_1^4+2\lambda\delta_1^2\delta_2 m_2)$$

$$+\lambda\delta_1\delta_2(\lambda m_2^2+\lambda\delta_1 m_2^2+2\delta_1)+m_2^2\delta_1^3(\delta_1+\delta_2+2\lambda m_2)\Big\},$$

$$a_{113} = \frac{(m_2-1)(\lambda\delta_2-\delta_1^2)}{\delta_1\delta_2^2 m_2^2(\lambda+\delta_1)},$$

$$a_{133} = -\frac{(\lambda\delta_2-\delta_1^2)}{\lambda^2\delta_1\delta_2^2 m_2^2(\lambda+\delta_1)^2}\Big\{2\lambda(m_2-1)(\lambda\delta_2+\delta_1^2 m_2)$$

$$+\delta_1 m_2^2(\lambda^2+\delta_1^2)+2\lambda\delta_1^2\Big\},$$

$$a_{123} = -2\frac{\sqrt{\delta_1(\lambda+\delta_1)(\lambda\delta_2-\delta_1^2)}}{\lambda^2\delta_2^2},$$

$$b_{122} = \frac{\sqrt{\delta_1(\lambda+\delta_1)(\lambda\delta_2-\delta_1^2)}}{\lambda^2\delta_2^2},$$

$$b_{222} = -\frac{(\lambda+\delta_1)\delta_1^2}{\lambda^3\delta_2^2},$$

$$b_{223} = -\sqrt{\frac{\lambda\delta_2-\delta_1^2}{\delta_1(\lambda+\delta_1)}}\left\{\frac{\delta_1(2\delta_1^2+\lambda\delta_2+3\lambda\delta_1)}{\lambda^3\delta_2^2}\right\},$$

$$b_{233} = -\frac{(\lambda\delta_2-\delta_1^2)(\delta_1^2+2\lambda\delta_2+3\lambda\delta_1)}{\lambda^3\delta_2^2(\lambda+\delta_1)},$$

$$b_{333} = -\left(\tfrac{\lambda\delta_2-\delta_1^2}{\delta_1(\lambda+\delta_1)}\right)^{3/2}\left(\tfrac{\delta_1}{\lambda^2\delta_2^2m_2^2}\right)\left\{(\lambda\delta_2-\delta_1^2)\right.$$

$$\left.+\delta_1m_2^2(\lambda+\delta_1)+\delta_2(m_2-1)(\lambda m_2+1)\right\},$$

$$b_{113} = \sqrt{\frac{\lambda\delta_2-\delta_1^2}{\delta_1(\lambda+\delta_1)}}\left(\frac{m_2-1}{\delta_2^2m_2^2}\right),$$

$$b_{133} = \left(\frac{\lambda\delta_2-\delta_1^2}{\delta_1(\lambda+\delta_1)}\right)^{3/2}\left(\frac{\delta_1m_2^2(\lambda+\delta_1)+2\lambda\delta_1(1-m_2)}{\lambda^2\delta_2^2m_2^2}\right),$$

$$b_{123} = 2\frac{\lambda\delta_2-\delta_1^2}{\lambda^2\delta_2^2},$$

$$c_{333} = -\left(\frac{\lambda\delta_2-\delta_1^2}{\lambda+\delta_1}\right)^2\left(\frac{m_2-1}{\lambda^2\delta_2^2m_2^2}\right),$$

$$c_{113} = -\frac{m_2-1}{\delta_2^2m_2^2},$$

$$c_{133} = 2\frac{(\lambda\delta_2-\delta_1^2)(m_2-1)}{\lambda\delta_2^2m_2^2(\lambda+\delta_1)}.$$

Normal form calculations in general are not unique. It is by a deliberate choice of transformations that (4.5) is independent of θ. In fact, (4.5) can be made independent of θ up to any degree ([49]). Hence we may ignore the θ-equation in (4.5) and restrict the analysis of the vector field in (4.5) to the

rx_3-plane. Also, since we will be considering only local arguments, we ignore the higher order terms in (4.5). Thus the normal form that we will consider is given by

$$\begin{aligned} \dot{r} &= c_2 r x_3 + c_6 r x_3^2 + c_3 r^3 \ , \\ \dot{x}_3 &= c_8 x_3^2 + c_9 r^2 x_3 + c_{10} x_3^3 \ , \end{aligned} \tag{4.7}$$

where

$$c_2 = \frac{(\lambda\delta_2 - \delta_1^2)(\lambda + m_2\delta_1)}{2\lambda\delta_1\delta_2 m_2(\lambda + \delta_1)} - \frac{\delta_1(\lambda\delta_2 + 2\lambda\delta_1 + \delta_1^2)}{2\lambda^2\delta_2(\lambda + \delta_1)},$$

$$c_3 = -\frac{\delta_1^2\{\delta_1(\lambda\delta_2 - \delta_1^2) + \lambda\delta_2(\delta_1 + 2\lambda)\}}{8\lambda^3\delta_2^2(\lambda\delta_2 - \delta_1^2)},$$

$$\begin{aligned} c_6 = &\frac{(\lambda\delta_2 - \delta_1^2)^2(4\lambda + 3\delta_1 m_2)}{4\lambda^2\delta_1\delta_2^2 m_2^2(\lambda + \delta_1)^2} + \frac{(\lambda\delta_2 - \delta_1^2)\{\delta_2 + m_2\delta_1 + 4(m_2 - 1)\}}{4\lambda\delta_2^2 m_2(\lambda + \delta_1)^2} \\ &- \frac{(\lambda\delta_2 - \delta_1^2)\{\delta_2 m_2(3m_2 - 2) + 5\delta_1(m_2 - 1)^2\}}{4\delta_1\delta_2^2 m_2^2(\lambda + \delta_1)^2} - \\ &\frac{\delta_1^2(\lambda\delta_2 - \delta_1^2)(3\lambda + 2\delta_1)}{4\lambda^3\delta_2^2(\lambda + \delta_1)^2} - \frac{\delta_1^3 + 2\lambda\delta_1\delta_2 + 2\delta_1\delta_2^2 m_2 + 4\lambda\delta_2^2 m_2 + 2\delta_1^2\delta_2 m_2}{4\lambda\delta_2^2 m_2(\lambda + \delta_1)^2}, \end{aligned}$$

$$c_7 = 0,$$

$$c_8 = -\frac{(m_2 - 1)(\lambda\delta_2 - \delta_1^2)}{\lambda\delta_2 m_2(\lambda + \delta_1)},$$

$$c_9 = -\frac{(m_2 - 1)\{\lambda(\lambda\delta_2 - \delta_1^2) + m_2\delta_1^3\}}{2\lambda\delta_2^2 m_2^2(\lambda\delta_2 - \delta_1^2)},$$

$$\begin{aligned} c_{10} = &\frac{m_2 - 1}{\delta_2^2 m_2^2(\lambda + \delta_1)^2}\left[(\lambda\delta_2 - \delta_1^2)\left\{(m_2 - 1) + \frac{\delta_1^2}{\lambda^2}\right\} + \frac{\delta_1^2\delta_2}{\lambda}\right] \\ &- \frac{m_2 - 1}{\delta_2^2 m_2^2(\lambda + \delta_1)^2}\left[m_2\delta_1^2 + \delta_2(m_2\delta_1 + \delta_2^2)\right]. \end{aligned}$$

Notice that c_3, c_8 and $c_9 < 0$, but the signs of the remaining coefficients are difficult to determine without further constraints. The biological constraint that the $x_3 = 0$ face is invariant for system (3.15) forces $c_7 = 0$. The x_3-equation in (4.7) is still analogous to the x_3-equation in (3.15). The r-equation

in (4.7) is a scaled measure of the square root of the sum of the squares of the lower trophic species x_1 and x_2. Hence the study of (4.7) is restricted to the positive quadrant of the rx_3-plane.

To further simplify the study of (4.7) we reduce the number of cases that need to be considered by rescaling. Letting $\overline{r} = \alpha r$ and $\overline{x}_3 = \beta x_3$ ([14]) system (4.7) becomes

$$\begin{aligned} \dot{\overline{r}} &= \tfrac{c_2}{\beta}\overline{r}\overline{x}_3 + \tfrac{c_6}{\beta^2}\overline{r}\overline{x}_3^2 + \tfrac{c_3}{\alpha^2}\overline{r}^3 \,, \\ \dot{\overline{x}}_3 &= \tfrac{c_8}{\beta}\overline{x}_3^2 + \tfrac{c_9}{\alpha^2}\overline{r}^2\overline{x}_3 + \tfrac{c_{10}}{\beta^2}\overline{x}_3^3 \,. \end{aligned}$$

Letting $\alpha = \sqrt{-c_3}$, $\beta = c_2$ (assuming $c_2 \neq 0$) and omitting the bars we obtain

$$\begin{aligned} \dot{r} &= rx_3 + arx_3^2 - r^3 \,, \\ \dot{x}_3 &= bx_3^2 - cr^2x_3 - dx_3^3 \,, \end{aligned} \tag{4.8}$$

with $a = c_6/c_2^2$, $b = c_8/c_2$, and $d = -c_{10}/c_2^2$ arbitrary scalars and $c = c_9/c_3 > 0$, a positive scalar.

Notice that the **sign** of the **rescaling constant** β is **unknown**. If $\beta > 0$ then $b < 0$ and the first quadrant of the rx_3-plane of system (4.7) is mapped to the first quadrant of system (4.8). If $\beta < 0$ then $b > 0$ and the first quadrant of the rx_3-plane of system (4.7) is mapped to the fourth quadrant of system (4.8). In either case $b \neq 0$.

Klebanoff ([26]) has done an unfolding analysis for a food chain with Jacobian matrix as in (4.3). His analysis required that $c_2 \neq 0$ and $c_7 = c_8 = 0$ in (4.5). In our case, although $c_2 \neq 0$ and $c_7 = 0$, $c_8 < 0$. The conditions $c_2 \neq 0$ and $c_7 = 0$ stem from the same reasons for both models. Namely, $c_2 \neq 0$ is due to the choice of rescaling, while $c_7 = 0$ is a result of the fact that if the top predator becomes extinct, it remains extinct. In the Klebanoff model, $c_8 = 0$ is a result of the lack of interaction between the highest and lowest trophic level species. As mentioned before, this is not the case for our model

and thus $c_8 < 0$. Despite the different constraint, we follow the analysis given in Klebanoff ([26]), making the appropriate changes to account for $c_8 \neq 0$.

There are three possible fixed points for (4.8). There is the trivial fixed point $(0,0)$, which corresponds to the fixed point $E^3_{S^*}$, and there is a second fixed point $(0, b/d)$. Recall that under the conditions in (4.2), one of the interior fixed points E^{Δ}_{3i} of (3.15) coalesces with $E^3_{S^*}$. Hence, $(0, b/d)$ must correspond to the remaining interior fixed point of (3.15). Finally, let $Z = (b-c)/(ac+d)$ and $R = \sqrt{Z + aZ^2}$. If $Z + aZ^2 > 0$, then there is a third fixed point (R, Z) that resides in the either the first or fourth quadrant of the rx_3–plane. This would correspond to a limit cycle for the original system (3.15).

We now proceed to determine an unfolding for (4.8). Note that due to the biological constraints of the model we do not attempt to determine a universal unfolding. First, since $x_3 = 0$ must remain invariant for the unfolding, we cannot introduce any perturbation terms in the x_3–equation independent of x_3. Second, recall that the vector field in (3.15) was restricted by the bifurcation conditions in (4.2). Ignoring these conditions for the moment, the Jacobian of (3.15) in real Jordan canonical form would be given by

$$\begin{pmatrix} \mu_1 & \omega & 0 \\ -\omega & \mu_1 & 0 \\ 0 & 0 & \mu_2 \end{pmatrix}.$$

Hence we introduce the following two parameter unfolding ([27]) of (4.8)

$$\begin{aligned} \dot{r} &= \mu_1 r + r x_3 + a r x_3^2 - r^3 \,, \\ \dot{x}_3 &= \mu_2 x_3 + b x_3^2 - c r^2 x_3 - d x_3^3 \,. \end{aligned} \tag{4.9}$$

Finally, note that the normal form in (4.5) was computed for an arbitrary vector field with linear part similar to (4.3). The terms that most influence the local dynamics of a vector field with linear part as in (4.3) are

present in (4.5). Comparing terms in (4.5) and (4.9), we see that the r^2 term in the x_3—equation could be another possible perturbation term for (4.9). However, since $x_3 = 0$ must remain invariant for the x_3—equation, the perturbation term $\mu_3 r^2$ is not acceptable. Hence the unfolding that we will consider is the two parameter unfolding in (4.9).

In the subsequent unfolding analysis we will consider the coefficients a, b, c, and d in (4.9) as constants. We do so in order to study the roles of the perturbation terms $\mu_1 r$ and $\mu_2 x_3$. The parameters μ_1 and μ_2 move the system through the various bifurcation phenomena. We will see that this two parameter unfolding is sufficient for displaying global bifurcations that are associated with horseshoe dynamics and chaos.

4.2 Isoclines and Fixed Points

We begin by considering the nullclines of (4.9). There are four possible nullclines. There are two trivial nullclines $r = 0$ and $x_3 = 0$ of $\dot{r} = 0$ and $\dot{x}_3 = 0$ respectively. In addition there are two nontrivial nullclines. First, for $\dot{r} = 0$ and $a \neq 0$ there is the nullcline given by the curve

$$\mu_1 + x_3 + a x_3^2 - r^2 = 0, \tag{4.10}$$

or equivalently,

$$\frac{4a^2}{1 - 4a\mu_1}(x_3 + \frac{1}{2a})^2 - \frac{4a}{1 - 4a\mu_1} r^2 = 1 \quad \text{if} \quad 1 - 4a\mu_1 \neq 0, \tag{4.11}$$

or the pair of lines

$$x_3 = -\frac{1}{2a} \pm \frac{1}{\sqrt{a}} r \quad \text{if} \quad 1 - 4a\mu_1 = 0 \quad a > 0. \tag{4.12}$$

If $a = 0$, the nullcline is a parabola given by

$$x_3 = r^2 - \mu_1. \tag{4.13}$$

For $a > 0$ the curve in (4.11) is a hyperbola with vertical symmetry if $1-4a\mu_1 < 0$. For $a > 0$ and $1-4a\mu_1 > 0$, the curve in (4.11) is a hyperbola with horizontal symmetry. For $a < 0$ and $1 - 4a\mu_1 > 0$, the curve in (4.11) is an ellipse. The curve in (4.11) has no solution set for $a < 0$ and $1 - 4a\mu_1 < 0$. The curve in (4.10) has only the point $(0, -1/(2a))$ for a solution when $1 - 4a\mu_1 = 0$ and $a < 0$.

Secondly, there is a nontrivial nullcline corresponding to $\dot{x}_3 = 0$, given by the curve

$$\mu_2 + bx_3 - dx_3^2 - cr^2 = 0,$$

or equivalently,

$$\frac{4d^2}{b^2 + 4d\mu_2}(x_3 - \frac{b}{2d})^2 + \frac{4cd}{b^2 + 4d\mu_2}r^2 = 1 \quad if \quad b^2 + 4d\mu_2 \neq 0. \tag{4.14}$$

Recall that d is an arbitrary scalar. First assume $d > 0$. For $b^2 + 4d\mu_2 > 0$, the curve in (4.14) is an ellipse. For $b^2 + 4d\mu_2 < 0$, the curve in (4.14) has no solution set, and for $b^2 + 4d\mu_2 = 0$, the curve has only the point $(0, b/(2d))$ as a solution.

Next assume $d < 0$. For $b^2 + 4d\mu_2 > 0$, the curve in (4.14) is a hyperbola with horizontal symmetry, and for $b^2 + 4d\mu_2 < 0$, it is a hyperbola with vertical symmetry. For $b^2 + 4d\mu_2 = 0$, the x_3-nullcline is a pair of lines given by

$$x_3 = \frac{b}{2d} \pm \sqrt{-\frac{c}{d}}r. \tag{4.15}$$

Lastly, for $d = 0$, the x_3-nullcline is a parabola given by

$$x_3 = \frac{c}{b}r^2 - \frac{\mu_2}{b}. \tag{4.16}$$

We now proceed to describe the direction of the flow of the r and x_3 components separately. The description is done for the **first quadrant only**.

The description for the fourth quadrant is similar, but the direction of the flow for the x_3 component is reversed.

For $a \neq 0$ and $1 - 4a\mu_1 \neq 0$, the nontrivial $r-$nullcline can be described by three different conic sections. Let

$$N_1(r, x_3) = \mu_1 + x_3 + ax_3^2 - r^2. \tag{4.17}$$

Since (4.17) is continuous and equal to zero only on the conic section, it can change signs only by crossing through the conic section. Thus it is enough to sample a point inside and a point outside the conic section to determine the sign of (4.17). Inside the conic section choose the point $(0, -1/(2a))$ and outside choose the point $(\pm R, -1/(2a))$ for $R > 0$ sufficiently large. Then

$$N_1(0, -1/(2a)) = \frac{4a\mu_1 - 1}{4a},$$

and

$$N_1(\pm R, -1/(2a)) < 0 \text{ for } R > 0 \text{ sufficiently large.}$$

Define the interior (i.e. inside) of a hyperbola to be the region between the branches and define the exterior (i.e. outside) to be the complement of the interior. Thus the $r-$nullcline ellipse or the hyperbola with vertical symmetry has $r-$components of trajectories increasing when inside these two conic sections and decreasing when outside. Conversely, $r-$components of trajectories decrease inside the hyperbola with horizontal symmetry and increase outside.

In the special case when the nullclines are lines (i.e. $a > 0$, $1 - 4a\mu_1 = 0$), the $r-$components of trajectories decrease in the region to the right of the point $(0, -1/(2a))$ and increase in the regions directly above and below $(0, -1/(2a))$. For the case when the nullcline is a parabola (i.e. $a = 0$), $r-$components of trajectories increase in the convex region of the parabola and decrease otherwise. Figure 4.1 summarizes these observations.

Consider next the nontrivial x_3−nullcline. Arguing as above, for $d > 0$ and $b^2 + 4d\mu_2 > 0$ the x_3−nullcline is an ellipse. The x_3−components of trajectories increase inside the ellipse and decrease outside. For $b^2 + 4d\mu_2 = 0$, the lengths of the axes of the ellipse have shrunk to zero.

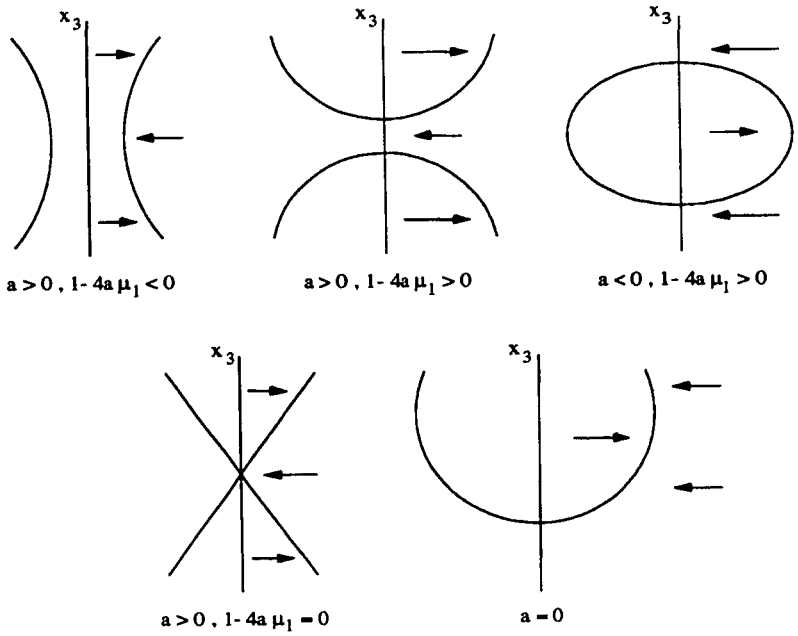

Figure 4.1 : The r−nullclines are symmetric about the x_3−axis. Arrows indicate direction of the flow and are assumed to lie in the positive quadrant.

Next, for $d < 0$ and $b^2 + 4d\mu_2 \neq 0$ the x_3−nullcline is a hyperbola with horizontal symmetry if $b^2 + 4d\mu_2 > 0$ and vertical symmetry if $b^2 + 4d\mu_2 < 0$. The x_3−components of solutions decrease (increase) inside the hyperbola with horizontal symmetry (vertical symmetry) and increase (decrease) when outside. In the special case when the nullclines are lines (i.e. $d < 0, b^2 + 4d\mu_2 = 0$), the x_3−components of solutions decrease in the region to the right of the point $(0, b/(2d))$ and increase in the regions directly above and below $(0, b/(2d))$.

Finally, for $d = 0$, the nullcline is a parabola with x_3−components of solutions increasing in the convex region of the parabola and decreasing otherwise. Figure 4.2 summarizes these observations.

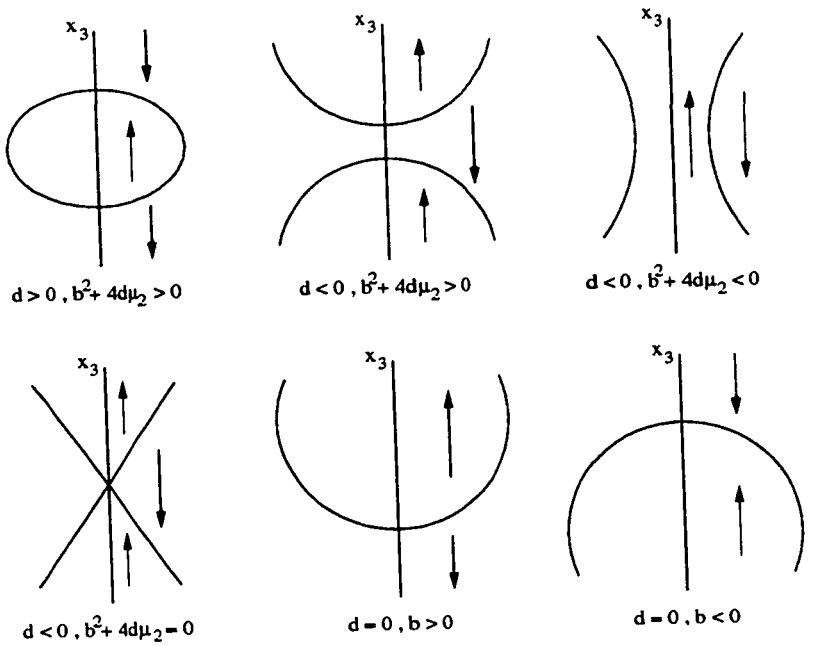

Figure 4.2 : The x_3−nullclines are symmetric about the x_3−axis. Arrows indicate direction of the flow and are assumed to lie in the positive quadrant.

Intersections of r and x_3− nullclines correspond to fixed points of (4.9). There are six possible fixed points for (4.9) given by $(0,0)$, $(\sqrt{\mu_1},0)$, $(0,\hat{x}_{3i})$ and $(\tilde{r}_i,\tilde{x}_{3i})$, where for $i = 1,2$, we have

$$\hat{x}_{3i} = \frac{b + (-1)^{i+1}\sqrt{b^2 + 4d\mu_2}}{2d}, \tag{4.18}$$

and,

$$\tilde{r}_i = \sqrt{\mu_1 + \tilde{x}_{3i} + a(\tilde{x}_{3i})^2}, \tag{4.19}$$

$$\tilde{x}_{3i} = \frac{-(c-b) + (-1)^{i+1}\sqrt{(c-b)^2 - 4(ac+d)(c\mu_1 - \mu_2)}}{2(ac+d)}. \tag{4.20}$$

The origin is always a fixed point of (4.9). The Jacobian of (4.9) evaluated at $(0,0)$ is

$$J(0,0) = \begin{pmatrix} \mu_1 & 0 \\ 0 & \mu_2 \end{pmatrix}.$$

Thus $(0,0)$ is locally asymptotically stable provided $\mu_1, \mu_2 < 0$. For $\mu_1 > 0$, $(\sqrt{\mu_1}, 0)$ is another fixed point of (4.9). The Jacobian of (4.9) evaluated at $(\sqrt{\mu_1}, 0)$ is

$$J(\sqrt{\mu_1}, 0) = \begin{pmatrix} -2\mu_1 & \sqrt{\mu_1} \\ 0 & \mu_2 - c\mu_1 \end{pmatrix}.$$

The associated eigenvalues of $(\sqrt{\mu_1}, 0)$ are $-2\mu_1$ and $\mu_2 - c\mu_1$. Provided $(\sqrt{\mu_1}, 0)$ exists (i.e. $\mu_1 > 0$), it is locally asymptotically stable if and only if $\mu_2 - c\mu_1 < 0$. Similarly, $(0, \hat{\tilde{x}}_{3i})$ exists provided $b^2 + 4d\mu_2 \geq 0$. The Jacobian of (4.9) evaluated at $(0, \hat{\tilde{x}}_{3i})$ is

$$J(0, \hat{\tilde{x}}_{3i}) = \begin{pmatrix} \mu_1 + \hat{\tilde{x}}_{3i} + a\left(\hat{\tilde{x}}_{3i}\right)^2 & 0 \\ 0 & \mu_2 + 2b\,\hat{\tilde{x}}_{3i} - 3d\left(\hat{\tilde{x}}_{3i}\right)^2 \end{pmatrix}.$$

Hence, $(0, \hat{\tilde{x}}_{3i})$ is locally asymptotically stable provided $\mu_1 + \hat{\tilde{x}}_{3i} + a\left(\hat{\tilde{x}}_{3i}\right)^2 < 0$ and $\mu_2 + 2b\,\hat{\tilde{x}}_{3i} - 3d\left(\hat{\tilde{x}}_{3i}\right)^2 < 0$.

Existence of limit cycles for the model in (3.15) requires that at least one of the fixed points $(\tilde{r}_i, \tilde{x}_{3i})$ resides in the first or fouth quadrant depending on the sign of the rescaling constant β. Hence, instead of providing conditions for the existence of $(\tilde{r}_i, \tilde{x}_{3i})$, we provide an example of a set of conditions that ensures that at least one of $(\tilde{r}_i, \tilde{x}_{3i})$ is in the first quadrant for $\beta > 0$ (i.e. $b < 0$). For example, if $\mu_1, a > 0$ then $\tilde{r}_i > 0$ if $\tilde{x}_{3i} > 0$. For $\tilde{x}_{3i} > 0$, we may choose $(ac + d) < 0$ and $0 < \mu_2 - c\mu_1 < \varepsilon$ for arbitrary $\varepsilon > 0$. Thus we have two positive distinct values for $\tilde{x}_{3i} > 0$. One can also choose values such that either one fixed point is in the first quadrant or there are no fixed points in

the first quadrant. Similarly, if $\beta < 0$, one can choose values such that none or one or two fixed points are in the fourth quadrant.

Then the Jacobian of (4.9) evaluated at $(\tilde{r}_i, \tilde{x}_{3i})$ is

$$J(\tilde{r}_i, \tilde{x}_{3i}) = \begin{pmatrix} \mu_1 + \tilde{x}_{3i} + a\,(\tilde{x}_{3i})^2 - 3\,(\tilde{r}_i)^2 & \tilde{r}_i\,(1 + 2a\tilde{x}_{3i}) \\ -2c\tilde{r}_i\tilde{x}_{3i} & \mu_2 + 2b\tilde{x}_{3i} - c\,(\tilde{r}_i)^2 - 3d\,(\tilde{x}_{3i})^2 \end{pmatrix}.$$

The associated eigenvalues are given by

$$\beta_{1,2} = \frac{tr\,(J(\tilde{r}_i, \tilde{x}_{3i})) \pm \sqrt{[tr(J(\tilde{r}_i, \tilde{x}_{3i}))]^2 - 4\det(J(\tilde{r}_i, \tilde{x}_{3i}))}}{2}, \tag{4.21}$$

where

$$tr\,(J(\tilde{r}_i, \tilde{x}_{3i})) = -2\mu_1 + (b-2)\tilde{x}_{3i} - 2(a+d)\,(\tilde{x}_{3i})^2\,, \tag{4.22}$$

and

$$\det\,(J(\tilde{r}_i, \tilde{x}_{3i})) = -2\,(\tilde{r}_i)^2\left\{c\mu_1 - \mu_2 - (ac+d)\,(\tilde{x}_{3i})^2\right\}. \tag{4.23}$$

Thus if $(\tilde{r}_i, \tilde{x}_{3i})$ exists, it is locally asymptotically stable if $\mathbf{Re}(\beta_{1,2}) < 0$.

4.3 Local Bifurcations

In this section we examine the local bifurcation behavior of the unfolded normal form in (4.9). Due to the complexity of the coefficients c_i in (4.9), a complete bifurcation analysis is difficult. Where possible we compute the relevant bifurcation curves. Otherwise, we give numerical examples of the local bifurcation phenomena in question. In any case, the bifurcation analysis is restricted to the first or fourth quadrant of the rx_3−plane.

4.3.1 Bifurcations of the Origin

Recall that the fixed point $(0,0)$ of (4.9) corresponds to the fixed point $E^3_{S^*}$ of system (3.15). We have already seen that $E^3_{S^*}$ can undergo both a transcritical

and a Hopf bifurcation. Thus, we expect the origin to undergo a transcritical bifurcation and a pitchfork bifurcation.

First, the origin undergoes a transcritical bifurcation at $\mu_2 = 0$. This follows from setting $r = 0$ in (4.9) and considering the resulting equation

$$\dot{x}_3 = G(x_3, \mu_2) = \mu_2 x_3 + b x_3^2 - d x_3^3.$$

For $\mu_2 = 0$ a transcritical bifurcation occurs at $x_3 = 0$ provided the following conditions hold ([49]) :

$$G(0,0) = \frac{\partial G}{\partial x_3}(0,0) = \frac{\partial G}{\partial \mu_2}(0,0) = 0,$$

$$\frac{\partial^2 G}{\partial x_3^2}(0,0) \neq 0 \text{ and } \frac{\partial^2 G}{\partial x_3 \partial \mu_2}(0,0) \neq 0.$$

The first three conditions are easily checked. Moreover,

$$\frac{\partial^2 G}{\partial x_3 \partial \mu_2}(x_3, \mu_2) = 1,$$

and

$$\frac{\partial^2 G}{\partial x_3^2}(x_3, \mu_2) = 2b - 6d x_3.$$

Hence, $\frac{\partial^2 G}{\partial x_3 \partial \mu_2}(0,0) \neq 0$ and $\frac{\partial^2 G}{\partial x_3^2}(0,0) = 2b \neq 0$ since $b \neq 0$. Thus, a transcritical bifurcation occurs at $(x_3, \mu_2) = (0,0)$.

Next, the origin undergoes a pitchfork bifurcation at $\mu_1 = 0$. This follows immediately from setting $x_3 = 0$ in (4.9) and considering the equation

$$\dot{r} = F(r, \mu_1) = r(\mu_1 - r^2). \tag{4.24}$$

For $\mu_1 < 0$, $r = 0$ is the only fixed point of (4.24) and is locally asymptotically stable. For $\mu_1 > 0$, there are three fixed points $r = 0$ and $r = \pm\sqrt{\mu_1}$. The fixed point $r = 0$ is now unstable and $r = \pm\sqrt{\mu_1}$ are stable (i.e. $\frac{\partial F}{\partial r}(\pm\sqrt{\mu_1}, \mu_1) = -2\mu_1$). Hence, a pitchfork bifurcation occurs at $(r, \mu_1) = (0,0)$.

4.3.2 Bifurcations on the Axes

There are three possible fixed points on the r and x_3 axes. There is the pair of fixed points $(0, \hat{x}_{3i})$ and for $\mu_1 > 0$, we have the fixed point $(\sqrt{\mu_1}, 0)$. The fixed points $(0, \hat{x}_{3i})$ correspond to the interior fixed points $E_{3i}^{\triangle}$ of system (3.15) and $(\sqrt{\mu_1}, 0)$ corresponds to the limit cycle in the x_1x_2-plane.

For $d \neq 0$, the fixed points $(0, \hat{x}_{3i})$ can arise and split via a saddle-node bifurcation. For $\mu_2 = -b^2/(4d)$ we have $\hat{x}_{31}=\hat{x}_{32}= b/(2d)$. Since the fixed points $(0, \hat{x}_{3i})$ remain on the x_3-axis, which is invariant for the flow generated by (4.9), we set $r = 0$ and consider again the equation

$$\dot{x}_3= G(x_3, \mu_2) = \mu_2 x_3 + b x_3^2 - d x_3^3.$$

For a saddle-node bifurcation to occur at $\hat{x}_3= b/(2d)$ for $\mu_2 = -b^2/(4d)$, we require the following conditions to hold ([49]) :

$$G(\frac{b}{2d}, -\frac{b^2}{4d}) = \frac{\partial G}{\partial x_3}(\frac{b}{2d}, -\frac{b^2}{4d}) = 0,$$

$$\frac{\partial G}{\partial \mu_2}(\frac{b}{2d}, -\frac{b^2}{4d}) \neq 0 \text{ and } \frac{\partial^2 G}{\partial x_3^2}(\frac{b}{2d}, -\frac{b^2}{4d}) \neq 0.$$

The first two conditions can be easily checked, and since $b \neq 0$ we have

$$\frac{\partial G}{\partial \mu_2}(\frac{b}{2d}, -\frac{b^2}{4d}) = \frac{b}{2d} \neq 0,$$

and

$$\frac{\partial^2 G}{\partial x_3^2}(\frac{b}{2d}, -\frac{b^2}{4d}) = 2b - 6d\left(\frac{b}{2d}\right) = -b \neq 0.$$

Hence, a saddle-node bifurcation occurs at $(r, x_3) = (0, b/(2d))$ with critical value $\mu_2 = -b^2/(4d)$. Depending on the signs of b and d, the saddle-node bifurcation can occur outside or inside the first (fourth) quadrant. Thus one of the fixed points $(0, \hat{x}_{3i})$ can enter or exit the first (fourth) quadrant via the transcritical bifurcation at the origin.

Next, the fixed points $(0, \hat{x}_{3i})$, provided $b^2 + 4d\mu_2 > 0$, can also undergo a pitchfork bifurcation giving birth to the interior fixed points $(\tilde{r}_i, \tilde{x}_{3i})$. This corresponds to the Hopf bifurcation about the interior fixed point E_{3i}^{Δ} for the original system (3.15). This can be easily seen by performing a center manifold reduction. Moving $(0, \hat{x}_{3i})$ to the origin, the system in (4.9) becomes

$$\begin{aligned}
\dot{r} &= \mu r + (1 + 2a\,\hat{x}_{3i}) r x_3 + a r x_3^2 - r^3 \,, \\
\dot{x}_3 &= (\mu_2 + 2b\,\hat{x}_{3i} - 3d(\hat{x}_{3i})^2) x_3 + (b - 3d\,\hat{x}_{3i}) x_3^2 - c\,\hat{x}_{3i}\, r^2 - c r^2 x_3 - d x_3^3 \,, \\
\dot{\mu} &= 0 \,,
\end{aligned}$$

where $\mu = \mu_1 + \hat{x}_{3i} + a(\hat{x}_{3i})^2$. The bifurcation value is $\mu = 0$. By the center manifold theorem, the center manifold of $(0, \hat{x}_{3i})$ is locally represented by $x_3 = g(r, \mu)$ with $g(0,0) = Dg(0,0) = 0$. Let

$$x_3 = g(r, \mu) = a_1 r^2 + a_2 r\mu + a_3 \mu^2 + \mathcal{O}(3),$$

then $g(r, \mu)$ must satisfy the quasi linear partial differential equation given by

$$\begin{aligned}
D_r g(r,\mu) \Big\{ \mu r + (1 + 2a\,\hat{x}_{3i}) r g(r,\mu) + a g^2(r,\mu) r - r^3 \Big\} \\
-(\mu_2 + 2b\,\hat{x}_{3i} - 3d(\hat{x}_{3i})^2) g(r,\mu) \\
-(b - 3d\,\hat{x}_{3i}) g^2(r,\mu) - c\,\hat{x}_{3i}\, r^2 - c r^2 g(r,\mu) - d g^3(r,\mu) = 0 \,.
\end{aligned}$$

Substituting $g(r, \mu) = a_1 r^2 + a_2 r\mu + a_3 \mu^2 + \mathcal{O}(3)$ in the above equation and equating coefficients of like powers we obtain

$$\begin{aligned}
a_1 &= \frac{c\hat{x}_{3i}}{\mu_2 + 2b\hat{x}_{3i} - 3d(\hat{x}_{3i})^2} \,, \\
a_2 &= 0, \\
a_3 &= 0,
\end{aligned}$$

provided $\mu_2 + 2b\,\hat{x}_{3i} - 3d(\hat{x}_{3i})^2 \neq 0$. Hence on the center manifold of $(0, \hat{x}_{3i})$ the dynamics of (4.9) are governed by the equation

$$\dot{r} = \mu r + \Big\{ (1 + 2a\,\hat{x}_{3i}) a_1^2 - 1 \Big\} r^3 + \mathcal{O}(4).$$

Thus a pitchfork bifurcation occurs at $(0, \hat{x}_{3i})$ with critical value $\mu = 0$, provided $a_1 \neq 0$ (i.e. $\hat{x}_{3i} \neq 0$).

Finally, for $\mu_1 > 0$ the fixed point $(\sqrt{\mu_1}, 0)$ can undergo a transcritical bifurcation. This corresponds to a transcritical bifurcation of limit cycles off the x_1x_2−plane for the original system (3.15). Recall that for $\mu_1 > 0$, $(\sqrt{\mu_1}, 0)$ is a sink if and only if $c\mu_1 - \mu_2 > 0$, otherwise it is a saddle type fixed point.

If $\beta < 0$, assume $-(c-b) > 0$ and $ac + d > 0$ in equation (4.20). The remaining three possible cases (for $\beta < 0$) are treated in a similar fashion. If $c\mu_1 - \mu_2 = 0$, then from (4.20) we have $(\tilde{r}_2, \tilde{x}_{32}) = (\sqrt{\mu_1}, 0)$. When $c\mu_1 - \mu_2 = \varepsilon$, for $\varepsilon > 0$ sufficiently small, the fixed point $(\tilde{r}_2, \tilde{x}_{32})$ is in the first quadrant above the point $(\sqrt{\mu_1}, 0)$. When $c\mu_1 - \mu_2 = -\varepsilon$, $(\tilde{r}_2, \tilde{x}_{32})$ is in the fourth quadrant just below $(\sqrt{\mu_1}, 0)$. Hence, at $c\mu_1 - \mu_2 = 0$, the fixed point $(\sqrt{\mu_1}, 0)$ undergoes a transcritical bifurcation. A similar argument holds for the case $\beta > 0$.

4.3.3 Bifurcations in the Interior

There are two possible interior fixed points $(\tilde{r}_i, \tilde{x}_{3i})$ of (4.9). They correspond to interior limit cycles for the original system (3.15).

First, the fixed points $(\tilde{r}_i, \tilde{x}_{3i})$ can arise and split via a saddle-node bifurcation. For a saddle-node bifurcation to occur we must have exactly one associated eigenvalue zero. From equation (4.21), this implies that we must have $\det(J(\tilde{r}_i, \tilde{x}_{3i})) = 0$ and $tr(J(\tilde{r}_i, \tilde{x}_{3i})) \neq 0$, where $tr(J(\tilde{r}_i, \tilde{x}_{3i}))$ and $\det(J(\tilde{r}_i, \tilde{x}_{3i}))$ are given by (4.22) and (4.23) respectively. Let

$$\mu = c\mu_1 - \mu_2 - \frac{(c-b)^2}{4(ac+d)},$$

then at $\mu = 0$ we have, from (4.20), $\tilde{x}_{31} = \tilde{x}_{32} = -(c-b)/2(ac+d) \equiv \tilde{x}$. Moreover, $\det(J(\tilde{r}_i, \tilde{x}_{3i})) = 0$ if and only if $\mu = 0$ (since $\tilde{r}_i > 0$). Then

at $\mu = 0$ we have $\det(J(\tilde{r}_i, \tilde{x}_{3i})) = 0$ and $tr(J(\tilde{r}_i, \tilde{x}_{3i})) \neq 0$ provided $\mu_1 \neq \frac{(b-2)}{2}\tilde{x} - (a+d)\tilde{x}^2$. Taking into consideration that we have at most two interior fixed points for system (4.9), and noting that small perturbations from $\mu = 0$ result in either no value or two distinct positive values for $\tilde{x}_{3i}$, then a saddle-node bifurcation occurs at $\mu = 0$. This of course corresponds to a saddle-node bifurcation of limit cycles in the interior for system (3.15).

Next, the fixed points $(\tilde{r}_i, \tilde{x}_{3i})$ can undergo a Hopf bifurcation. In general for a Hopf bifurcation to occur about one of the fixed points $(\tilde{r}_i, \tilde{x}_{3i})$ we must have at least a pair of pure imaginary associated eigenvalues. This would imply $tr(J(\tilde{r}_i, \tilde{x}_{3i})) = 0$ and $\det(J(\tilde{r}_i, \tilde{x}_{3i})) > 0$. However due to the complexity of the expressions in (4.22) and (4.23), it is difficult to show a Hopf bifurcation occurs in general. Instead we provide two numerical examples of a Hopf bifurcation. The first is an example of a subcritical Hopf bifurcation and the second is an example of a supercritical bifurcation.

First assume $a = c = 1$, $b = d = -2$ and $\mu_2 = 1$. Thus from equations (4.19) and (4.20) we have

$$\tilde{x}_{31} = \frac{-3 + \sqrt{9 + 4(\mu_1 - 1)}}{-2} \text{ and } \tilde{r}_1 = \sqrt{\mu_1 + \tilde{x}_{31} + (\tilde{x}_{31})^2}.$$

In addition,

$$tr(J(\tilde{r}_1, \tilde{x}_{31})) = -2\mu_1 - 4\tilde{x}_{31} + 2(\tilde{x}_{31})^2,$$

$$\det(J(\tilde{r}_1, \tilde{x}_{31})) = -2\tilde{r}_1^2 \left\{\mu_1 - 1 + (\tilde{x}_{31})^2\right\}.$$

At $\mu_1 = -1$, we have $(\tilde{r}_1, \tilde{x}_{31}) = (1, 1)$ and $trJ((\tilde{r}_1, \tilde{x}_{31})) = 0$ with $\det(J(\tilde{r}_1, \tilde{x}_{31})) = 2 > 0$. Thus the associated eigenvalues at $\mu_1 = -1$ are $\beta_{1,2} = \pm i\sqrt{2}$. In a neighborhood of $\mu_1 = -1$, the real parts of the eigenvalues are

$$\mathbf{Re}(\beta_{1,2}) = \frac{tr(J(\tilde{r}_1, \tilde{x}_{31}))}{2}.$$

Hence the transversality condition evaluated at $\mu_1 = -1$ is

$$\frac{d}{d\mu_1}(\mathbf{Re}(\beta_{1,2})) = \frac{1}{2}\left\{-2 - 4\frac{d}{d\mu_1}(\tilde{x}_{31}(\mu_1)) + 4\left(\frac{d}{d\mu_1}(\tilde{x}_{31}(\mu_1))\right)\tilde{x}_{31}(\mu_1)\right\},$$

with

$$\frac{d}{d\mu_1}(\tilde{x}_{31}(\mu_1)) = -\frac{1}{\sqrt{9 + 4(\mu_1 - 1)}}.$$

Thus at $\mu_1 = -1$, we have

$$\frac{d}{d\mu_1}(\mathbf{Re}(\beta_{1,2})) = \frac{1}{2}\{-2 - 4(-1) + 4(-1)\} = -1 \neq 0.$$

Hence a Hopf bifurcation occurs about $(\tilde{r}_1, \tilde{x}_{31}) = (1, 1)$ with bifurcation value $\mu_1 = -1$.

To determine the stability of the emerging limit cycle, we shift $(1, 1)$ to the origin subject to the bifurcation condition $\mu_1 = -1$, and obtain the following vector field

$$\begin{pmatrix} \dot{r} \\ \dot{x}_3 \end{pmatrix} = \begin{pmatrix} -2 & 3 \\ -2 & 2 \end{pmatrix}\begin{pmatrix} r \\ x_3 \end{pmatrix} + \begin{pmatrix} 3rx_3 + x_3^2 - 3r^2 + rx_3^2 - r^3 \\ -2rx_3 + 4x_3^2 - r^2 - r^2x_3 + 2x_3^3 \end{pmatrix}.$$

Applying the similarity transformation

$$\begin{pmatrix} r \\ x_3 \end{pmatrix} = \begin{pmatrix} -2 & \sqrt{2} \\ -2 & 0 \end{pmatrix}\begin{pmatrix} u \\ v \end{pmatrix},$$

to the vector field above, we obtain

$$\begin{pmatrix} \dot{u} \\ \dot{v} \end{pmatrix} = \begin{pmatrix} 0 & -\sqrt{14} \\ \sqrt{14} & 0 \end{pmatrix}\begin{pmatrix} u \\ v \end{pmatrix} + \begin{pmatrix} f(u,v) \\ g(u,v) \end{pmatrix},$$

where

$$\begin{aligned} f(u,v) &= -2u^2 + 4\sqrt{2}uv + v^2 + 4u^3 - 4\sqrt{2}u^2v - 2uv^2, \\ g(u,v) &= -(2\sqrt{2} - \tfrac{4}{\sqrt{2}})u^2 - 2uv + 2\sqrt{2}v^2 + (2\sqrt{2} - \tfrac{4}{\sqrt{2}})u^3 \\ &\quad -4\sqrt{2}uv^2 - 2v^3. \end{aligned}$$

Using the vague attractor condition ([14]),

$$\alpha = \frac{1}{16}\{f_{uuu} + f_{uvv} + g_{uuv} + g_{vvv} + \frac{1}{s}((f_{uv}(f_{uu} + f_{vv}) - g_{uv}(g_{uu} + g_{vv}) - f_{uu}g_{uu} + f_{vv}g_{vv})\}$$

evaluated at $(u, v) = (0, 0)$, we obtain $\alpha = \sqrt{2} > 0$. Thus we have a subcritical Hopf bifurcation about $(1, 1)$ at $\mu_1 = -1$.

The resulting Hopf bifurcation about $(\tilde{r}_i, \tilde{x}_{3i})$ can be supercritical as well. For example, assume $a = 3$, $b = 2$, $c = 1$, $d = -2$ and $\mu_2 = 1$. Then at $\mu_1 = -1$, there is a Hopf bifurcation at $(\tilde{r}_1, \tilde{x}_{31}) = (1, -1)$. Proceeding as above, we obtain $\alpha = -5/6 < 0$, and the transversality is equal to $-7/3$. Thus we have a supercritical Hopf bifurcation.

A Hopf bifurcation in the rx_3-plane, for system (4.9), implies the existence of invariant tori and quasi periodic motion for the original system (3.15). We will discuss this phenomenon in more detail in the following section on global bifurcations of the normal form (4.9).

4.4 Global Bifurcations

We begin this section by initially ignoring the problem of the undetermined sign of the rescaling constant β. That is, we assume a, b, d are arbitrary scalars, c a positive scalar and restrict our analysis to the positive quadrant of rx_3-plane. After determining what global bifurcations are possible under these conditions, we then consider the rescaling constant β and how it effects these global bifurcations.

There are two types of global bifurcations that are of interest to us. The first type is the homoclinic bifurcation. This type of global bifurcation occurs when the stable and unstable manifolds of a saddle type fixed point

intersect. Since we are considering a smooth vector field, and since initial value problems have unique solutions, it follows that the stable and unstable manifolds of the saddle point must not only intersect at a single point but rather along a smooth closed curve. The $r-$axis and x_3-axis are invariant for (4.9) and thus if a homoclinic bifurcation is to occur it must occur in the interior of the positive quadrant. Existence of a homoclinic bifurcation for the planar system (4.9) implies that there is a fixed point inside the homoclinic loop. Since there are at most two interior fixed points for (4.9), the homoclinic bifurcation must involve both of them. One is a saddle type fixed point and the other a sink or source contained inside the loop.

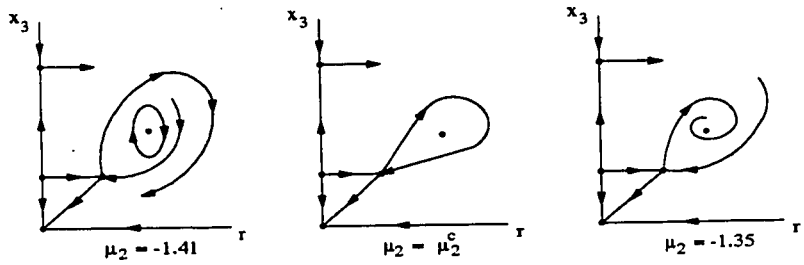

Figure 4.3 : Let μ_2 be the bifurcation parameter with $\mu_1 = -0.41$, $a = 0.4$, $b = 4.0$, $c = 1.5$ and $d = 1.0$. A homoclinic bifurcation occurs for μ_2 between -1.41 and -1.35.

We demonstrate the occurrence of a homoclinic bifurcation for (4.9) by considering the possible intersections of nullclines of (4.9) and then determining how the separatices change due to the bifurcation. Figure 4.3 illustrates a homoclinic bifurcation for (4.9). Figures 4.4 and 4.5 depict the same type of homoclinic bifurcation but in different parameter ranges. In both of these examples the fixed point $(\sqrt{\mu_1}, 0)$ exists in the positive quadrant and in one case the transcritical bifurcation at the origin has not yet occurred while in the other case the origin has undergone a transcritical bifurcation.

For the full system (3.15), the homoclinic loop manifests itself as a pinched torus in three-space. Due to the presence of the saddle type limit cycle the flow is not toroidal. Under small perturbations we expect the homoclinic connection to break and the stable and unstable manifolds of the saddle to intersect transversely, giving rise to horseshoe dynamics near the saddle type limit cycle.

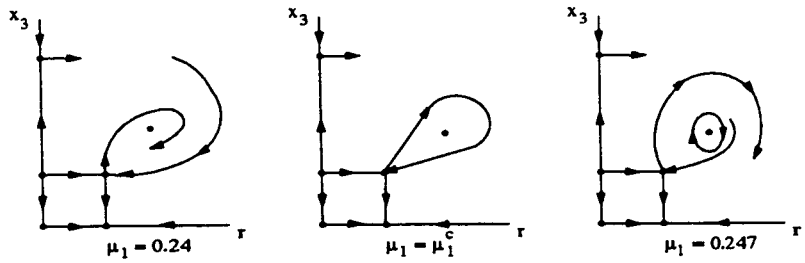

Figure 4.4 : Let μ_1 be the bifurcation parameter with $\mu_2 = -1.0$, $a = -0.25$, $b = 10.0$, $c = 5.0$ and $d = 4.0$. A homoclinic bifurcation occurs for μ_1 between 0.24 and 0.247.

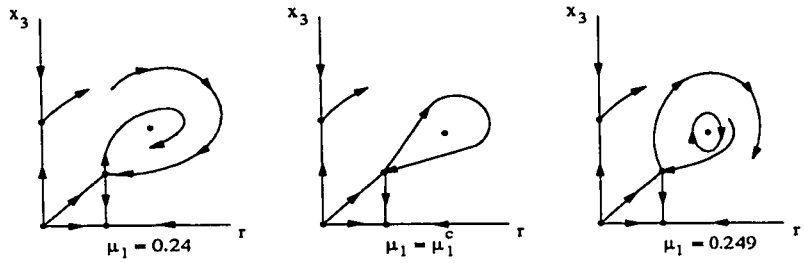

Figure 4.5 : Let μ_1 be the bifurcation parameter with $\mu_2 = 0.5$, $a = -0.25$, $b = 7.0$, $c = 5.0$ and $d = 2.5$. A homoclinic bifurcation occurs for μ_1 between 0.24 and 0.249.

The second type of global bifurcation that we are interested in is the heteroclinic bifurcation. The simplest heteroclinic loop occurs when the stable and unstable manifolds of a fixed point coincide with the unstable and stable manifolds, respectively, of another fixed point. A heteroclinic loop can only occur for (4.9) if it involves the fixed points on the r—axis or x_3—axis since

one of $(\tilde{r}_i, \tilde{x}_{3i})$ is always a sink or source and thus must be contained inside the loop. Again, by examining the possible intersections of nullclines and then determining how the separatices change via the bifurcation, we demonstrate the occurrence of a heteroclinic loop for (4.9).

First, notice that if the fixed point $(\sqrt{\mu_1}, 0)$ is to be a part of a heteroclinic loop then we must have $c\mu_1 - \mu_2 < 0$. When $(\sqrt{\mu_1}, 0)$ exists (i.e. $\mu_1 > 0$) it always has the $r-$axis as part of its stable manifold, hence if it is to be a part of a heteroclinic loop, it must be a saddle which implies $c\mu_1 - \mu_2 < 0$. Moreover, under these conditions, the flow on the x_3-axis must decrease near the origin. Thus $\mu_2 < 0$. However, since $c > 0$, then $c\mu_1 - \mu_2 > 0$. Therefore the fixed point $(\sqrt{\mu_1}, 0)$ cannot be a part of a heteroclinic loop. If we allow c to be negative, then we could have a heteroclinic cycle as depicted in Figure 4.6. However, even with $c < 0$, the heteroclinic bifurcation depicted in Figure 4.6 is still not possible for the original system (3.15) since solutions must be bounded.

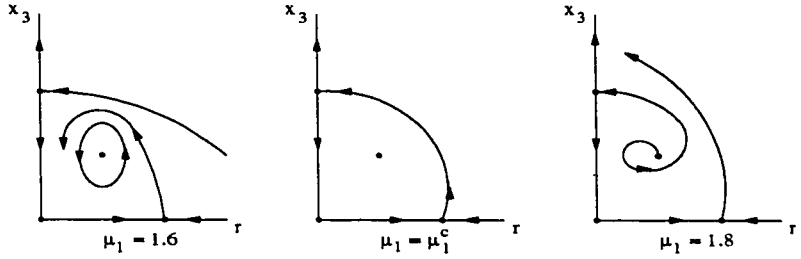

Figure 4.6 : Fix $\mu_2 = -1.0$, $a = -1.0$, $b = 0.4$, $c = -1.0$ and $d = 0.0$. Let μ_1 be the bifurcation parameter, then a heteroclinic bifurcation occurs for μ_1 between -1.6 and -1.8.

Taking the above observation into consideration, if a heteroclinic loop is to occur for system (4.9) for realistic parameter values, it must involve the two fixed points on the x_3-axis. Figure 4.7 depicts such a heteroclinic cycle. For the full system (3.15), this type of heteroclinic cycle manifests itself as an

invariant sphere. Under small perturbations the sphere breaks up resulting in horseshoe dynamics.

Note that a heteroclinic loop similar to Figure 4.7 but with the direction of the flow reversed is not possible for system (3.15) since solutions must be bounded. Also, a heteroclinic loop similar to Figure 4.7 but involving both fixed points $(\tilde{r}_i, \tilde{x}_{3i})$ is not possible. This would require the r-nullcline to cross the x_3-axis once between the saddle-type fixed points $(0, \hat{x}_{3i})$ but yet intersect the x_3-nullcline twice in the interior. Consideration of the nullclines in Figures 4.1 and 4.2 shows this to be impossible.

We now consider the rescaling constant β and the effect it has on these global bifurcations. Note that regardless of the sign of β, the heteroclinic bifurcation of Figure 4.6 is not possible.

First assume $\beta > 0$. Thus our analysis is confined to the first quadrant of the rx_3-plane and $b < 0$. In the global bifurcations depicted in Figures 4.3, 4.4 and 4.7 there are two saddle type fixed points on the x_3-axis and $\mu_2 < 0$. From equation (4.18), it is clear for both fixed points $(0, \hat{x}_{3i})$ to reside in the positive quadrant we require at least $d < 0$. But then this forces $\mu_2 > 0$. Hence these global bifurcations are not possible for $\beta > 0$.

Next, consider the homoclinic bifurcation depicted in Figure 4.5. For this bifurcation to occur we require at least both fixed points $(\tilde{r}_i, \tilde{x}_{3i})$ to reside in the first quadrant and $c\mu_1 - \mu_2 > 0$. From equation (4.20), since $b < 0$ then $-(c - b) < 0$ and thus $(ac + d) < 0$. But then this forces $c\mu_1 - \mu_2 < 0$. Hence, this homoclinic bifurcation is not possible for $\beta > 0$.

Assume $\beta < 0$. Our analysis is now restricted to the fourth quadrant of the rx_3-plane and $b > 0$. By an argument similar to the one used in the case when $\beta > 0$, the global bifurcations depicted in Figures 4.3, 4.4 and 4.7 are not possible.

Whether or not the homoclinic bifurcation of Figure 4.5 is possible for $\beta < 0$ remains an open question. Although there is no simple immediate reason why this bifurcation cannot happen for system (4.9), we have not been able to find a viable set of parameters for this bifurcation to occur.

Remark : Guckenheimer and Holmes ([14]) found a heteroclinic orbit of the type shown in Figure 4.7 for this particular type of codimension 'two' bifurcation. The truncated normal form they considered had two saddle-type fixed points on the x_3- axis, $\vec{p}_1$ and $\vec{p}_2$. The fixed point $\vec{p}_1$ had a two dimensional stable manifold, $W^s(\vec{p}_1)$, and a one dimensional unstable manifold, $W^u(\vec{p}_1)$, while $\vec{p}_2$ had a one dimensional stable manifold and a two dimensional unstable manifold. $W^s(\vec{p}_1)$ coincided with $W^u(\vec{p}_2)$ to form an invariant sphere in three-space as was also the case for Figure 4.7.

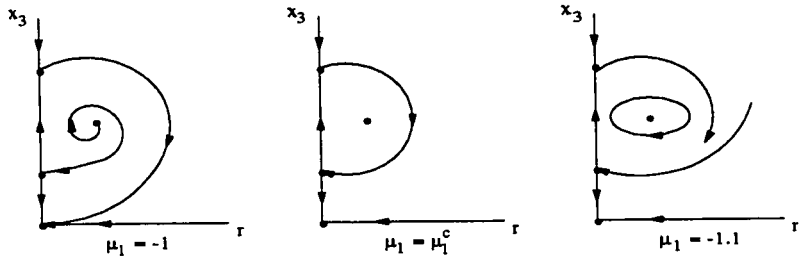

Figure 4.7 : Fix $\mu_2 = -1.0$, $a = 0.0$, $b = 4.0$, $c = 6.0$ and $d = 1.0$. Let μ_1 be the bifurcation parameter, then a heteroclinic bifurcation occurs for μ_1 between -1.0 and -1.1.

Generically, one would not expect the one dimensional unstable manifold $W^u(\vec{p}_1)$ and the one dimensional stable manifold $W^s(\vec{p}_2)$ to intersect in three-space. Similarly, one would expect the two dimensional unstable manifold $W^u(\vec{p}_2)$ and the two dimensional stable manifold $W^s(\vec{p}_1)$ to intersect along one dimensional curves in three-space. One also expects that higher order terms of the normal form to affect this structure. The fact that this is indeed the case was shown by Broer and Vegter ([3]). They showed that

when this structure breaks up, the branch of $W^u(\vec{p}_1)$ inside the sphere falls into $W^s(\vec{p}_1)$, or, similarly the branch of $W^s(\vec{p}_2)$ inside the sphere falls into $W^u(\vec{p}_2)$, producing a Sil'nikov bifurcation about one of the fixed points $\vec{p}_1$, $\vec{p}_2$.

Taking this into consideration, it is not unreasonable to hypothesize that a similar scenario may occur for the homoclinic bifurcations in Figures 4.3, 4.4, and 4.5. That is, when higher order terms are considered in the normal form (4.9), the homoclinic structure breaks giving rise to a Sil'nikov phenomenon about one of the fixed points $(\tilde{r}_i, \tilde{x}_{3i})$. For the original system this would imply a Sil'nikov bifurcation about a limit cycle in the interior of the positive octant. This of course remains an open question which we plan to investigate further.

4.5 Parameter Comparison

In the previous two sections we described the dynamical behavior of the normal form near bifurcation. Now we would like to determine how the parameters of the unfolded normal form in (4.9) are related to the parameters of the original system in (3.15). This would enable us to determine how the dynamical behavior of the unfolding can be obtained in the original model. However, this task can be rather complicated and quite often impossible to accomplish. These complications and difficulties are common to all such normal form calculations and are discussed in [50] and [14], for example. For the sake of completeness, we include a similar discussion here.

Consider the system of differential equations given by

$$\dot{\mathbf{x}} = f_\mu(\mathbf{x}) \text{ for } \mathbf{x} \in \mathbf{R}^n,\ \mu \in \mathbf{R}^p,\ p \geq 1. \tag{4.1}$$

Assume $\mathbf{x}_0$ is a fixed point of (4.1) and that there is a finite codimension m

bifurcation at $(\mathbf{x}_0, \mu_0)$. For the purpose of this discussion, let $f_\mu(\mathbf{x})$ be analytic at $(\mathbf{x}_0, \mu_0)$. The normal form theorem tells us that we can always compute a normal form for f_μ, about $(\mathbf{x}_0, \mu_0)$, to any degree $d \geq 2$. The first thing we do in order to compute a normal form for f_{μ_0} is to Taylor expand f_{μ_0} about the fixed point $\mathbf{x}_0$. After translating $\mathbf{x}_0$ to the origin and truncating at degree d we obtain the sum $g(\mathbf{x})$, called a $d-$jet of f_{μ_0} about $\mathbf{x}_0$, given by

$$g(\mathbf{x}) = \sum_{k=1}^{d} g_k(\mathbf{x})$$

where $g_k \in P_k^n$.

Next, we apply the linear transformation T_1 to $g(\mathbf{x})$, which puts the Jacobian into real Jordan canonical form. We then apply $d-1$ near linear transformations T_i $(i = 2, ...d)$ which take the degree i terms into 'normal' form. Recall that the choice of near linear transformations T_i are not unique in general and each near linear transformation is chosen in such a way as to not change the lower degree terms that have already been 'normalized'. Define V_d^n to be the set of all $d-$jets in $\mathbf{R}^n$ about $\mathbf{x} = \mathbf{0}$. Then there is a map

$$T : V_d^n \to V_d^n$$

given by $T = T_d \circ T_{d-1} \circ ... \circ T_1$. Hence, T is a transformation which takes our $d-$jet, $g(\mathbf{x})$, into a normal form $T(g(\mathbf{x}))$.

For any $f_k(\mathbf{x}) \in P_k^n$, we may write $f_k(\mathbf{x}) = \mu_k b_k$, where μ_k denotes f_k's coefficient matrix and b_k is the column vector consisting of the standard basis for P_k^n. If we let $\mu = (\mu_1, ..., \mu_d)^T$ denote the vector of coefficient matrices μ_k for $f(\mathbf{x}) \in V_d^n$, then we may define the parameter space, Ω_d^n, of the $d-$jets in $\mathbf{R}^n$ (about $\mathbf{x} = 0$) to be the set

$$\Omega_d^n = \left\{ \mu = (\mu_1, ..., \mu_d)^T : f(\mathbf{x}) = \sum_{k=1}^{d} \mu_k b_k \in V_d^n,\ \mu_k \in \mathbf{R}^{q_k} \right\}$$

where $q_k = n\begin{pmatrix} n+k-1 \\ k \end{pmatrix}$. Notice that, by construction, Ω_d^n is isomorphic to $\mathbf{R}^p$ where $p = \sum_{k=1}^{d} q_k$.

Next, we define the homeomorphism

$$h : V_d^n \to \Omega_d^n$$

by

$$h(f(\mathbf{x})) = h(\sum_{k=1}^{d} \mu_k b_k) := (\mu_1, ..., \mu_d)^T,$$

where $f(\mathbf{x}) = \sum_{k=1}^{d} \mu_k b_k \in V_d^n$. Thus, the study of the vector field $f(\mathbf{x}) \in V_d^n$ can be reduce to the study of its coefficients in Ω_d^n via the homeomorphism h. Similarly, the corresponding normal form $T(f(\mathbf{x}))$ can be reduced to the study of its coefficients via the same homeomorphism. Our goal is to compare the parameters of the original vector field $g(\mathbf{x})$ to the parameters of the normal form $T(g(\mathbf{x}))$. To accomplish this, we define the map

$$T^* : \Omega_d^n \to \Omega_d^n$$

by $T^* = h \circ T \circ h^{-1}$. Hence the following diagram commutes.

$$\begin{array}{ccc} V_d^n & \xrightarrow{T} & V_d^n \\ {\scriptstyle h}\downarrow & & {\scriptstyle h}\downarrow \\ \Omega_d^n & \xrightarrow{T^*} & \Omega_d^n \end{array}$$

The transformation T^* takes the parameters $\mu_0 \in \Omega_d^n$ of the original $d-$jet to the coefficients $\nu_0 \in \Omega_d^n$ of the $d-$jet in normal form. That is, $T^*\mu_0 = \nu_0$.

As mentioned above, the study of the original $d-$jet, $g(\mathbf{x})$, can now be reduced to considering its corresponding coefficients. We must now consider small perturbations in the vector of coefficient matrices and thus need to define a norm on Ω_d^n. Define

$$||\mu - \mu_0|| = \sum_{k=1}^{d} ||\mu_k - (\mu_0)_k||_{mat}$$

where $||...||_{mat}$ is the standard matrix norm given by

$$||A||_{mat} = \max_{i,j} |a_{ij}|, \ A = (a_{ij}).$$

Consider μ such that $||\mu - \mu_0||$ is small and let $\nu = T^*\mu$. Since T is a C^∞ transformation, by definition, T^* is continuous and we may write

$$T^*\mu = \nu = \nu_0 + \varepsilon$$

where $\varepsilon \to 0$ as $\mu \to \mu_0$. Hence $\nu_0 + \varepsilon$ represents the unfolding of the normal form. That is to say, ν_0 is the coefficient vector of the $d-$jet in normal form (at bifurcation) and the non-zero entries in ε (whose corresponding entries in ν_0 are zero) give rise to the unfolding which describes the behavior of the original vector field f_μ.

Caution :

Let $\nu_0 + \delta$, for $||\delta||$ small, represent another unfolding of the normal form.

1) Assume $\delta \neq \varepsilon$. That is to say, δ has at least one nonzero entry in a position where ε has a zero entry. In this case, it may be impossible to obtain the unfolding $\nu_0 + \delta$ from the original model. There may be no transformation T that takes the original model into a normal form that has $\nu_0 + \delta$ as its vector of coefficient matrices.

2) If $\nu_0 + \delta$ can be obtained from a different normal form transformation, then one would expect the unfolding $\nu_0 + \delta$ to exhibit topologically distinct dynamical behavior from $\nu_0 + \varepsilon$.

In a neighborhood of a bifurcation there may be unfoldings that can not be obtained by varying the parameters in the original model. In general,

a model of a real system is only an approximation and hence it is reasonable to assume that the model itself undergoes a bifurcation. In this case, all small perturbations from bifurcation (which are reasonable for the model) could be possible and thus must be considered.

Example 3: Consider the following system of linear differential equations given by

$$\begin{aligned} \dot{x_1} &= -bx_2 \\ \dot{x_2} &= cx_1 + dx_2 \end{aligned} \tag{4.2}$$

where b, c are positive scalars and d is an arbitrary scalar. The origin is the only fixed point of (4.2), with associated eigenvalues

$$\zeta_{1,2} = \frac{d \pm \sqrt{d^2 - 4bc}}{2}.$$

At $d = 0$ there is a bifurcation. Let $\mathbf{x} = (x_1, x_2)$ and

$$\mathbf{f}(\mathbf{x}) = \begin{pmatrix} f_1(x_1, x_2) \\ f_2(x_1, x_2) \end{pmatrix} = \begin{pmatrix} -bx_2 \\ cx_1 + dx_2 \end{pmatrix},$$

then, using the notation of this section, we may write $\mathbf{f}(\mathbf{x}) = \mu_1 b_1$ where

$$\mu_1 (= \mu) = \begin{pmatrix} 0 & -b \\ c & d \end{pmatrix} \text{ and } b_1 = \begin{pmatrix} x_1 \\ x_2 \end{pmatrix}.$$

Thus there is a bifurcation at

$$\mu_0 = \begin{pmatrix} 0 & -b \\ c & 0 \end{pmatrix}, \text{ i.e. } \mu_1^{(4)} = d = 0.$$

For system (4.2), the 1−jet about $(0, 0)$ (at bifurcation) is given by

$$g(\mathbf{x}) = \begin{pmatrix} 0 & -b \\ c & 0 \end{pmatrix} \begin{pmatrix} x_1 \\ x_2 \end{pmatrix},$$

and the normal form is given by

$$T(g(\mathbf{x})) = F(\mathbf{x}) = A^{-1}\mu_0 A\mathbf{x} = \begin{pmatrix} 0 & \sqrt{bc} \\ -\sqrt{bc} & o \end{pmatrix} \begin{pmatrix} x_1 \\ x_2 \end{pmatrix},$$

where

$$A = \begin{pmatrix} 0 & \sqrt{\frac{b}{c}} \\ 1 & 0 \end{pmatrix}.$$

The parameter transformation, T^*, is defined by the equation

$$T^*\mu_0 = \nu_0 = \begin{pmatrix} 0 & \sqrt{bc} \\ -\sqrt{bc} & 0 \end{pmatrix},$$

and hence

$$T^* = \begin{pmatrix} -\sqrt{\frac{c}{b}} & 0 \\ 0 & -\sqrt{\frac{b}{c}} \end{pmatrix}.$$

Thus in general we have

$$T^*\mu = \begin{pmatrix} -\sqrt{\frac{c}{b}} & 0 \\ 0 & -\sqrt{\frac{b}{c}} \end{pmatrix} \begin{pmatrix} 0 & -b \\ c & d \end{pmatrix} = \begin{pmatrix} 0 & \sqrt{bc} \\ -\sqrt{bc} & -d\sqrt{\frac{b}{c}} \end{pmatrix} = \nu,$$

or equivalently,

$$T^*\mu = \begin{pmatrix} 0 & \sqrt{bc} \\ -\sqrt{bc} & 0 \end{pmatrix} + \begin{pmatrix} 0 & 0 \\ 0 & -d\sqrt{\frac{b}{c}} \end{pmatrix} = \nu_0 + \varepsilon.$$

Thus ε represents a choice of unfolding parameters for $F(\mathbf{x})$.

One could have chosen an unfolding of $F(\mathbf{x})$ that was not representative of the original system (4.2). For example, one could choose the unfolding $F^1(\mathbf{x})$ given by

$$F^1(\mathbf{x}) = \begin{pmatrix} a & \sqrt{bc} \\ -\sqrt{bc} & 0 \end{pmatrix} \begin{pmatrix} x_1 \\ x_2 \end{pmatrix} = \nu_0\mathbf{x} + \delta\mathbf{x},$$

where

$$\delta = \begin{pmatrix} a & 0 \\ 0 & 0 \end{pmatrix}.$$

Clearly $T^*\mu$ can not equal $\nu_0 + \delta$, and hence the unfolding is not representative of (4.2). It is still however an unfolding of $F(\mathbf{x})$, and in fact it does not introduce any dynamical behavior different from $\nu_0 + \varepsilon$.

On the other hand, if we had chosen an unfolding of the form

$$F^2(\mathbf{x}) = \begin{pmatrix} 0 & \sqrt{bc} \\ -\sqrt{bc} & a \end{pmatrix} \begin{pmatrix} x_1 \\ x_2 \end{pmatrix},$$

then we could compare coefficients in $F^2(\mathbf{x})$ with the original parameters. Let

$$F^2(\mathbf{x}) = \nu\mathbf{x} = \begin{pmatrix} v_1^{(1)} & v_1^{(2)} \\ v_1^{(3)} & v_1^{(4)} \end{pmatrix} \begin{pmatrix} x_1 \\ x_2 \end{pmatrix},$$

then we have $v_1^{(1)} = 0$, $v_1^{(2)} = \sqrt{bc}$, $v_1^{(3)} = -\sqrt{bc}$ and $v_1^{(4)} = a = -d\sqrt{\frac{b}{c}}$.

What does all this mean for our choice of normal form and subsequent unfolding? First, we were unable to compare parameters as we did in the example above. Second, we do not know if our choice of unfolding is topologically equivalent to an unfolding for which one could compare parameters. Third, we are not sure whether or not the unfolding captures all possible dynamical behavior produced by the original model, or conversely, if the unfolding predicts more behavior than the original model is capable of producing. Fourth, this particular Hopf-transcritical bifurcation may be a codimension ∞ bifurcation (this is an open question for this particular bifurcation), and thus it may be impossible to compare parameters.

4.6 Comparing Bifurcation Behavior

In the previous section we saw that we could not determine how the parameters of the unfolded normal form in (4.9) were related to the parameters of the original system in (3.15). However, we can attempt to identify the bifurcation behavior of the normal form in the original system. In order to accomplish this (at least numerically) we use the bifurcation software package AUTO ([11]).

Below are two bifurcation diagrams for the original system (3.15). In both bifurcation diagrams, solid curves denote curves of fixed points while dashed curves denote curves of limit cycles. Moreover, circles mark Hopf bifurcation points, squares denote transcritical bifurcation points, triangles represent saddle-node bifurcation points and diamonds indicate period doubling bifurcation points. For both diagrams, S^0 is used as the bifurcation parameter.

First, consider Diagram 4.8. The line K_1 represents the planar fixed point $E^3_{S\bullet}$. At $S^0 = 1$, $E^3_{S\bullet}$ is stable and remains stable until we reach the Hopf bifurcation at $S^0 = 1.625$. As S^0 increases past 1.625, we have the emergence of a limit cycle in the x_1x_2-plane and $E^3_{S\bullet}$ is a saddle type fixed point with a two dimensional unstable manifold. At $S^0 = 2.5$, $E^3_{S\bullet}$ undergoes a transcritical bifurcation and for $S^0 > 2.5$, $E^3_{S\bullet}$ is completely unstable. Curve K_2 represents the interior fixed points $E^{\triangle}_{3i}$. The fixed points $E^{\triangle}_{3i}$ are born via a saddle-node bifurcation at $S^0 = 2.45$. The saddle-node bifurcation occurs outside the positive octant (i.e. $x_{3i} < 0$). As S^0 increases, one of the interior fixed points $E^{\triangle}_{3i}$ enters the positive octant via the planar transcritical bifurcation. Increasing S^0 past 2.5, $E^{\triangle}_{3i}$ undergoes a Hopf bifurcation at $S^0 = 2.61075$ followed by a second Hopf bifurcation at $S^0 = 3.59524$. For $S^0 \in (2.5, 2.61075)$, $E^{\triangle}_{3i}$ is a saddle type equilibrium point with a one dimensional stable manifold. $E^{\triangle}_{3i}$ is stable for $S^0 \in (2.61075, 3.59524)$ and for $S^0 \in (3.59524, 5]$ it is again a

saddle type fixed point with a one dimensional stable manifold.

Curve K_3 denotes the planar limit cycle born via the Hopf bifurcation about $E^3_{S^*}$. For $S^0 \in (1.625, 3.68224)$, the limit cycle is stable. At $S^0 = 3.68224$ there is a transcritical bifurcation of limit cycles. For $S^0 > 3.68224$, the planar limit cycle is unstable with the x_1x_2-plane as its stable manifold. Next consider curve K_4 from top to bottom. At $S^0 = 3.3$ there is a saddle type limit cycle just below the x_1x_2-plane in the negative cone. As S^0 increases, the limit cycle enters the positive octant via the transcritical bifurcation at $S^0 = 3.68224$. For $S^0 \in (3.68224, 3.72069)$ this interior limit cycle is stable. At $S^0 = 3.72069$, there is a saddle-node bifurcation of limit cycles. Along curve K_4 for $S^0 \in (2.61075, 3.72069)$ we have an interior saddle type limit cycle.

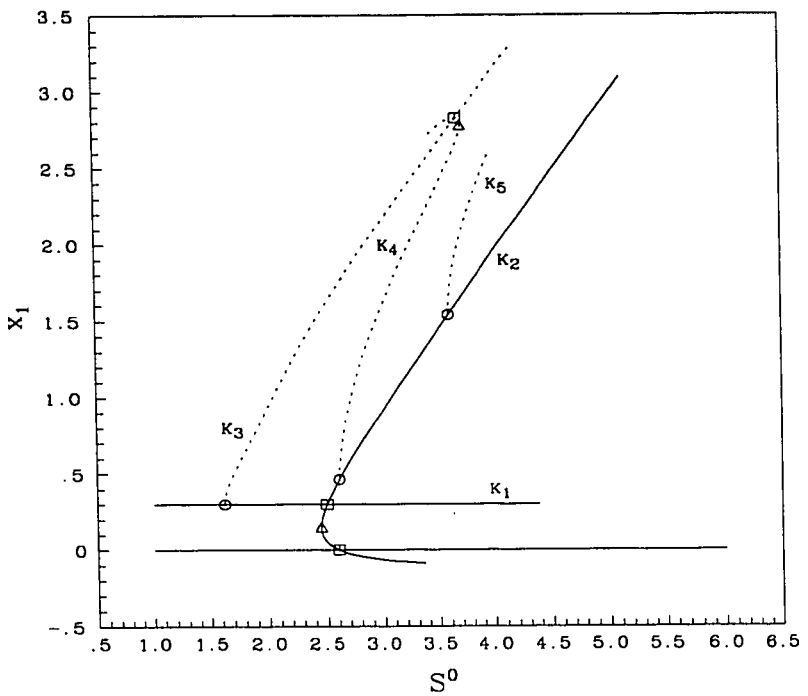

Diagram 4.8 : Parameter values are $\lambda = 0.2$, $\delta_1 = 0.3$, $\delta_2 = 1.2$, $m_1 = 1.5$ and $m_2 = 3.0$.

Finally, curve K_5 represents an interior stable limit cycle. We refrain

from discussing curve K_5 until the following chapter where we consider an intermediate case for model (2.3).

Diagram 4.8 encompasses all of the local bifurcations witnessed in the normal form (4.9) with one exception. There is no bifurcation to a torus in Diagram 4.8, which would correspond to a Hopf bifurcation about $(\tilde{r}_i, \tilde{x}_{3i})$ for the normal form. In all our numerical simulations of the original system (3.15) and subsequent bifurcation analysis using AUTO we have not seen anything that would indicate this type of bifurcation. Thus, with respect to the original system (3.15), we speculate that a bifurcation to a torus is either not possible or if it is possible, it occurs for a relatively small parameter region. What does this mean in terms of our normal form in (4.9)? Our choice of normal form has a $\theta-$independence which probably is not possessed by the original system. As a result, we have probably introduced bifurcation behavior in the normal form that is not present for the original system. If this is the case, then not all of the global bifurcations described for the normal form occur in the original system (3.15). The normal form global bifurcations all involve a Hopf bifurcation in the positive quadrant of the rx_3-plane.

Recall the concluding remark to Section 4.4. The heteroclinic bifurcation in Figure 4.7 is affected by the addition of higher order terms in such a way as to produce a Sil'nikov bifurcation about one of the fixed points $(0, \hat{x}_{3i})$. If the homoclinic bifurcations depicted in Figures 4.3, 4.4 and 4.5 are affected in a similar fashion, then they would represent a Sil'nikov bifurcation about a limit cycle for the original system (3.15). Note that neither the heteroclinic nor the homoclinic bifurcations in this case would require the presence of the Hopf bifurcation about $(\tilde{r}_i, \tilde{x}_{3i})$. Thus the homoclinic bifurcation depicted in Figure 4.5 may still be possible for the original system according to the normal form analysis.

Diagram 4.9 lends some support to this notion. Curve K_1 denotes the fixed point $E^3_{S^\bullet}$. As was the case in Diagram 4.8, $E^3_{S^\bullet}$ undergoes a Hopf bifurcation ($S^0 = 0.465$) and a transcritical bifurcation ($S^0 = 0.9$) and the stability description of $E^3_{S^\bullet}$ is the same. That is, as S^0 increases, $E^3_{S^\bullet}$ changes from locally asymptotically stable to a saddle type fixed point with a two dimensional unstable manifold, and eventually, to completely unstable. Curve K_3 represents the planar limit cycle born via the Hopf bifurcation about $E^3_{S^\bullet}$, and is at least locally asymptotically stable for $S^0 \in (0.465, 1.1)$.

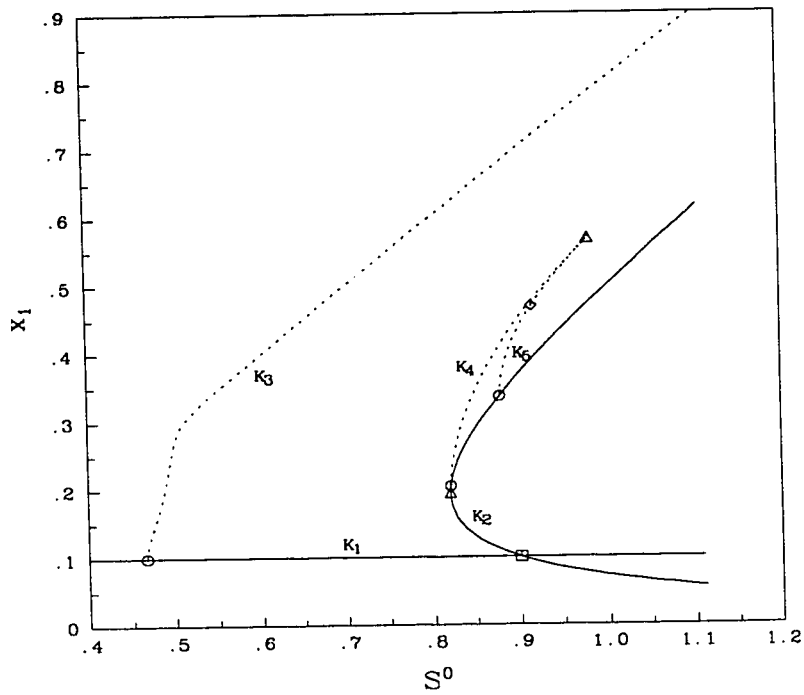

Diagram 4.9 : Parameter values are $\lambda = 0.2$, $\delta_1 = 0.1$, $\delta_2 = 0.2$, $m_1 = 1.1$ and $m_2 = 1.5$.

Curve K_2 denotes the interior equilibria $E^{\triangle}_{3i}$. At $S^0 = 0.818901$, there is a saddle-node bifurcation in the positive octant giving rise to two branches of interior fixed points. One branch of fixed points is initially of saddle type with a two dimensional unstable manifold. The other, initially, is completely

unstable. As S^0 increases, the completely unstable interior fixed point escapes the positive octant via the planar transcritical bifurcation. The saddle type fixed point undergoes a Hopf bifurcation at $S^0 = 0.819363$ and at $S^0 = 0.877366$. For $S^0 \in (0.819363, 0.877366)$ this interior fixed point is stable and for $S^0 \in (0.877366, 1.1)$ it is again a saddle type fixed point with a two dimensional unstable manifold.

Curve K_5 represents the interior limit cycle born via the Hopf bifurcation at $S^0 = 0.877366$. For $S^0 \in (0.877366, 0.91592)$, the limit cycle is asymptotically stable. At $S^0 = 0.91592$, there is a period doubling bifurcation and the limit cycle is now of saddle type until we reach the saddle-node bifurcation at $S^0 = 0.980338$. Curve K_4 is the other interior limit cycle and is of saddle type for $S^0 \in (0.819363, 0.980338)$.

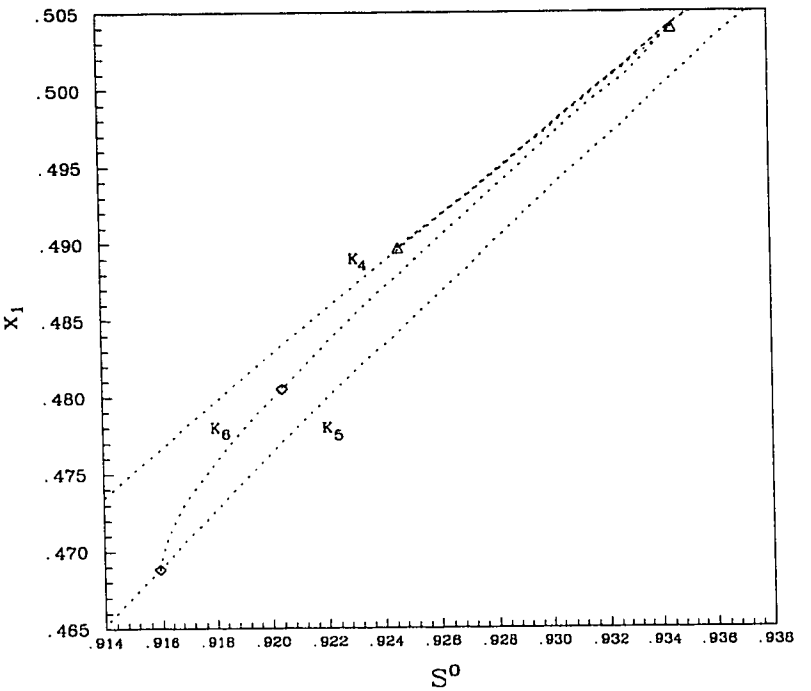

Diagram 4.9a : A closer look at the region about the period doubling bifurcation on curve K_5.

Diagram 4.9a is a blow up of the region about the period doubling bifurcation on curve K_5. Curve K_6 denotes the period 2 limit cycle. The period 2 limit cycle is stable until we reach another period doubling bifurcation at $S^0 = 0.920424$. For $S^0 > 0.920424$, it is of saddle type and undergoes a saddle-node and reverse saddle-node bifurcation respectively at $S^0 = 0.924593$ and $S^0 = 0.934524$. One could continue now to follow the period 4 limit cycle, however, the diagram quickly becomes complicated and AUTO's limitations are tested. Instead, we take a test value of $S^0 = 0.922$ and numerically simulate system (3.15). Figure 4.10 depicts what appears to be a **locally** asymptotically stable attractor for system (3.15) for $S^0 = 0.922$. This attractor could be the result of a Sil'nikov bifurcation about an interior limit as described above.

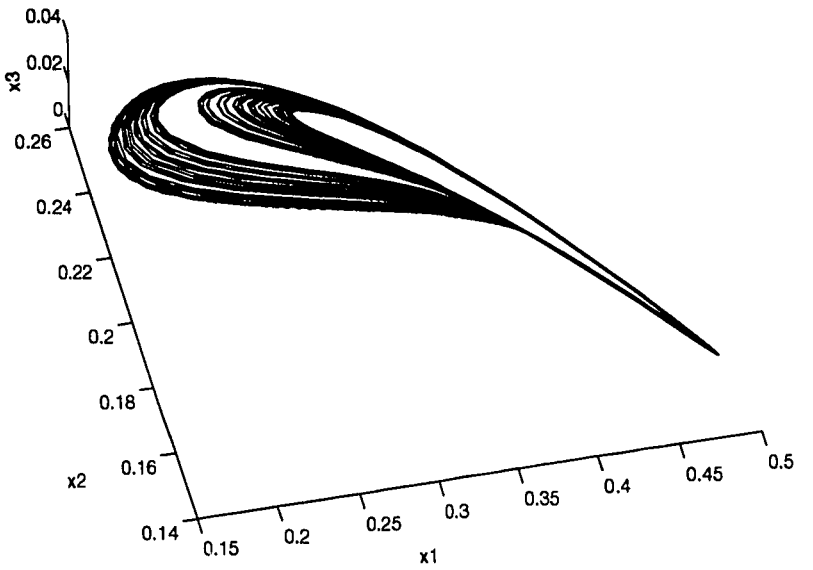

Figure 4.10 : A locally asymptotically stable attractor at $S^0 = 0.922$.

Remark : Recall the Sil'nikov bifurcation about a saddle-focus fixed point in $\mathbf{R}^3$ ([39]). Near the homoclinic connection there is a countable infinity of periodic orbits of saddle type. Moreover, from the subsequent bifurcation analysis of Glendinning and Sparrow ([13]), these periodic orbits are born in

pairs via saddle-node bifurcations. Reconsider the AUTO bifurcation Diagram 4.9a. The period 2 limit cycle (curve K_6) is of saddle type for $S^0 > 0.929424$. The branches of period 2 limit cycles created via the subsequent saddle-node bifurcations are of saddle type. As S^0 approaches the value 0.980338 (the saddle-node bifurcation value of the interior limit cycles K_4 and K_5), AUTO indicates several more saddle-node bifurcations that occur relatively close to one another. These new branches are again of saddle type. That is, AUTO seems to suggest the possibility of a countable infinity of period 2 limit cycles of saddle type. If in fact this is a Sil'nikov bifurcation of a limit cycle in this neighborhood, then there seems to be analogous bifurcation behavior to a Sil'nikov bifurcation about a fixed point.

Chapter 5

Case 4: The Intermediate Case

There are several cases of model (2.3), consisting of various combinations of prototype response functions, that we have not considered yet. In particular, there is one that provides additional insight into the 'exotic' behavior witnessed in system (3.15). This case is described by $h(S)$ and $p_2(x_2)$ being linear uptake functions while $p_1(x_1)$ is a Michaelis-Menten response function. We will refer to this case of model (2.3) as the intermediate case, and consider it below.

5.1 Stability Analysis

The intermediate case of model (2.3) is given by the following system of differential equations

$$\begin{aligned} S' &= S^0 - S - x_1\tfrac{S}{\lambda}, \\ x_1' &= x_1(-1+\tfrac{S}{\lambda}) - x_2\tfrac{m_1x_1}{\delta_1(m_1-1)+x_1}, \\ x_2' &= x_2(-1+\tfrac{m_1x_1}{\delta_1(m_1-1)+x_1}) - x_3\tfrac{x_2}{\delta_2}, \\ x_3' &= x_3(-1+\tfrac{x_2}{\delta_2}), \end{aligned} \tag{5.1}$$

where $m_1 > 1$. As was the case with system (3.11), system (5.1) has five fixed points that may exist in the nonnegative cone. E_0, E_λ and E_{S^*} are as in case

3 and the two interior fixed points are given by

$$E_i^{\Delta} = (S_i^{\Delta}, x_{1i}^{\Delta}, \delta_2, x_{3i}^{\Delta}) \text{ for } i = 1, 2,$$

where S_i^{Δ}, x_{1i}^{Δ} and x_{3i}^{Δ} are as in (3.12).

The local stability description of $E_{S^*} = (S^*, \delta_1, x_2^*, 0)$ is identical to case 3 with the obvious changes. Namely, E_λ and E_{S^*} coalesce at $S^0 = \lambda + \delta_1$ and E_λ loses stability via a transcritical bifurcation as S^0 increases past $\lambda + \delta_1$. At the same time E_{S^*} enters the nonnegative cone. The associated eigenvalues of E_{S^*} are

$$-1, -1 + \frac{x_2^*}{\delta_2} \text{ and } \frac{1}{2}\left\{-\gamma \pm \sqrt{\gamma^2 - \frac{4(S^0 - \lambda - \delta_1)(m_1 - 1)}{\lambda m_1}}\right\},$$

with γ given in (3.13). Thus, $E_{S^*} \in int\mathbf{R}_+^4$ and is locally asymptotically stable provided

$$\lambda + \delta_1 < S^0 < \begin{cases} (\lambda + \delta_1)(1 + \frac{\delta_2}{\delta_1}) \text{ i.e. } x_2^* < \delta_2, \\ \\ (\lambda + \delta_1)(1 + \frac{m_1\delta_1}{\lambda}) \text{ i.e. } \gamma > 0. \end{cases}$$

Notice that the condition above is identical to the condition in (3.14). Proceeding as we did for the model in case 3, we can consider the following three dimensional system

$$\begin{aligned} x_1' &= x_1(-1 + \tfrac{S^0 - x_1 - x_2 - x_3}{\lambda}) - x_2 \tfrac{m_1 x_1}{\delta_1(m_1 - 1) + x_1}, \\ x_2' &= x_2(-1 + \tfrac{m_1 x_1}{\delta_1(m_1 - 1) + x_1}) - x_3 \tfrac{x_2}{\delta_2}, \\ x_3' &= x_3(-1 + \tfrac{x_2}{\delta_2}). \end{aligned} \tag{5.2}$$

As was the case for system (3.15), the fixed point $E_{S^*}^3$ of system (5.2) undergoes a Hopf bifurcation at $S^0 = (\lambda + \delta_1)(1 + m_1\delta_1/\lambda)$ (i.e. $\gamma = 0$) and a transcritical bifurcation at $S^0 = (\lambda + \delta_1)(1 + \delta_2/\delta_1)$ (i.e. $x_2^* = \delta_2$). Hence, the two systems (3.15) and (5.2) share the same local bifurcations, and bifurcation values, about $E_{S^*}^3$.

Moreover, a saddle-node bifurcation involving the interior fixed points, E_{3i}^{Δ}, occurs and it may occur in the positive octant. In fact, if a saddle-node bifurcation of E_{3i}^{Δ} occurs in $int\mathbf{R}_+^3$, it occurs in the same manner as in case 3. That is it must occur after the planar Hopf bifurcation but before the planar transcritical bifurcation about $E_{S\bullet}^3$. The parameter values given in Example 2 (with the exception of m_2) provide an example of this bifurcation for this case as well.

The Jacobian of (5.2) evaluated at $E_{S\bullet}^3$ is similar to the matrix in (4.3) via the same similarity transformation T given in (4.6). Thus, as did system (3.15), system (5.2) lends itself to the same normal form computation and analysis of the previous chapter.

Proceeding as we did in the previous chapter, we compute a normal form for (5.2) expanded about the fixed point $E_{S\bullet}^3$ subject to the same constraints given in (4.2). Note that the normal form calculation here is the same as in (4.4) except the corresponding Taylor coefficients are different. Truncating the normal form up to third order and ignoring the θ—equation, the normal form in cylindrical coordinates is given by

$$\begin{aligned}\dot{r} &= \xi_2 r x_3 + \xi_6 r x_3^2 + \xi_3 r^3,\\ \dot{x}_3 &= \xi_8 x_3^2 + \xi_9 r^2 x_3 + \xi_{10} x_3^3,\end{aligned}$$

where

$$\xi_2 = \frac{\lambda\delta_2 - \delta_1^2}{2\lambda\delta_2(\lambda+\delta_1)} - \frac{\delta_1(\lambda\delta_2-\delta_1^2)}{2\lambda^2\delta_2(\lambda+\delta_1)} - \frac{\delta_1^2}{\lambda\delta_2(\lambda+\delta_1)},$$

$$\xi_3 = -\frac{\delta_1^3}{8\lambda^3\delta_2^2} - \frac{\delta_1+2\lambda}{8\lambda^2\delta_2},$$

$$\xi_6 = \frac{\delta_1(\lambda\delta_2-\delta_1^2)}{4\lambda\delta_2^2(\lambda+\delta_1)^2} - \frac{(\lambda\delta_2-\delta_1^2)(3\lambda\delta_1^3+2\delta_1^4+3\lambda^3\delta_2+5\lambda^3\delta_1)}{4\lambda^3\delta_1\delta_2^2(\lambda+\delta_1)^2}$$
$$-\frac{(\delta_1+\delta_2)\{\delta_1\delta_2-2\lambda(\delta_1-\delta_2)\}}{2\lambda\delta_2^2(\lambda+\delta_1)^2},$$

$$\xi_8 = -\frac{(\lambda\delta_2 - \delta_1^2)}{\lambda\delta_2(\lambda + \delta_1)},$$

$$\xi_9 = -\frac{\delta_1^3}{2\lambda\delta_2^2(\lambda\delta_2 - \delta_1^2)},$$

$$\xi_{10} = \frac{\lambda\delta_2 - \delta_1^2}{\delta_2^2(\lambda + \delta_1)^2} - \frac{\delta_1(\delta_1 + \delta_2)}{\delta_2^2(\lambda + \delta_1)^2}.$$

Notice that ξ_3, ξ_8 and $\xi_9 < 0$. Performing the same rescaling by letting $\overline{r} = \alpha r$, $\overline{x}_3 = \beta x_3$ with $\alpha = \sqrt{-\xi_3}$, $\beta = \xi_2$ (assuming $\xi_2 \neq 0$) and omitting the bars we obtain

$$\begin{aligned} \dot{r} &= r x_3 + a r x_3^2 - r^3, \\ \dot{x}_3 &= b x_3^2 - c r^2 x_3 - d x_3^3, \end{aligned} \tag{5.3}$$

where $a = \xi_6/\xi_2^2$, $b = \xi_8/\xi_2$, and $d = -\xi_{10}/\xi_2^2$ are arbitrary scalars and $c = \xi_9/\xi_3 > 0$. Reasoning in the same manner as we did for the normal form in (4.8), we choose the same two parameter unfolding of (5.3)

$$\begin{aligned} \dot{r} &= \mu_1 r + r x_3 + a r x_3^2 - r^3, \\ \dot{x}_3 &= \mu_2 x_3 + b x_3^2 - c r^2 x_3 - d x_3^3. \end{aligned} \tag{5.4}$$

Fixed points of (5.4) are identical to the fixed points of (4.9). The normal form analysis (i.e. local and global bifurcations) for (4.8) carries over to (5.4) without any changes. Thus, the normal form analysis would suggest that system (5.2) has the same dynamical behavior as system (3.15). That is, system (5.2) can exhibit 'chaotic' behavior.

As we will see below, although the two systems (3.15) and (5.2) do share similar local bifurcation behavior, system (5.2) does not seem to possess (at least numerically) the global bifurcation behavior of system (3.15). This does not necessarily mean that the choice of normal form for system (5.2) is inadequate. The normal form coefficients, ξ_i, are comparatively simpler than their counterparts c_i for system (3.15). They are still complicated enough to prevent anything but a superficial treatment. However, unlike the normal form

coefficients c_i of system (3.15), here it is possible to deduce a few relationships among the coefficients ξ_i. For instance,

$$\xi_2 = \frac{1}{2\lambda}\left\{\delta_2(\lambda+\delta_1)\xi_{10} - \frac{\delta_1^2}{\lambda\delta_2}\right\},$$

which gives the relationship, that if $\xi_{10} < 0$ then $\xi_2 < 0$. Also,

$$\xi_3 = -\frac{1}{4}\left(\frac{\delta_1}{\lambda}\right)^2\left\{\xi_9 - \frac{1}{\lambda\delta_2^2\xi_8}\right\},$$

and since $\xi_3 < 0$ then $\lambda\delta_2^2\xi_9 > \xi_8$. Even with the knowledge of these additional relationships we can only deduce one extra constraint on the coefficients a, b, c and d of the unfolding in (5.4). Namely, if $\xi_{10} < 0$, then b, $d > 0$. However, even with this additional constraint it is not obvious whether the homoclinic bifurcation depicted in Figure 4.5 can or cannot occur. It is clear that the normal form coefficients ξ_i are more restrictive and thus it may be the case that we never achieve a viable set of values for a, b, c and d such that this homoclinic bifurcation can occur.

Direct comparison of the normal form parameters with the original parameters is again not possible. Thus we resort to AUTO bifurcation diagrams to illustrate the above observations. We will use the same descriptive legend as before. Namely, solid curves denote curves of fixed points, dashed curves are curves of limit cycles, and we use the same symbols to denote the various bifurcation points. S^0 is again the bifurcation parameter.

First consider Diagram 5.1. With the exception of curve K_5 in Diagram 4.8, the two bifurcation Diagrams 5.1 and 4.8 are similar. In fact, the bifurcation behavior and stability description of the fixed points and limit cycles, represented by curves K_1 through K_4, are identical to that of Diagram 4.8. The only difference is that some of the bifurcation values have changed. In particular, the transcritical bifurcation of limit cycles (intersection of curves

K_3 and K_4) occurs at $S^0 = 3.38427$, the saddle-node bifurcation of limit cycles along curve K_4 is at $S^0 = 3.38615$ and the Hopf bifurcation on curve K_2 happens at $S^0 = 2.60898$. Hence, (with the noted exception of a bifurcation to a torus) Diagram 5.1 captures all the local bifurcations of the normal form in (5.4).

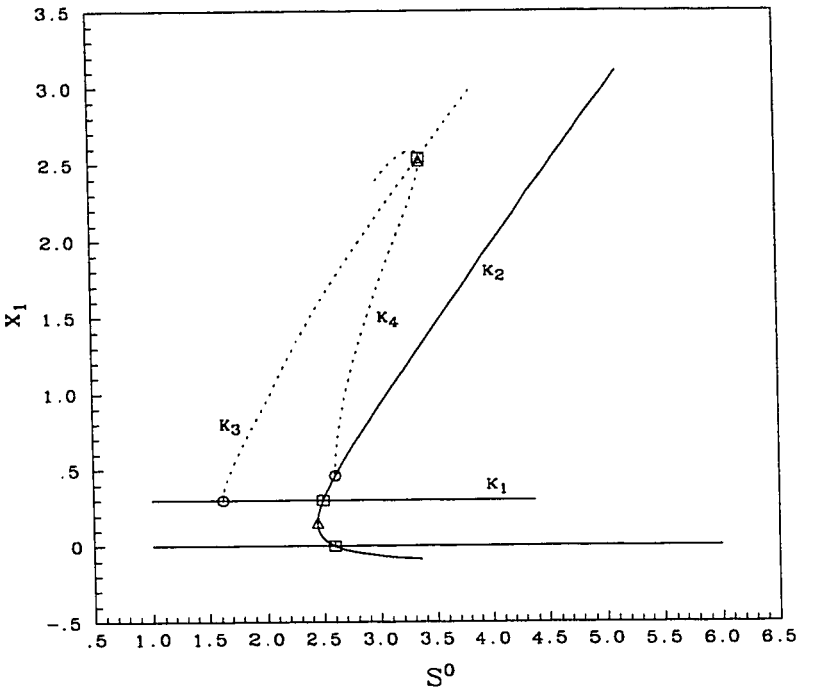

Diagram 5.1 : Parameter values are $\lambda = 0.2$, $\delta_1 = 0.3$, $\delta_2 = 1.2$, and $m_1 = 1.5$.

Next consider Diagram 5.2, which is the analog of Diagram 4.9. Once again, the two AUTO bifurcation diagrams are similar with the exception curve K_5 of Diagram 4.9. The bifurcation behavior and stability description of the fixed points and limit cycles along curves K_1 through K_4 are again identical to Diagram 4.9. The only difference is the Hopf bifurcation value on K_2, which is now $S^0 = 0.81914$. The absence of curve K_5 here seems to prevent the occurrence of a period doubling bifurcation and any other complicated

dynamical behavior. The most complicated behavior here is that of bystability in the positive octant. Both the planar limit cycle and E_{3i}^{Δ} are asymptotically stable for $S^0 \in (0.81914, 1.1)$ and the saddle-type interior limit cycle (K_4) serves as a separatrix.

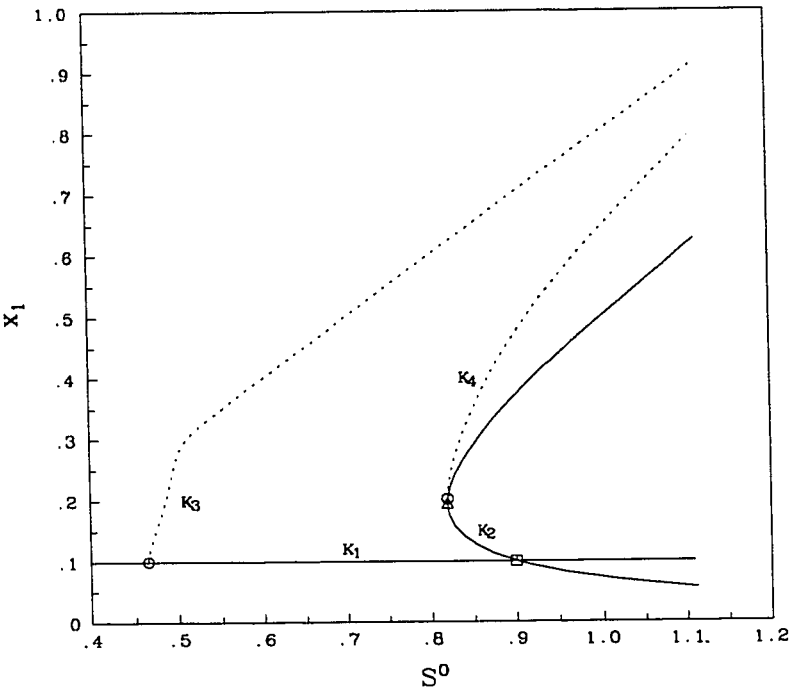

Diagram 5.2 : Parameter values are $\lambda = 0.2$, $\delta_1 = 0.1$, $\delta_2 = 0.2$, and $m_1 = 1.1$.

In all the parameter regions that we tested we could not produce a curve of limit cycles analogous to curve K_5 for system (5.2). In fact, we could not produce any other bifurcation phenomena other than what is depicted in Diagrams 5.1 and 5.2. Also of note is, that if the planar transcritical bifurcation of $E_{S^*}^3$ occurs before the planar Hopf bifurcation, then the interior fixed point E_{3i}^{Δ} that enters the positive octant (via the transcritical bifurcation) appears to be always asymptotically stable with respect to initial conditions $x_{i0} > 0$. In this case there seems to be no interior limit cycles born via Hopf bifurcations

in the interior. The curve of limit cycles, K_5, appears to play an integral role in the 'exotic' dynamically behavior of system (3.15), and it's apparent absence in system (5.2) seems to prevent any 'exotic' dynamics from occurring.

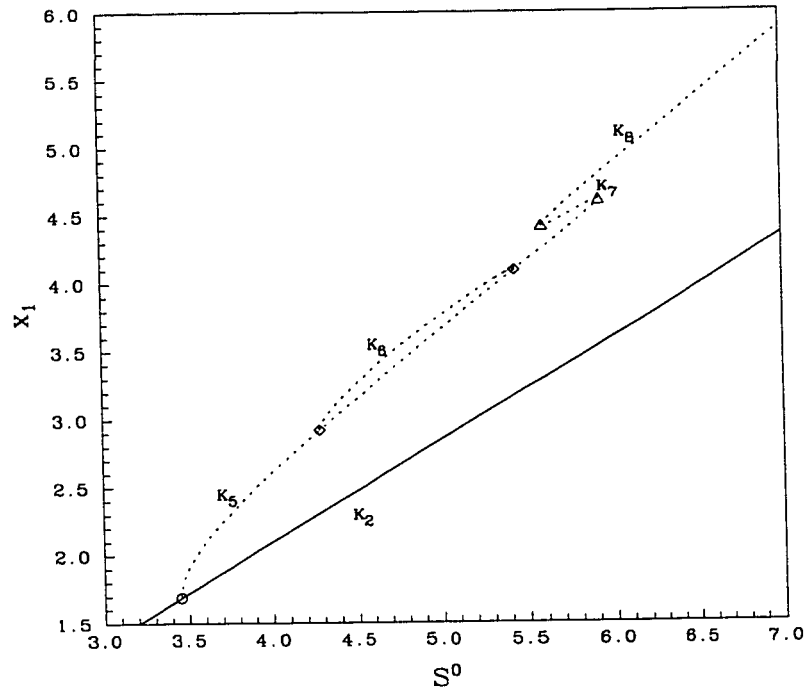

Diagram 5.3 : Parameter values are $\lambda = 0.9$, $\delta_1 = 0.9$, $\delta_2 = 0.3$, and $m_2 = 1.74$.

5.2 Cases 2 and 3 Revisited

In the previous section we saw that curve K_5 played an instrumental role in the dynamical behavior of systems (5.2) and (3.15). The absence of curve K_5 for system (5.2) seems to inhibit any complex dynamical behavior from arising. If the 'codimension two' bifurcation in the x_1x_2-plane is solely responsible for the 'chaotic' behavior of model (3.15), then the intermediate case of the model in (5.2) should also exhibit this behavior. We can not show analytically

that model (5.2) is not 'chaotic', but there is good numerically evidence that this is the case. So, what can account for this difference? The two systems (5.2) and (3.15) differ in the structure of the uptake function $p_2(x_2)$. What are the dynamical effects of changing $p_2(x_2)$ from a linear to a Michaelis-Menten response function?

Recall case 1 of the model described by the system of equations in (3.1). In this case all uptake functions were linear and we had a complete global description of the dynamics. The food chain in (3.1) was characterized by an orderly transfer of global stability from one fixed point to another via transcritical bifurcations. At each stage of this transfer, conditions became favorable such that a new species survived.

We then moved on to consider case 2 of the model which consisted of changing $p_2(x_2)$ from a linear response function to a Michaelis-Menten response function. Example 1 illustrated that the change in $p_2(x_2)$ now at least allowed the birth of an interior limit cycle via a Hopf bifurcation about E_{3i}^{Δ}. However, this is not the only bifurcation that the change in $p_2(x_2)$ produces. Consider the AUTO bifurcation Diagram 5.3. The parameter values used here are from Example 1, and instead of using m_2 as the bifurcation parameter (as we did in Example 1) we use S^0. At $S^0 = 2.4$ there is a transcritical bifurcation about $E_{S^\bullet}^3$ and as S^0 increases, E_{3i}^{Δ} (curve K_2) enters the positive octant and is initially stable. At $S^0 = 3.45106$, E_{3i}^{Δ} undergoes a Hopf bifurcation (Example 1) producing the branch of limit cycles K_5. The limit cycle is stable for $S^0 \in (3.45106, 4.28297)$. At $S^0 = 4.28297$, there is a period doubling bifurcation and the limit cycle is of saddle type for $S^0 \in (4.28297, 5.43488)$. The period 2 limit cycle is stable in this range of S^0. There is a second period doubling bifurcation at $S^0 = 5.43488$ on curve K_5, and for $S^0 \in (5.43488, 5.92155)$ the limit cycle is again stable. At $S^0 = 5.92155$, there is a reverse saddle-node

bifurcation producing a saddle type branch of limit cycles (curve K_7). Finally, at $S^0 = 5.59079$, there is a saddle–node bifurcation with a new stable branch of limit cycles (K_8). Hence the change in $p_2(x_2)$ is capable of producing more than a simple branch of interior limit cycles.

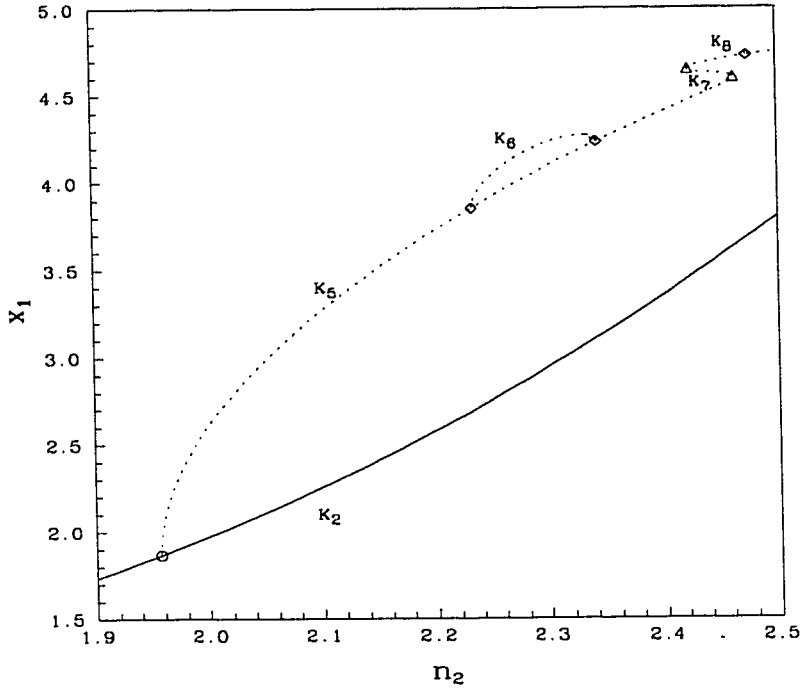

Diagram 5.4 : Parameter values are $n_1 = -1.0$, $S^0 = 5.0$, $\lambda = 0.2$, $\delta_1 = 0.3$ and $m_2 = 3.0$.

Case 3 of the model consisted of now changing both $p_1(x_1)$ and $p_2(x_2)$ from linear to Michaelis-Menten response functions. The bifurcation structure of case 2, depicted in Diagram 5.3, should also be present for case 3. Recall the local bifurcation conditions, about $E^3_{S^\bullet}$ for case 3, given in (4.2). Let

$$n_1 = \frac{\lambda x_2^*}{\delta_1^2} - m_1, \text{ and } n_2 = x_2^* - \delta_2.$$

Then at $n_1 = 0$ there is a Hopf bifurcation about $E^3_{S^\bullet}$ and at $n_2 = 0$ there is a transcritical bifurcation. Using n_1 and n_2 we can move system (3.15) through

the Hopf and transcritical bifurcations independently. Fix $n_1 = -1$ (i.e. no Hopf bifurcation) and let n_2 be the bifurcation parameter. Diagram 5.4 is an AUTO bifurcation diagram for system (3.15). Notice that the bifurcation structure of Diagram 5.3 is present here in Diagram 5.4. The intermediate case given by (5.2) does not seem to posses this type of bifurcation structure. Using n_2 as the bifurcation parameter to now move system (5.2) through the planar transcritical bifurcation produces only a stable branch of interior equilibria E_{3i}^{Δ}.

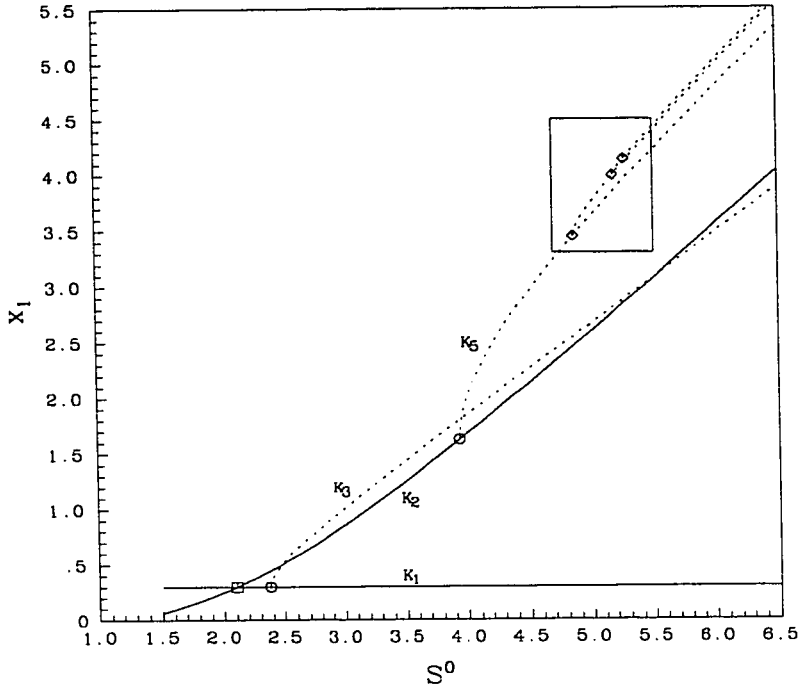

Diagram 5.5 : Parameter values are $\lambda = 0.2$, $\delta_1 = 0.3$, $\delta_2 = 0.96$, $m_1 = 2.5$ and $m_2 = 3.0$.

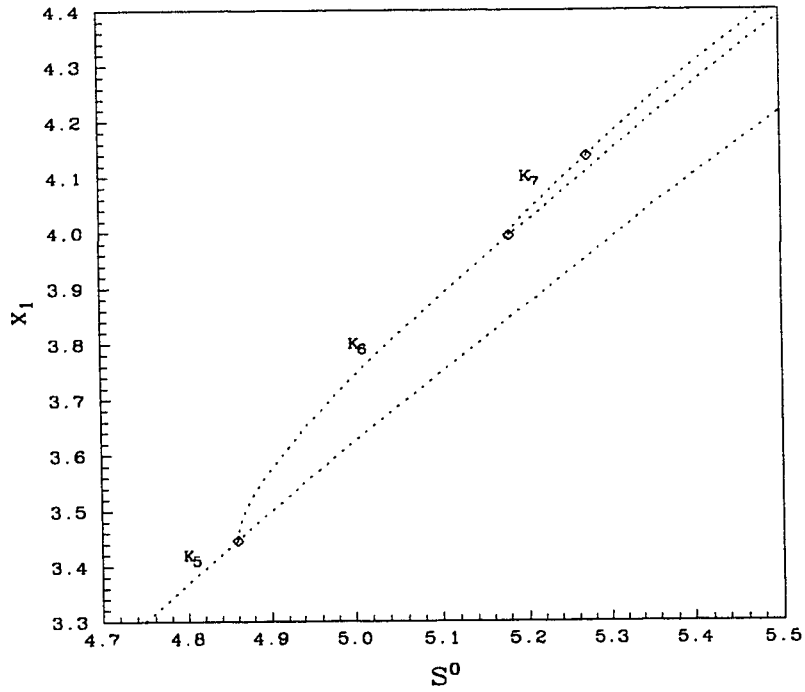

Diagram 5.5a : A closer look at the region about the period doubling bifurcations of Diagram 5.5.

Up to this point we have avoided discussing the attractors depicted in Figures 3.7 and 3.8. In both of the numerical simulations that produced these attractors, the planar transcritical bifurcation occurred before the planar Hopf bifurcation. Thus, already the sequence of bifurcations that leads to these attractors is different from the sequence that produced the locally asymptotically stable attractor in Figure 4.10. As a result the normal form analysis is somewhat inadequate to explain the attractors in Figures 3.7 and 3.8. Instead, consider Diagram 5.5 which is an AUTO simulation using the parameter values of Figure 3.7. There is a transcritical bifurcation at $S^0 = 2.1$ and a Hopf bifurcation at $S^0 = 2.375$ about $E^3_{S^*}$ (curve K_1). Curve K_3 represents the planar limit cycle and it is of saddle type. E^{Δ}_{3i} (curve K_2) enters the positive octant via the planar transcritical bifurcation and is at least initially

stable until it loses stability via the Hopf bifurcation at $S^0 = 3.93797$. The interior limit cycle, created by this Hopf bifurcation, is initially stable and at $S^0 = 4.85950$ it undergoes a period doubling bifurcation losing it's stability. At this point a further increase in S^0 results in a cascade of period doubling limit cycles. At each stage of the period doubling the resulting higher period limit cycle is stable. This cascade results in the attractor seen in Figure 3.7.

One way of thinking about this attractor is in terms of an addition of a planar Hopf bifurcation to the bifurcation structure of Diagram 5.4. That is, adding a Hopf bifurcation about $E^3_{S^\bullet}$ results in the destruction of curve K_6 in Diagram 5.4, producing a period doubling cascade.

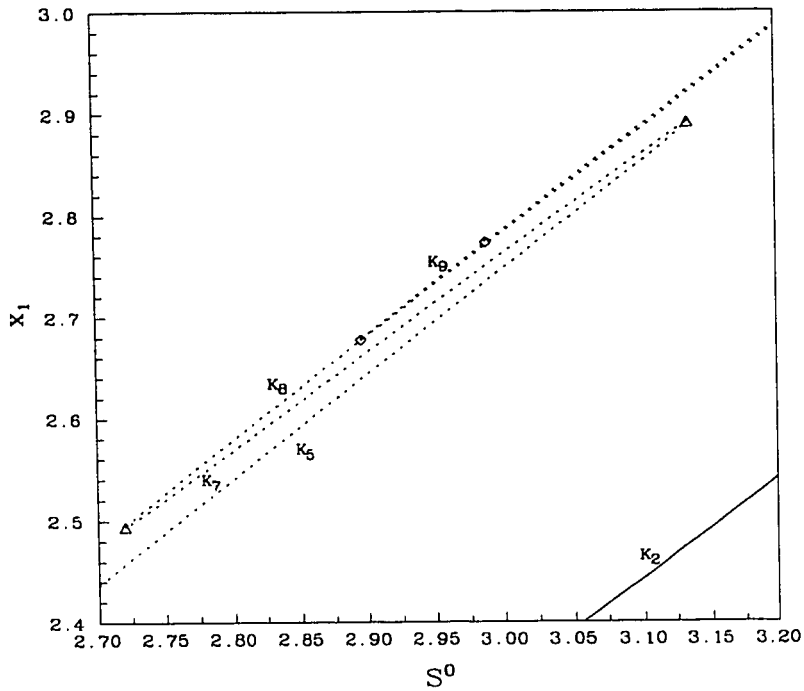

Diagram 5.6 : Parameter values are $\lambda = 0.2$, $\delta_1 = 0.3$, $\delta_2 = 0.2$, $m_1 = 2.5$ and $m_2 = 3.0$.

Next, consider Diagram 5.6, which is an AUTO simulation using the parameter values of Figure 3.8. Once again the transcritical bifurcation ($S^0 =$

0.83333) in the x_1x_2-plane occurs before the planar Hopf bifurcation ($S^0 = 2.375$). The planar limit cycle is again of saddle type. E_{3i}^{Δ} enters the positive octant via the transcritical bifurcation about $E_{S^*}^3$ and is initially stable until the Hopf bifurcation at $S^0 = 1.38630$, at which point it loses stability. Curve K_5 denotes the branch of limit cycles born from this Hopf bifurcation. Diagram 5.6 depicts the bifurcation phenomena along curve K_5. Initially the limit cycle is stable until it reaches the reverse saddle-node bifurcation value $S^0 = 3.13518$. The branch K_7 of limit cycles, produced by this bifurcation, is of saddle type. Following curve K_7 (S^0 is now decreasing) we reach another saddle-node bifurcation at $S^0 = 2.71984$. The new branch of limit cycles (K_8) created now is initially stable and loses stability as it passes through the period doubling bifurcation at $S^0 = 2.89611$. At this point a further increase in S^0 results in another period doubling bifurcation along the branch of period 2 limit cycles (K_9), producing a branch of period 4 limit cycles. Thus, it appears that we have the beginning of a period doubling cascade. Unfortunately, at this point AUTO's limitations are tested when we try to follow the branch of period 4 limit cycles. However, it does appear that a saddle-node bifurcation occurs before a period doubling bifurcation along this branch of period 4 limit cycles. Also, in a neighborhood of $S^0 = 4.0$, curve K_9 undergoes several saddle-node bifurcations. Hence, this does not appear to be a cascade like the one previous. For $S^0 \in (2.71984, 3.13518)$ there are three limit cycles (a behavior not reflected by the normal form) in the positive octant. More importantly, for $S^0 \in (2.89611, 3.13518)$ two of these limit cycles (K_7 and K_8) are of saddle type and thus allow for the possibility of a Sil'nikov type bifurcation about one of these limit cycles.

At $S^0 = 2.8$, there are two stable limit cycles in the interior (K_5 and K_8) and one saddle type limit cycle (K_7). The saddle type limit cycle serves as

a separatrix in the interior, and depending on the initial conditions, solutions tend to one of the stable limit cycles. At $S^0 = 2.91$, the limit cycle denoted by curve K_8 has lost it's stability to a period 2 limit cycle. Once again, the saddle type limit cycle (K_7) serves as a separatrix and depending on initial conditions, solutions either tend to the stable limit cycle or the stable period 2 limit cycle. This behavior seems to continue through to the attractor of Figure 3.8. That is, at $S^0 = 3.12$, the saddle type limit cycle (K_7) is still acting as a separatrix and drawing solutions to either the stable limit cycle (K_6) or the attractor. This saddle type limit cycle seems to be located below the bottom of the attractor (just above the x_1x_2-plane) and the stable limit cycle is just below it. Hence, the attractor in this case seems to be a result of a Sil'nikov bifurcation about a limit cycle.

In terms of the bifurcation structure of Diagram 5.3, one can think of the addition of the planar Hopf bifurcation in this case as moving the period doubling bifurcation value along curve K_8 down the curve to reside between the two saddle-node bifurcation values. Thus allowing for the possibility of a Sil'nikov type bifurcation about one of the saddle type limit cycles.

Chapter 6

Summary and Discussion

Our work on the three species chemostat food chain was motivated by recent comparable work ([18], [26]) on the three species food chain of the type in (4.1). These models share several characteristic traits. First, they both display persistence of species at the bottom trophic levels in the absence of higher trophic level species. Secondly, there are coupled predator-prey oscillations with higher trophic level species oscillating at lower amplitudes than the bottom trophic level species. Lastly, both models have a fixed point of the form $(\overline{x}_1, \overline{x}_2, 0)$, with $(\overline{x}_1, \overline{x}_2, 0)$ having an unstable manifold transverse to the x_1x_2-plane and this fixed point may undergo a codimension two bifurcation. Much of the work done on the food chain (4.1) has centered around the case when the response functions are Michaelis-Menten, partly because this is a biologically reasonable scenario but also because the food chain in this case can exhibit chaotic dynamics ([18], [26]). From a mathematical point of view, the Michaelis-Menten case can prove to be quite challenging. As a result, our approach to the study of the three species chemostat food chain was slightly different. We first considered the linear response function case. Then, by changing the response functions one at a time, we built towards the

Michaelis-Menten case with chaos. Nonetheless, we profited greatly from the work done on the three species food chain.

The periodically forced two species predator-prey chemostat has been shown to be chaotic ([37]) using AUTO. As well, there is numerical evidence to indicate that the perodically operated chemostat with two or three competitor populations can have chaotic dynamics for certain parameter ranges ([30], [31]). In all cases, it was shown that if the periodicities were sufficiently strong, then chaotic dynamics were possible. Our results show that chaos is possible in the chemostat without any imposed periodicities in the model. Chaos in the three species chemostat food chain is a result of species interactions. Nonlinearities in the response functions, $p_i(x_i)$, can generate chaos. Thus it is important to understand the role of the structure of the uptake functions with respect to the dynamics of the model.

Recall that for general monotone uptake functions, the fixed point E_0 was globally asymptotically stable for $S^0 < \lambda$. Next, restricting $p_1(x_1)$ to being one of the three prototype response functions in (2.4), we were able to show that E_λ is globally asymptotically stable for $\lambda < S^0 < \lambda + \delta_1$. Thus the condition $S^0 > \lambda$ ensured the survivability of population x_1. At this point we were forced to consider only prototype response functions due to the mathematical difficulties presented by general monotone response functions. The first case we considered was when all response functions were linear. In this case, we had two additional fixed points E_{S^*} and E^Δ. The model was characterized by an orderly transfer of global stability from one fixed point to another via transcritical bifurcations. At each stage of the transfer, conditions became sufficient for a new population to survive. The condition $S^0 > (\lambda + \delta_1)(1 + \delta_2/\delta_1)$ provided coexistence of the three populations in terms of fixed point stability.

Next, we considered case 2. The only difference between case 1 and case 2 is that in case 2, $p_2(x_2)$ is of Michaelis-Menten form rather than of linear form. Once again, we had two additional fixed points E_{S^*} and E^{Δ}, and there was an orderly transfer of global stability from E_0 to E_λ to E_{S^*} via transcritical bifurcations. The transfer of global stability from E_{S^*} to E^{Δ} was interrupted. Although the condition $S^0 > (\lambda + \delta_1)(1 + \delta_2/\delta_1)$ was not sufficient to show global asymptotic stability of E^{Δ}, it was however a necessary and sufficient condition for uniform persistence in this case. Unlike case 1, here coexistence of the three populations could be attained in terms of several different types of invariant sets. Coexistence of the three species could take the form of fixed point stability (E^{Δ}), limit cycle stability and period 2 limit cycle stability (Diagram 5.3). This case of the model also provided us with an example of coexistence in the form of multiple invariant sets. From Diagram 5.3 we see that it is possible to have a saddle interior limit cycle which acts as a separatrix in the positive cone. Depending on initial conditions, trajectories tended to one of two stable interior limit cycles. Hence the change in $p_2(x_2)$ was at least responsible for the creation of a Hopf bifurcation about E^{Δ}, as well as period doubling and saddle-node bifurcations of limit cycles in the positive cone. Case 2 however, did fall short in terms of exhibiting chaotic behavior.

Next, we considered case 3. The only difference between case 2 and case 3 is that in case 3, $p_1(x_1)$ is of Michaelis-Menten form rather than of linear form. Once again, E_{S^*} was a fixed point. However, now it was possible to have none, one or two interior fixed points E_i^{Δ}. The orderly transfer of global stability from on fixed point to another of case 1, was now interrupted at an earlier stage than case 2. Specifically, it was interrupted between E_λ and E_{S^*}, due to the planar limit cycle born via a Hopf bifurcation about E_{S_*}. We now had a codimension two bifurcation about E_{S^*}, and adopted a

normal form approach (similar to [26]) to further facilitate the understanding of the dynamics of this case. As mentioned above, the three species chemostat food chain and the three species food chain (4.1) share certain characteristic traits, but they do differ. Namely, there is an absence of direct interaction between prey and superpredator in the food chain (4.1). This is not the case for the food chain in the chemostat. This difference manifested itself in the choice of unfolding for the normal form computed about E_{S^*}. Our choice was a two parameter unfolding as opposed to the three parameter unfolding in ([26]). Despite this difference, we were able to reproduce the local and global bifurcations found in ([26]) for the three species chemostat food chain, with the exception of the pitchfork bifurcation about $(r, x_3) = (0, 0)$.

The unfolded normal form reflected the behavior of the original model relatively well when the planar Hopf bifurcation occurred before the planar transcritical bifurcation. However, the unfolded normal form was inadequate in reflecting the original model's behavior when the order of the planar bifurcations were reversed. Why this is the case is still an open question. Perhaps we need to consider higher order terms in the normal form. At least the consideration of fourth order terms would allow for the possibility of three interior fixed points, and thus reflect the possibility of three interior limit cycles for the original system (Diagram 5.6). Or, it could be the case that our somewhat 'artificial' choice of normal form is not an appropriate one. Nonetheless, the consideration of this particular third order normal form did motivate us to search for and locate the locally asymptotically chaotic attractor in Figure 4.10. Also, we were able to compare the chaotic dynamics of case 3 to the underlying bifurcation structure of case 2.

In an attempt to better understand the role of the codimension two bifurcation about E_{S^*}, we then considered the intermediate case of the model.

This case consisted of changing $p_2(x_2)$ back to a linear response function in case 3. We still had the codimension two bifurcation about E_{S^*} in this case. The unfolded normal form for this case did reflect all of the local bifurcation behavior of the original system. However, in the case of global bifurcations, the unfolded normal form predicted more behavior than the original system was capable of displaying (probably due to the lack of information regarding the normal form coefficients, i.e. sign, magnitude etc..). The intermediate case did not display any chaotic behavior. The presence of only the codimension two bifurcation in the x_1x_2-plane is not sufficient for chaos to occur in the three species food chain.

Hence we concluded that it is the nonlinearities in both $p_1(x_1)$ and $p_2(x_2)$ that are responsible for the chaotic dynamics of the three species chemostat food chain. In determining whether or not the three species food chain in the chemostat is capable of chaotic dynamics, it is enough to consider the structure of the uptake functions $p_1(x_1)$ and $p_2(x_2)$.

The reader might have already noted that the Hopf and saddle-node bifurcation values on curve K_2 in Diagrams 4.9 and 5.2 occur relatively close to each other. Thus it is reasonable to consider whether or not these two bifurcations can occur simultaneously. That is, is it possible to have a second codimension two bifurcation that occurs in the positive cone? By considering the associated characteristic equation of E_i^{Δ}, it is clear that the intermediate case cannot undergo such a bifurcation inside or outside the positive cone. Similarly, case 3 cannot undergo a bifurcation of this type in the positive cone. However, this codimension two bifurcation can occur outside the positive cone for case 3. In fact, it is possible for this bifurcation to occur just below the x_1x_2-plane. To what extent this bifurcation affects the dynamics in the positive cone is unclear. The x_1x_2-plane is invariant with respect to the flow,

hence it is unclear how this codimension two bifurcation affects the dynamics in the positive cone or, if it affects them at all. For the three species food chain, consideration of whether or not this bifurcation can occur in $\mathbf{R}^4$ may be a good indication if there are sufficient nonlinearities in $p_1(x_1)$ and $p_2(x_2)$ to produce chaos in certain parameter regions.

Like the work of [18], [30], [31], [35], [37], and [38], our results tend to question the conventional thinking that chaos in nature is rare. Our work suggests that for reasonable parameter values chaos is possible. From a biological point of view, if information of long term behavior is required then the role of chaos becomes crucial. Over a short time period chaos can appear to be regular oscillatory motion. However, over longer time periods the effects of sensitivity to initial conditions become more pronounced and chaos plays an important role. From a mathematical point of view, (as pointed out in [18]) if a model can exhibit chaotic behavior then one has to be cautious about conclusions drawn from linear stability analyses of fixed points. For example, conclusions made on the bases of return time arguments ([36]).

We conclude this chapter with a few remarks on two open questions. First, the two species predator-prey chemostat model has been shown (numerically) to have the same bifurcation behavior (with the exception of the case of washout of both populations) as the classical two species food chain ([38]). Similarly, the periodically forced two species predator-prey chemostat model has been shown to have the same bifurcation structure as its periodic food chain counter part ([37]). Although we have seen a lot of shared bifurcation behavior between our model and the three species food chain, it is still an open question of whether or not they have the same bifurcation structure.

Secondly, the periodically forced two species predator-prey chemostat has been shown to be chaotic ([35], [37]). Chaos for this model can occur via

a period doubling cascade of limit cycles or through torus destruction. What effect does the addition of periodically forced terms to our model, and the three species food chain in (4.1), have on the existing chaotic behavior? Do we now have three routes to chaos, a period doubling cascade, a Sil'nikov bifurcation of a limit cycle and torus destruction?

Appendix A

Maple Program For Calculation Of Third Order Normal Form

The following is a Maple V (version 3.0) program for the computation of a normal form of a vector field of the form

$$\begin{pmatrix} \dot{x} \\ \dot{y} \\ \dot{z} \end{pmatrix} = \begin{pmatrix} 0 & w & 0 \\ -w & 0 & 0 \\ 0 & 0 & 0 \end{pmatrix} \begin{pmatrix} x \\ y \\ z \end{pmatrix} + f_2(x,y,z) + f_3(x,y,z), \qquad \text{(A.1)}$$

where f_i, for $i = 1, 2$, are power series terms about the point $(0,0,0)$ of degree 2 and 3 respectively, and are given in lines 8 and 9 below. Before running the program, the Maple linear algebra package should be opened first. Maple commands are proceeded by the symbol >. All other text below is inserted comment for the benefit of the reader, and all notation is from the introductory chapter.

```
> with(linalg):
> jac := [[0, w, 0], [-w, 0, 0], [0, 0, 0]]:
```

$> f2cof := [[a11, a12, a22, a23, a33, a13], [b11, b12, b22, b23, b33, b13],$
$[c11, c12, c22, c23, c33, c13]]:$

$> f3cof := [[a111, a112, a122, a222, a223, a233, a333, a113, a133, a123],$
$[b111, b112, b122, b222, b223, b233, b333, b113, b133, b123],$
$[c111, c112, c122, c222, c223, c233, c333, c113, c133, c123]]:$

$> X := [x, y, z]:$

$> TH2 := [x\hat{}2, x * y, y\hat{}2, y * z, z\hat{}2, x * z]:$

$> TH3 := [x\hat{}3, x\hat{}2{*}y, x{*}y\hat{}2, y\hat{}3, y\hat{}2{*}z, y{*}z\hat{}2, z\hat{}3, x\hat{}2{*}z, x{*}z\hat{}2, x{*}y{*}z]:$

$> f2 := multiply(matrix(f2cof), TH2):$

$> f3 := multiply(matrix(f3cof), TH3):$

First put the second order terms in normal form. We do this by choosing $h_2(\mathbf{y})$ such that the transformation $\mathbf{x} = \mathbf{y} + h_2(\mathbf{y})$, applied to (A.1), eliminates all 'nonessential' second order terms. First, we need to represent H_2 (vector space of vector-valued monomials of degree 2) as $H_2 = L_J(H_2) \oplus G_2$, where G_2 is a space complementary to $L_J(H_2)$. Secondly, we need to find bases for $L_J(H_2)$ and G_2. We then decompose $f2cof$ to obtain $f2res \in G_2$. Finally, we solve for $h_2(\mathbf{y})$.

$> quadb := [[x\hat{}2, 0, 0], [x * y, 0, 0], [y\hat{}2, 0, 0], [y * z, 0, 0], [z\hat{}2, 0, 0], [x * z, 0, 0],$
$[0, x\hat{}2, 0], [0, x * y, 0], [0, y\hat{}2, 0], [0, y * z, 0], [0, z\hat{}2, 0], [0, x * z, 0],$
$[0, 0, x\hat{}2], [0, 0, x * y], [0, 0, y\hat{}2], [0, 0, y * z], [0, 0, z\hat{}2], [0, 0, x * z]]:$

$> dqb := [seq([[\mathrm{diff}(quadb[i][1], x), \mathrm{diff}(quadb[i][1], y), \mathrm{diff}(quadb[i][1], z)],$
$[\mathrm{diff}(quadb[i][2], x), \mathrm{diff}(quadb[i][2], y), \mathrm{diff}(quadb[i][2], z)],$
$[\mathrm{diff}(quadb[i][3], x), \mathrm{diff}(quadb[i][3], y), \mathrm{diff}(quadb[i][3], z)]], i = 1..18)]:$

$>$ for i from 1 to 18 do $LQ[i] := multiply(matrix(dqb[i]), matrix(jac))$; od:

$> qlie := expand([seq(add(multiply(matirx(jac), quadb[i]),$

$scalarmul(multiply(LQ[i], X), -1)), i = 1..18)])$:

We want to compute $L_J(H_2)$. We do this by determining the action of $L_J(*)$ on each basis element in *quadb* (i.e. *qlie*), and then determine a matrix representation of $L_J(*)$, $m2$, with respect to the basis *quadb*.

$> m2 := transpose(matrix([seq([\text{coeff}(qlie[i][1], x\hat{}2),$
$\text{coeff}(\text{coeff}(qlie[i][1], x), y), \text{coeff}(qlie[i][1], y\hat{}2),$
$\text{coeff}(\text{coeff}(qlie[i][1], y), z), \text{coeff}(qlie[i][1], z\hat{}2),$
$\text{coeff}(\text{coeff}(qlie[i][1], x), z), \text{coeff}(qlie[i][2], x\hat{}2),$
$\text{coeff}(\text{coeff}(qlie[i][2], x), y), \text{coeff}(qlie[i][2], y\hat{}2),$
$\text{coeff}(\text{coeff}(qlie[i][2], y), z), \text{coeff}(qlie[i][2], z\hat{}2),$
$\text{coeff}(\text{coeff}(qlie[i][2], x), z), \text{coeff}(qlie[i][3], x\hat{}2),$
$\text{coeff}(\text{coeff}(qlie[i][3], x), y), \text{coeff}(qlie[i][3], y\hat{}2),$
$\text{coeff}(\text{coeff}(qlie[i][3], y), z), \text{coeff}(qlie[i][3], z\hat{}2),$
$\text{coeff}(\text{coeff}(qlie[i][3], x), z)], i = 1..18)])):$

Compute G_2. We do this by finding the space of vectors orthogonal to each column of $m2$ or equivalently the nullspace of the transpose of $m2$. Columns of *qns* form a basis for G_2.

$> qns1 := nullspace(transpose(m2)):$
$> qns2 := convert(qns1, list):$
$> qns := transpose(matrix(qns2)):$

Compute the range of $L_J(*)$. This is the column space of $m2$. Columns of *qcspb* form a basis for the range of $L_J(*)$.

$> qcspb1 := colspace(m2):$

$> qcspb2 := convert(qcspb1, list):$

$> qcspb := transpose(matrix(qcspb2)):$

$> rq := rank(m2):$

Concatenate the two bases, qns and $qcspb$, to form a new basis of H_2. Then decompose $f2cof$, such that $f2cof = qinrang + f2res$, where $qinrang$ is in $L_J(H_2)$ and $f2res \in G_2$.

$> qbasis := concat(qcspb, qns):$

$> F2 := [a11, a12, a22, a23, a33, a13, b11, b12, b22, b23, b33, b13,$
$c11, c12, c22, c23, c33, c13]:$

$> qcoefs := linsolve(qbasis, F2):$

$> qtemp1 := [seq(scalarmul(col(qbasis, j), qcoefs[j]), j = 1..rq)]:$

$> qinrang := evalm(sum(qtemp1[k], k = 1..rq)):$

$> qtemp2 := [seq(scalarmul(col(qbasis, j), qcoefs[j]), j = rq + 1..18)]:$

$> f2res := evalm(sum(qtemp2[k], k = 1..18 - rq)):$

$> f2res1 := [seq(f2res[i], i = 1..6)]:$

$> f2res2 := [seq(f2res[i], i = 7..12)]:$

$> f2res3 := [seq(f2res[i], i = 13..18)]:$

$> negrang := scalarmul(qinrang, -1):$

Determine $h_2(\mathbf{y})$ by solving $m2 * h2 = -qinrang$.

$> HH2 := linsolve(m2, negrang, dd, v):$

$> H2 := [seq(expand(HH2[i]), i = 1..18)]:$

```
> for i from 1 to 4 do v[i] := 0; od:
> h21 := [seq(H2[i], i = 1..6)]:
> h22 := [seq(H2[i], i = 7..12)]:
> h23 := [seq(H2[i], i = 13..18)]:
> h2cof := [h21, h22, h23]:
> h2 := multiply(matrix(h2cof), TH2):
```

Next, determine the third order terms now that they have changed due to the second order near identity transformation $\mathbf{x} = \mathbf{y} + h_2(\mathbf{y})$.

```
> df2 := [seq([diff(f2[i], x),diff(f2[i], y),diff(f2[i], z)], i = 1..3)]:
> dh2 := [seq([diff(h2[i], x),diff(h2[i], y),diff(h2[i], z)], i = 1..3)]:
> term11 := multiply(matrix(df2), matrix(dh2)):
> term12 := multiply(jac, X):
> TERM[1] := multiply(term11, term12):
> term21 := multiply(matrix(dh2), matrix(jac)):
> term22 := multiply(term21, h2):
> TERM[2] := scalarmul(term22, -1):
> term31 := multiply(matrix(dh2), f2):
> TERM[3] := scalarmul(term31, -1):
> TERM[4] := multiply(matrix(df2), h2):
> newf3 := [0, 0, 0]:
> for i from 1 to 2 do newf3 := add(add(TERM[i], TERM[5 - i]), newf3);
  od:
> new1f3 := expand(newf3[1]):
> new2f3 := expand(newf3[2]):
> new3f3 := expand(newf3[3]):
```

$> NF3 :=$ [coeff($new1f3, x\hat{}3$),coeff(coeff($new1f3, x\hat{}2$), y),
coeff(coeff($new1f3, x$), $y\hat{}2$),coeff($new1f3, y\hat{}3$),
coeff(coeff($new1f3, y\hat{}2$), z),coeff(coeff($new1f3, y$), $z\hat{}2$),
coeff($new1f3, z\hat{}3$),coeff(coeff($new1f3, x\hat{}2$), z),
coeff(coeff($new1f3, x\hat{}2$), y),coeff(coeff(coeff($new1f3, x$), y), z),
coeff($new2f3, x\hat{}3$),coeff(coeff($new2f3, x\hat{}2$), y),
coeff(coeff($new2f3, x$), $y\hat{}2$),coeff($new2f3, y\hat{}3$),
coeff(coeff($new2f3, y\hat{}2$), z),coeff(coeff($new2f3, y$), $z\hat{}2$),
coeff($new2f3, z\hat{}3$),coeff(coeff($new2f3, x\hat{}2$), z),
coeff(coeff($new2f3, x\hat{}2$), y),coeff(coeff(coeff($new2f3, x$), y), z),
coeff($new3f3, x\hat{}3$),coeff(coeff($new3f3, x\hat{}2$), y),
coeff(coeff($new3f3, x$), $y\hat{}2$),coeff($new3f3, y\hat{}3$),
coeff(coeff($new3f3, y\hat{}2$), z),coeff(coeff($new3f3, y$), $z\hat{}2$),
coeff($new3f3, z\hat{}3$),coeff(coeff($new3f3, x\hat{}2$), z),
coeff(coeff($new3f3, x\hat{}2$), y),coeff(coeff(coeff($new3f3, x$), y), z)]:

Put the third order terms in normal form. First, we need to represent H_3 (vector space of vector-valued monomials of degree 3) as $H_3 = L_J(H_3) \oplus G_3$, where G_3 is a space complementary to $L_J(H_3)$. Secondly, we need to find bases for $L_J(H_3)$ and G_3. We then decompose $f3cof$ to obtain $f3res \in G_3$.

$> cubb :=$ [[$x\hat{}3, 0, 0$], [$x\hat{}2 * y, 0, 0$], [$x * y\hat{}2, 0, 0$], [$y\hat{}3, 0, 0$], [$y\hat{}2 * z, 0, 0$],
[$y * z\hat{}2, 0, 0$], [$z\hat{}3, 0, 0$], [$x\hat{}2 * z, 0, 0$], [$x * z\hat{}2, 0, 0$], [$x * y * z, 0, 0$],
[$0, x\hat{}3, 0$], [$0, x\hat{}2 * y$], [$0, x * y\hat{}2, 0$], [$0, y\hat{}3, 0$], [$0, y\hat{}2 * z, 0$],
[$0, y * z\hat{}2, 0$], [$0, z\hat{}3, 0$], [$0, x\hat{}2 * z, 0$], [$0, x * z\hat{}2, 0$], [$0, x * y * z, 0$],
[$0, 0, x\hat{}3$], [$0, 0, x\hat{}2 * y$], [$0, 0, x * y\hat{}2$], [$0, 0, y\hat{}3$], [$0, 0, y\hat{}2 * z$],
[$0, 0, y * z\hat{}2$], [$0, 0, z\hat{}3$], [$0, 0, x\hat{}2 * z$], [$0, 0, x * z\hat{}2$], [$0, 0, x * y * z$]]:

```
> dcb := [seq([[diff(cubb[i][1],x),diff(cubb[i][1],y),diff(cubb[i][1],z)],
          [diff(cubb[i][2],x),diff(cubb[i][2],y),diff(cubb[i][2],z)],
          [diff(cubb[i][3],x),diff(cubb[i][3],y),diff(cubb[i][3],z)]],i = 1..30)]:
> for i from 1 to 30 do LC[i] := multiply(matrix(dcb[i]),matrix(jac)); od:
> clie := expand([seq(add(multiply(matrix(jac),cubb[i]),
          scalarmul(multiply(LC[i],X),-1)),i = 1..30)]):
```

We want to compute $L_J(H_3)$. We do this by determining the action of $L_J(*)$ on each basis element in *cubb* (i.e. *clie*), and then determine a matrix representation of $L_J(*)$, $m3$, with respect to the basis *cubb*.

```
> m3 := transpose(matrix([seq([coeff(clie[i][1],x^3),
          coeff(coeff(clie[i][1],x^2),y),coeff(coeff(clie[i][1],x),y^2),
          coeff(clie[i][1],y^3),coeff(coeff(clie[i][1],y^2),z),
          coeff(coeff(clie[i][1],y),z^2),coeff(clie[i][1],z^3),
          coeff(coeff(clie[i][1],x^2),z),coeff(coeff(clie[i][1],x),z^2),
          coeff(coeff(coeff(clie[i][1],x),y),z),coeff(clie[i][2],x^3),
          coeff(coeff(clie[i][2],x^2),y),coeff(coeff(clie[i][2],x),y^2),
          coeff(clie[i][2],y^3),coeff(coeff(clie[i][2],y^2),z),
          coeff(coeff(clie[i][2],y),z^2),coeff(clie[i][2],z^3),
          coeff(coeff(clie[i][2],x^2),z),coeff(coeff(clie[i][2],x),z^2),
          coeff(coeff(coeff(clie[i][2],x),y),z),coeff(clie[i][3],x^3),
          coeff(coeff(clie[i][3],x^2),y),coeff(coeff(clie[i][3],x),y^2),
          coeff(clie[i][3],y^3),coeff(coeff(clie[i][3],y^2),z),
          coeff(coeff(clie[i][3],y),z^2),coeff(clie[i][3],z^3),
          coeff(coeff(clie[i][3],x^2),z),coeff(coeff(clie[i][3],x),z^2),
          coeff(coeff(coeff(clie[i][3],x),y),z)],i = 1..30)])):
```

Compute G_3. We do this by finding the space of vectors orthogonal to each column of $m3$ or equivalently the nullspace of the transpose of $m3$. However, here we do not use the nullspace of the transpose of $m3$, instead we use a similar set of vectors ,cns, which retains the θ independence of the normal form equations in cylindrical coordinates. Columns of cns form a basis for G_3.

$> cns1 := nullspace(transpose(m3))$:

$> cns2 := convert(cns1, list)$:

> for k from 1 to 6 do for i from 1 to 30 do if $abs(cns2[k][i]) = 3$ then
$cns2[k][i] := cns2[k][i]/3$ fi; od; od:

Compute the range of $L_J(*)$. This is the column space of $m3$. Columns of $ccspb$ form a basis for the range of $L_J(*)$.

$> cns := transpose(matrix(cns2))$:

$> ccspb1 := colspace(m3)$:

$> ccspb2 := convert(ccspb1, list)$:

$> ccspb := transpose(matrix(ccspb2))$:

$> rc := rank(m3)$:

Concatenate the two bases, cns and $ccspb$, to form a new basis of H_3. Then decompose $f3cof$, such that $f3cof = cinrang + f3res$, where $cinrang$ is in $L_J(H_3)$ and $f3res \in G_3$.

$> cbasis := concat(ccspb, cns)$:

$> ccoefs := linsolve(cbasis, NF3)$:

$> ctemp1 := [seq(scalarmul(col(cbasis, j), ccoefs[j]), j = 1..rc)]:$

$> cinrang := evalm(sum(ctemp1[n], n = 1..rc)):$

$> ctemp2 := [seq(scalarmul(col(cbasis, j), ccoefs[j]), j = rc + 1..30)]:$

$> f3res := evalm(sum(ctemp2[n], n = 1..30 - rc)):$

$> f3res1 := [seq(f3res[j], j = 1..10)]:$

$> f3res2 := [seq(f3res[j], j = 11..20)]:$

$> f3res3 := [seq(f3res[j], j = 21..30)]:$

$> f := (x, y, z) \rightarrow dotprod(jac[1], X) + dotprod(f2res1, TH2)$
$+dotprod(f3res1, TH3):$

$> g := (x, y, z) \rightarrow dotprod(jac[2], X) + dotprod(f2res2, TH2)$
$+dotprod(f3res2, TH3):$

$> h := (x, y, z) \rightarrow dotprod(jac[3], X) + dotprod(f2res3, TH2)$
$+dotprod(f3res3, TH3):$

Change to cylindrical coordinates and get the normal form coefficients c_i.

$> polarf := subs(x = r * cos(t), y = r * sin(t), z = z, f(x, y, z)):$

$> polarg := subs(x = r * cos(t), y = r * sin(t), z = z, g(x, y, z)):$

$> polarh := subs(x = r * cos(t), y = r * sin(t), z = z, h(x, y, z)):$

$> rdot := expand(cos(t) * polarf + sin(t) * polarg):$

$> thetadot := expand((cos(t)/r) * polarf - (sin(t)/r) * polarg)):$

$> zdot := expand(polarh):$

$> c1 :=$coeff$(thetadot, z):$

$> c2 :=$coeff(coeff$(rdot, r), z):$

$> c3 :=$coeff$(rdot, r\hat{}3):$

$> c4 :=$coeff$(thetadot, r\hat{}2):$

$> c5 :=$coeff$(thetadot, z\hat{}2):$

```
> c6 :=coeff(coeff(rdot,r),z^2):
> c7 :=coeff(zdot,r^2):
> c8 :=coeff(zdot,z^2):
> c9 :=coeff(coeff(zdot,r^2),z):
> c10 :=coeff(zdot,z^3):
```

Appendix B

Maple Program For Calculation Of 3-Jet

The following is a Maple V (version 3.0) program for the computation of the coefficients of a 3–jet of the vector field in (3.15) about the fixed point $E^3_{S^*}$. Before running the program, the Maple linear algebra package should be opened first. Maple commands are proceeded by the symbol >. All other text below is inserted comment for the benefit of the reader. Note that the same program can be run for the calculation of the 3–jet for the intermediate case of the model in Chapter 5. Simply make the appropriate changes in lines 3 and 4 below.

$> with(linalg)$:

$> f := (x,y,z) \rightarrow -x + x*(S-x-y-z)/L - y*m1*x/(d1*(m1-1)+x)$:

$> g := (x,y,z) \rightarrow y*(-1 + m1*x/(d1*(m1-1)+x))$

$\qquad -z*m2*y/(d2*(m2-1)+y)$:

$> h := (x,y,z) \rightarrow z*(-1 + m2*y/(d2*(m2-1)+y))$:

$> linf := [\text{diff}(f(x,y,z),x), \text{diff}(f(x,y,z),y), \text{diff}(f(x,y,z),z)]$:

$> ling := [\mathrm{diff}(g(x,y,z),x),\mathrm{diff}(g(x,y,z),y),\mathrm{diff}(g(x,y,z),z)]:$

$> linh := [\mathrm{diff}(h(x,y,z),x),\mathrm{diff}(h(x,y,z),y),\mathrm{diff}(h(x,y,z),z)]:$

$> JAC := [linf, ling, linh]:$

Apply the bifurcation conditions in (4.2).

$> m1 := L * d2/(d1\hat{}2):$

$> u := sqrt((d1/L+1) * d2 * (m1-1)/(d1 * m1)):$

$> jac := simplify(subs(x = d1, y = d2, z = 0, JAC)):$

$> jacb := subs(jac[1][1] = 0, jac):$

$> T := matrix([[0, u * m1 * d1/(d2 * (m1-1)), 1],$
$[1, 0, -(d2 * (m1-1)/(m1 * (d1+L)))],$
$[0, 0, d2 * (m1-1)/(d1 * m1)]]):$

$> Tinv := inverse(T):$

$> jord := multiply(Tinv, mulltiply(matrix(jacb), T)):$

Second and third order terms to be transformed.

$> quadf := simplify(subs(x = d1, y = d2, z = 0, [\mathrm{diff}(f(x,y,z),x\$2),$
$\mathrm{diff}(f(x,y,z),x,y),\mathrm{diff}(f(x,y,z),y\$2),\mathrm{diff}(f(x,y,z),y,z),$
$\mathrm{diff}(f(x,y,z),z\$2),\mathrm{diff}(f(x,y,z),x,z)])):$

$> quadg := simplify(subs(x = d1, y = d2, z = 0, [\mathrm{diff}(g(x,y,z),x\$2),$
$\mathrm{diff}(g(x,y,z),x,y),\mathrm{diff}(g(x,y,z),y\$2),\mathrm{diff}(g(x,y,z),y,z),$
$\mathrm{diff}(g(x,y,z),z\$2),\mathrm{diff}(g(x,y,z),x,z)])):$

$> quadh := simplify(subs(x = d1, y = d2, z = 0, [\mathrm{diff}(h(x,y,z),x\$2),$
$\mathrm{diff}(h(x,y,z),x,y),\mathrm{diff}(h(x,y,z),y\$2),\mathrm{diff}(h(x,y,z),y,z),$
$\mathrm{diff}(h(x,y,z),z\$2),\mathrm{diff}(h(x,y,z),x,z)])):$

$$> cubf := simplify(subs(x = d1, y = d2, z = 0, [\text{diff}(f(x,y,z), x\$3),$$
$$\text{diff}(f(x,y,z), x\$2, y), \text{diff}(f(x,y,z), x, y\$2), \text{diff}(f(x,y,z), y\$3),$$
$$\text{dif}(f(x,y,z), y\$2, z), \text{diff}(f(x,y,z), y, z\$2), \text{diff}(f(x,y,z), z\$3),$$
$$\text{diff}(f(x,y,z), x\$2, z), \text{diff}(f(x,y,z), x, z\$2), \text{diff}(f(x,y,z), x, y, z)])):$$

$$> cubg := simplify(subs(x = d1, y = d2, z = 0, [\text{diff}(g(x,y,z), x\$3),$$
$$\text{diff}(g(x,y,z), x\$2, y), \text{diff}(g(x,y,z), x, y\$2), \text{diff}(g(x,y,z), y\$3),$$
$$\text{diff}(g(x,y,z), y\$2, z), \text{diff}(g(x,y,z), y, z\$2), \text{diff}(g(x,y,z), z\$3),$$
$$\text{diff}(g(x,y,z), x\$2, z), \text{diff}(g(x,y,z), x, z\$2), \text{diff}(g(x,y,z), x, y, z)])):$$

$$> cubh := simplify(subs(x = d1, y = d2, z = 0, [\text{diff}(h(x,y,z), x\$3),$$
$$\text{diff}(h(x,y,z), x\$2, y), \text{diff}(h(x,y,z), x, y\$2), \text{diff}(h(x,y,z), y\$3),$$
$$\text{dif}(h(x,y,z), y\$2, z), \text{diff}(h(x,y,z), y, z\$2), \text{diff}(h(x,y,z), z\$3),$$
$$\text{diff}(h(x,y,z), x\$2, z), \text{diff}(h(x,y,z), x, z\$2), \text{diff}(h(x,y,z), x, y, z)])):$$

$$> X := [x, y, z]:$$

$$> T2 := [x\hat{}2/2, x * y, y\hat{}2/2, y * z, z\hat{}2/z, x * z]:$$

$$> T3 := [x\hat{}3/6, x\hat{}2 * y/2, x * y\hat{}2/2, y\hat{}3/6, y\hat{}2 * z/2, y * z\hat{}2/2,$$
$$z\hat{}3/6, x\hat{}2 * z/2, x * z\hat{}2/2, x * y * z]:$$

$$> xlin := (x, y, z) \rightarrow dotprod(jacb[1], X):$$

$$> ylin := (x, y, z) \rightarrow dotprod(jacb[2], X):$$

$$> zlin := (x, y, z) \rightarrow dotprod(jacb[3], X):$$

$$> xquad := (x, y, z) \rightarrow dotprod(quadf, T2):$$

$$> yquad := (x, y, z) \rightarrow dotprod(quadg, T2):$$

$$> zquad := (x, y, z) \rightarrow dotprod(quadh, T2):$$

$$> xcub := (x, y, z) \rightarrow dotprod(cubf, T3):$$

$$> ycub := (x, y, z) \rightarrow dotprod(cubg, T3):$$

$$> zcub := (x, y, z) \rightarrow dotprod(cubh, T3):$$

$$> w := multiply(T, [a, b, c]):$$

Transformed second order terms.

$$> nquadvec := multiply(Tinv, [subs(x = w[1], y = w[2], z = w[3], xquad(x, y, z)),$$
$$subs(x = w[1], y = w[2], z = w[3], yquad(x, y, z)),$$
$$subs(x = w[1], y = w[2], z = w[3], zquad(x, y, z))]):$$
$$> nxdotquad := expand(nquadvec[1]):$$
$$> a11 := simplify(\text{coeff}(nxdotquad, a\hat{}2)):$$
$$> a12 := simplify(\text{coeff}(\text{coeff}(nxdotquad, a), b)):$$
$$> a22 := simplify(\text{coeff}(nxdotquad, b\hat{}2)):$$
$$> a23 := simplify(\text{coeff}(\text{coeff}(nxdotquad, b), c)):$$
$$> a33 := simplify(\text{coeff}(nxdotquad, c\hat{}2)):$$
$$> a13 := simplify(\text{coeff}(\text{coeff}(nxdotquad, a), c)):$$
$$> nydotquad := expand(nquadvec[2]):$$
$$> b11 := simplify(\text{coeff}(nydotquad, a\hat{}2)):$$
$$> b12 := simplify(\text{coeff}(\text{coeff}(nydotquad, a), b)):$$
$$> b22 := simplify(\text{coeff}(nydotquad, b\hat{}2)):$$
$$> b23 := simplify(\text{coeff}(\text{coeff}(nydotquad, b), c)):$$
$$> b33 := simplify(\text{coeff}(nydotquad, c\hat{}2)):$$
$$> b13 := simplify(\text{coeff}(\text{coeff}(nydotquad, a), c)):$$
$$> nzdotquad := expand(nquadvec[3]):$$
$$> c11 := simplify(\text{coeff}(nzdotquad, a\hat{}2)):$$
$$> c12 := simplify(\text{coeff}(\text{coeff}(nzdotquad, a), b)):$$
$$> c22 := simplify(\text{coeff}(nzdotquad, b\hat{}2)):$$
$$> c23 := simplify(\text{coeff}(\text{coeff}(nzdotquad, b), c)):$$
$$> c33 := simplify(\text{coeff}(nzdotquad, c\hat{}2)):$$
$$> c13 := simplify(\text{coeff}(\text{coeff}(nzdotquad, a), c)):$$

Transformed third order terms.

```
> ncubvec := multiply(Tinv, [subs(x = w[1], y = w[2], z = w[3], xcub(x, y, z)),
                             subs(x = w[1], y = w[2], z = w[3], ycub(x, y, z)),
                             subs(x = w[1], y = w[2], z = w[3], zcub(x, y, z))]):
> nxdotcub := expand(ncubvec[1]):
> a111 := simplify(coeff(nxdotcub, a^3)):
> a112 := simplify(coeff(coeff(nxdotcub, a^2), b)):
> a122 := simplify(coeff(coeff(nxdotcub, a), b^2)):
> a222 := simplify(coeff(nxdotcub, b^3)):
> a223 := simplify(coeff(coeff(nxdotcub, b^2), c)):
> a233 := simplify(coeff(coeff(nxdotcub, b), c^2)):
> a333 := simplify(coeff(nxdotcub, c^3)):
> a113 := simplify(coeff(coeff(nxdotcub, a^2), c)):
> a133 := simplify(coeff(coeff(nxdotcub, a), c^2)):
> a123 := simplify(coeff(coeff(coeff(nxdotcub, a), b), c)):
> nydotcub := expand(ncubvec[2]):
> b111 := simplify(coeff(nydotcub, a^3)):
> b112 := simplify(coeff(coeff(nydotcub, a^2), b)):
> b122 := simplify(coeff(coeff(nydotcub, a), b^2)):
> b222 := simplify(coeff(nydotcub, b^3)):
> b223 := simplify(coeff(coeff(nydotcub, b^2), c)):
> b233 := simplify(coeff(coeff(nydotcub, b), c^2)):
> b333 := simplify(coeff(nydotcub, c^3)):
> b113 := simplify(coeff(coeff(nydotcub, a^2), c)):
> b133 := simplify(coeff(coeff(nydotcub, a), c^2)):
> b123 := simplify(coeff(coeff(coeff(nydotcub, a), b), c)):
```

```
> nzdotcub := expand(ncubvec[3]):
> c111 := simplify(coeff(nzdotcub, a^3)):
> c112 := simplify(coeff(coeff(nzdotcub, a^2), b)):
> c122 := simplify(coeff(coeff(nzdotcub, a), b^2)):
> c222 := simplify(coeff(nzdotcub, b^3)):
> c223 := simplify(coeff(coeff(nzdotcub, b^2), c)):
> c233 := simplify(coeff(coeff(nzdotcub, b), c^2)):
> c333 := simplify(coeff(nzdotcub, c^3)):
> c113 := simplify(coeff(coeff(nzdotcub, a^2), c)):
> c133 := simplify(coeff(coeff(nzdotcub, a), c^2)):
> c123 := simplify(coeff(coeff(coeff(nzdotcub, a), b), c)):
```

Coefficients of the new transformed linear, second order and third order terms.

```
> xdotlin := row(jord, 1):
> ydotlin := row(jord, 2):
> zdotlin := row(jord, 3):
> xdotquad := [a11, a12, a22, a23, a33, a13]:
> ydotquad := [b11, b12, b22, b23, b33, b13]:
> zdotquad := [c11, c12, c22, c23, c33, c13]:
> xdotcub := [a111, a112, a122, a222, a223, a233, a333, a113, a133, a123]:
> ydotcub := [b111, b112, b122, b222, b223, b233, b333, b113, b133, b123]:
> zdotcub := [c111, c112, c122, c222, c223, c233, c333, c113, c133, c123]:
```

The normal form coefficients (computed in Appendix A) of the $r-$equation and x_3-equation.

$$> c2 := simplify((a13 + b23)/2):$$

$$> c3 := simplify((3a111 + a122 + b112 + 3b222)/8 - a11 * a12/(8 * u) -$$
$$a12 * a22/(8 * u) + a11 * b11/(4 * u) + b11 * b12/(8 * u) -$$
$$a22 * b22/(4 * u) + b12 * b22/(8 * u) - 3 * a23 * c11/(16 * u) -$$
$$3 * b13 * c11/(16 * u) + 3 * a13 * c12/(16 * u) + b23 * c12/(16 * u) -$$
$$a23 * c22/(16 * u) - b13 * c22/(16 * u)):$$

$$> c6 := simplify((a133 + b233)/2 - a12 * a33/(2 * u) - a33 * b22/u +$$
$$a11 * b33/u + b12 * b33/u - b33 * c13/u + a33 * c23/u -$$
$$a23 * c33/(4 * u) - b13 * c33/(4 * u)):$$

$$> c7 := simplify((c11 + c22)/2):$$

$$> c8 := c33:$$

$$> c9 := simplify((c113 + c223)/2 + a23 * c11/(2 * u) + b13 * c11/(2 * u) -$$
$$a13 * c12/(2 * u) + b11 * c13/(2 * u) + b22 * c13/(2 * u) -$$
$$a11 * c23/(2 * u) - a22 * c23/(2 * u) + c12 * c33/(2 * u)):$$

$$> c10 := simplify(c333 + b33 * c13/u - a33 * c23/u):$$

Bibliography

[1] R.A Amstrong and R.McGehee, *Competitive exclusion*, Amer. Nat. 115 (1980); 151-170.

[2] D.K. Arrowsmith and C.M. Place, *An introduction to dynamical systems*, Cambridge University Press, 1990.

[3] H.W. Broer and G. Vegter, *Subordinate Sil'nikov bifurcations near some singularities of vector fields having low codimension*, Ergodic Theory and Dynamical Systems 4 (1984); 509-525.

[4] H.R. Bungay and M.L. Bungay, *Microbial interactions in continuous culture*, Advances in Appl. Microbiol. 10 (1968); 794-803.

[5] G. Bulter, H.I. Freedman, and P. Waltman, *Uniformly persistent systems*, Proc. of the Amer. Math. Soc. 96 (1986); 425-430.

[6] G. Butler and P. Waltman, *Persistence in dynamical systems*, J. of Diff. Eqns. 63 (1986); 255-263.

[7] G. Bulter and G.S.K. Wolkowicz, *Predator-mediated competition in the chemostat*, J. of Math. Biol. 24 (1986); 167-191.

[8] G. Bulter and G.S.K. Wolkowicz, *A mathematical model of the chemostat with a general class of functions describing nutrient uptake*, SIAM J. of Appl. Math. 45 (1985); 138-151.

[9] A. Cunningham and R.M. Nisbet, *Transients and oscillations in continuous cultures*, Math. in Microbiol., Academic Press, N.Y., (1983); 77-103.

[10] G. D'Anes, P.V. Kokotovic, and D. Gotlieb, *A nonlinear regulator problem for a model of biological waste treatment*, IEEE Transactions on Automatic Control AC-16 (1971); 341-347.

[11] E.J. Doedel, *AUTO : Software for continuation and bifurcation problems in ordinary differential equations*, CIT Press, Pasadena, 1986.

[12] H.I. Freedman and P. Waltman, *Persistence in a model of three interacting predator-prey populations*, Math. Biosc. 68 (1984); 213-231.

[13] P. Glendinning and C. Sparrow, *Local and global behavior near homoclinic orbits*, Statist. Phys. 35 (1984); 645-696.

[14] J. Guckenhiemer and P. Holmes, *Nonlinear oscillations, dynamical systems, and bifurcations of vector fields*, Appl. Math. Sc. 42, Springer-Verlag, 1983.

[15] T. Hacker, *Flight stability and control*, American Elsevier, 1970.

[16] J.K. Hale, *Ordinary differential equations*, R.E. Krieger Publishing Co., Florida, 1980.

[17] S.R. Hansen and S.P. Hubbell, *Single nutrient microbial competition: Agreement between experimental and theoretical forecast outcomes*, Science 207 (1980); 1491-1493.

[18] A. Hastings and T. Powell, *Chaos in a three species food chain*, Ecology 72 (1991); 896-903.

[19] D. Herbert, R.Elsworth, and R.C. Telling, *The continuous culture of bacteria: A theoretical and experimental study*, J. of Gen. Microbiol. 4 (1956); 601-622.

[20] M.W. Hirsch and C. Pugh, *Stable manifolds and hyperbolic sets*, Global Analysis, Proc. of Symps. on Pure Math. 14, Amer. Math. Soc., Providence, R.I., (1970); 133-165.

[21] G.P. Hoshchild, *Basic theory of algebraic groups and Lie algebras*, Graduate Texts in Math. 75, Springer-Verlag, 1981.

[22] S.B. Hsu, *Limiting behavior for competing species*, SIAM J. of Appl. Math. 34 (1978); 760-763.

[23] S.B. Hsu, S.P. Hubbell, and P. Waltman, *A mathematical theory for single nutrient competition in continuous cultures of micro-organisms*, SIAM J. of Appl. Math. 32 (1977); 366-383.

[24] G.E. Hutchinson, *A treatise on limnology*, vII, Introduction to Lake Biology and Limnology, Wiley, N.Y. (1967).

[25] J.L. Jost, J.F. Drake, A.G. Fredrickson, and H.M. Tsuchiya, *Interactions of Tetrahymena pyriforms, Eschericha coli, Azotobacter vinelandii, and glucose in a minimal medium*, J. of Bacteriology 113 (1973); 834-840.

[26] A. Klebanoff and A. Hastings, *Chaos in three species food chains*, J. of Math. Biol. 32 (1994); 427-451.

[27] W.F. Langford, *A review of interactions of Hopf and steady-state bifurcations*, Nonlinear Dynamics and Turbulence, Pitman: London (1985); 215-237.

[28] J.W.M. La Riviere, *Microbial ecology of liquid waste*, Adv. in Microbial Ecol. 1 (1977); 215-259.

[29] J. LaSalle, *Some extensions of Liapunov's second method*, IRE Trans. Circuit, CT-7 (1960); 520-527.

[30] P. Lenas and S. Pavlou, *Coexistence of three competing microbial populations in a chemostat with periodically varying dilution rate*, Math. Biosc. 129 (1995); 111-142.

[31] P. Lenas and S. Pavlou, *Periodic, quasi-periodic, and chaotic coexistence of two competing microbial populations in a periodically operated chemostat*, Math. Biosc. 121 (1994); 61-110.

[32] R. Miller, *Nonlinear Volterra equation*, W.A. Benjamin, N.Y., 1971.

[33] J. Monod, *Recherches sur la croissance des cultures bacterienness*, Hermann et Cie., Paris, 1942.

[34] A. Novick and L. Szilard, *Experiments with the chemostat on spontaneous mutations of bacteria*, Proc. of Nat. Acad. of Sc. 36 (1950); 708-719.

[35] S. Pavlou and I.G. Kevrekidis, *Microbial predation in a periodically operated chemostat: A global study of the interaction between natural and externally imposed frequencies*, Math. Biosc. 108 (1992); 1-55.

[36] S.L. Pimm, *Food chains and return times*, in D.R. Strong, D. Simberloff, L.G. Abele, and A.B. Thistle, editors. Ecological Communities. Princeton University Press, N.J., (1984); 397-412.

[37] S. Rinaldi and A. Gragnani, *A universal bifurcation diagram for seasonally perturbed predator-prey models*, Bull. of Math. Biol. 57 (1995); 701-712.

[38] S. Rinaldi, S. Muratori, and Y.A. Kuznetsov, *Multiple attractors, catastrophes and chaos in seasonally perturbed predator-prey communities*, Bull. of Math. Biol. 55 (1993); 15-35.

[39] L.P. Sil'nikov, *A case of the existence of a denumerable set of periodic motions*, Sov. Math. Dokl. 6 (1965); 163-166.

[40] S. Smale, *Differentiable dynamical systems*, Bull. of Amer. Math.Soc. 73 (1967); 747-817.

[41] H.L. Smith and P. Waltman, *The theory of the chemostat*, Cambridge University Press, 1995.

[42] G. Stephanopoulos and G. Lapidus, *Chemostat dynamics of plasmid-bearing plasmid-free mixed recombinant cultures*, Chem. Eng. Sc. 43 (1988); 49-57.

[43] P.A. Taylor and P.J.L. Williams, *Theoretical studies on the coexistence of competing species under continuous-flow conditions*, Can. J. of Microbiol. 21 (1975); 90-98.

[44] M. Tang and H. Xia, *Global asymptotic behavior of a class of competitive systems*, Dynamics of Continuous, Discrete and Impulsive Systems 1 (1995); 19-35.

[45] H.R. Theime, *Convergence results and a Poincare-Bendixson trichotomy for asymptotically autonomous differential equations*, J. of Math. Biol. 30 (1992); 755-763.

[46] V. Volterra, *Variations and fluctuations of the number of individuals in animal species living together*, J. of Cons. Int. Explor. Mer. 3 (1928); 3-51.

[47] P. Waltman, S.P. Hubbell, and S.B. Hsu, *Theoretical and experimental investigations of microbial competition in continuous culture*, in T. Burton (ed.), Modelling and Differential Equations in Biology, Marcel Dekker, N.Y. (1980); 107-152.

[48] P.S Welch, *Limnology*, McGraw-Hill Publishing Co., 1952.

[49] S. Wiggins, *Introduction to applied nonlinear dynamical systems and chaos*, Texts in Appl. Math., Springer-Verlag, 1990.

[50] S. Wiggins, *Global bifurcations and chaos*, Appl. Math. Sc. 73, Springer-Verlag, 1988.

[51] G.S.K. Wolkowicz and H. Xia, *Global asymptotic behavior of a chemostat model with discrete delays*, SIAM J. of Appl. Math. 57 (1997).

[52] G.S.K. Wolkowicz, H. Xia, and S. Ruan, *Competition in the chemostat: A distributed delay model and its global asymptotic behavior*, To appear in SIAM J. of Appl. Math.

[53] G.S.K. Wolkowicz and L. Zhiqi, *Global dynamics of a mathematical model of competition in the chemostat: General response functions and differential death rates*, SIAM J. of Appl. Math. 52 (1992); 222-233.

[54] R.D. Yang and A.E. Humphrey, *Dynamics and steady state studies of phenol biodegradation in pure and mixed cultures*, Biotech. Bioeng. 17 (1956); 601-622.

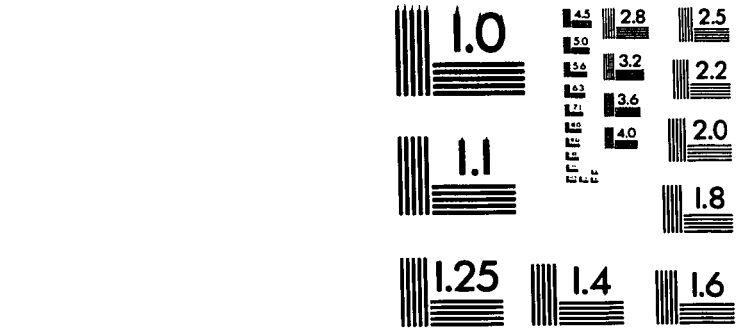

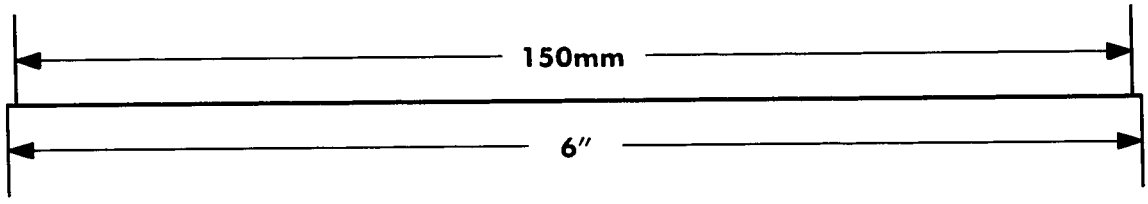

APPLIED IMAGE, Inc
1653 East Main Street
Rochester, NY 14609 USA
Phone: 716/482-0300
Fax: 716/288-5989